Okinawa Institute of Science and Technology

Graduate University

Thesis submitted for Degree
Doctor for Philosophy

Deciphering the role of AP-1 transcription factor JunB in CD4$^+$ T cells

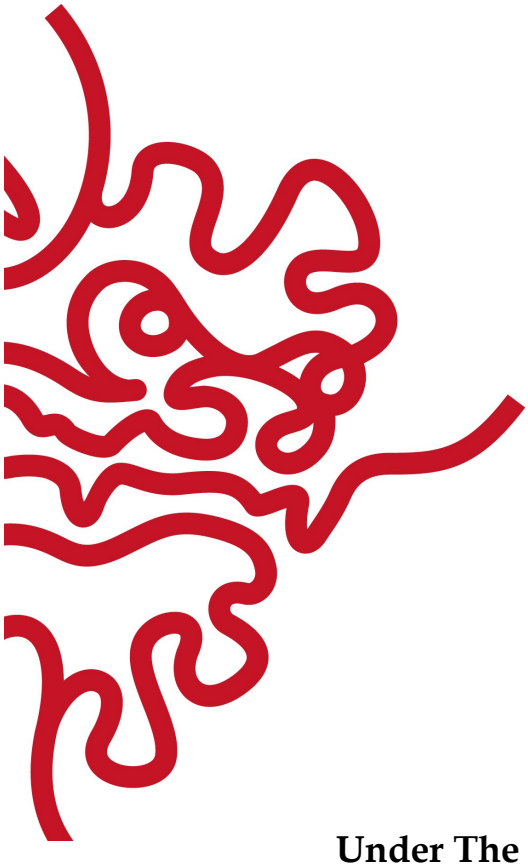

By

Tsunghan Hsieh

Under The Supervision of:
Associate Professor Dr. Hiroki Ishikawa
October 20th 2021

Declaration of original and sole authorship

I, Tsunghan Hsieh, declare that this thesis entitled *Deciphering the role of AP-1 transcription factor JunB in CD4$^+$ T cells* and the data presented in it are original and my own work.

I confirm that:

- No part of this work has previously been submitted for a degree at this or any other university.
- References to the work of others have been clearly acknowledged. Quotations from the work of others have been clearly indicated and attributed to them.
- In cases where others have contributed to part of this work, such contribution has been clearly acknowledged and distinguished from my own work.
- None of this work has been previously published elsewhere.

Date: October 20th, 2021

謝宗翰. Tsunghan Hsieh.

Abstract

Differentiation of distinct $CD4^+$ T effector cell subsets is a key event for adaptive immune responses. Upon recognition of antigens, naïve $CD4^+$ T cells differentiate into functionally distinct $CD4^+$ effector T cell subsets, which control different types of adaptive immunity. The differentiation of $CD4^+$ T effector cells is regulated by the BATF-containing AP-1 heterodimers and their associating proteins IRF4, BATF and IRF4 are induced by T cell receptor (TCR) and co-stimulatory signals and regulate expression of genes required for a broad spectrum of biological functions across diverse $CD4^+$ effector T cell subsets. These transcription factors have been shown to be essential for lineage specification, metabolic activity, and survival of various $CD4^+$ effector T cell subsets, including T helper 1 (Th1), Th2, Th9, Th17, follicular T helper (Tfh) and effector regulator T (eTreg) cells. In contrast to IRF4 and BATF, the role of the major BATF-heterodimeric partner, JunB, in $CD4^+$ T cell differentiation is still not fully understood. In this thesis, I demonstrate that JunB promotes the survival of TCR-stimulated $CD4^+$ T cells under Th1-, Th2-, and Th17-polarizing conditions. Consistent with this, accumulation of antigen-primed JunB-deficient $CD4^+$ T cells are dramatically impaired in mice immunized with complete Freund's adjuvant (CFA), LPS, or papain. RNA-sequencing (RNA-seq) and chromatin immunoprecipitation sequencing (ChIP-seq) analyses reveal that JunB directly regulates expression of various genes that are commonly induced in priming of naïve $CD4^+$ T cells, including a pro-apoptotic gene *Bcl2l11* (encoding Bim), and genes that are specifically induced in Th1, Th2, and Th17 cells. Furthermore, JunB colocalizes with BATF and IRF4 at genomic regions for more than 70% of JunB direct responsive genes. Taken together, JunB, in collaboration with BATF and IRF4, serves a critical function in differentiation of diverse $CD4^+$ T cells by controlling common and lineage-specific gene expression.

Acknowledgements

I would like to express my greatest gratitude to all the people who help me throughout this adventure.

Dr. Hiroki Ishikawa, as my academic supervisor, he has showed me the importance to keep high precision and righteous attitude during research. I thank for the teaching and mentoring.

Dr. Daiki Sasaki, Dr. Naoyuki Taira, Mr. Yu Seto, and Ms. Mio Miyagi provide their professional skills in helping me set various experiments. Without your help, the project cannot be accomplished.

Ms. Sarkar, my lab mate, joined this lab with me at the same time. We have worked in similar projects and shared thoughts, ideas, and information with each other. Those works have built camaraderie between us, and I believe we will bear this bond through the whole lifetime.

I would thank Dr. Zih-Jie Shen, who is my ex-colleague mate and now a researcher in Weill Cornell Medical College/New York Presbytarian Hospital. He generously shares his insights in pursuing career in scientific field – and helps me to improve my terrible scientific writing.

Great appreciations to my parents, Jing-Chen Hsieh and Jui-Hsiang Hsieh, although they are not with me, they do their best in supporting me to start my life in Japan. I also want to thank my sister, Han-Yun Hsien, as she is the major person to take care my parents when I was not in Taiwan.

Lastly, I want to express my deepest and honest gratitude to my most reliable partner – either in family or in lab – Hsiaochiao Chien. Without you, our family will not be complete and our life in pursuing truth will not be so diversified.

List of abbreviations

ACE2	Angiotensin-converting enzyme 2
AICE	AP-1-IRF4 composite element
AP-1	Activator Protein 1
APC	Antigen presenting cell
AIDS	Acquired immune disease syndrome
ATF	Activating transcription factor
ATP	Adenosine triphosphate
BATF	Basic leucine zipper transcription factor ATF-like
BCR	B cell receptor
bp	Base pair
bZIP	Basic leucine zipper
cAMP	Cyclic adenosine monophosphate
CD	Cluster of differentiation
CFA	Complete Freund's adjuvant
ChIP	Chromatin immunoprecipitation
CLP	Common lymphoid progenitor
CRE	cAMP responsive element
COVID-19	Corona virus disease 2019
CRP	C-reactive protein
CTLA-4	Cytotoxic T lymphocyte-associated protein 4
CXCR-5	C-X-C motif chemokine receptor 5
DBD	DNA binding domain
ECAR	Extracellular acidification rate
EICE	ETS-IRF4 composite element
ELISA	Enzyme linked immunosorbent assay
EMSA	Electrophoretic mobility shifting assay
ETP	Early thymocyte progenitor
eTreg	Effector regulator T helper cells
ETS	E26 transformation specific
FACS	Fluorescence-activated cell sorting
GATA-3	GATA-binding protein 3
HIV	Human immunodeficiency virus
IL	Interleukin
ILC	Innate lymphoid cell
IFN	Interferon

Ig	Immunoglobulin
ISRE	Interferon-stimulated response element
kbp	Kilo base pair
LPS	Lipopolysaccharide
MAC	Membrane attack complex
MASP	MBL-associated serine protease
MBL	Mannan-binding lectin
MHC	Major histocompatibility complex
NAD^+	Nicotinamide adenine dinucleotide
NK cell	Nature killer cell
OCR	Oxygen consumption rate
PCR	Polymerase chain reaction
PRR	Pattern recognition receptors
RORγt	RAR-related orphan receptor gamma
RT-qPCR	Quantitative reverse transcription PCR
SAP	Serum amyloid protein
SARS-CoV2	Severe acute respiratory syndrome corona virus 2
SIRT1	Silent mating type information regulation 2 homolog 1
STAT	Signal transducer and activator of transcription
TAD	Transactivation domain
T-bet	T-box expressed in T cells
TCA	Tricarboxylic acid
TCR	T cell receptor
TF	Transcription factor
Tfh cell	Follicular T helper cell
TGF	Tumor growth factor
Th cell	T helper cells
TPA	12-O-tetradecanoylphorbol-12-acetate
Treg cell	Regulatory T helper cell
TSS	Transcription starting sites
TTS	Transcription termination sites

Table of contents

List of figures

List of tables

Chapter 1: General introduction

Overview of Immune system

Mammals live in an environment full of pathogens and have evolved two sophisticated immune systems to prevent infection: innate and adaptive immune systems. The innate immune system operates in a rapid and non- -specific way to provide the first line of defense. On the other hand, the adaptive immune system protects host in a pathogen-specific manner.

The first line of defense of innate immune system is tissues such as skin and mucosal membrane that create physical barriers impermeable for pathogens. In addition, lytic enzymes secreted by epithelial cells surrounding those barrier tissues can also help to remove microbes adhered to host surface tissues. The second responders are innate immune cells. These cells utilize their pattern-recognition receptors (PRRs) to sense pathogen-derived molecules such as lipoprotein, lipopolysaccharides (LPS), flagellin, and pathogen-derived DNA and RNA (1). Upon perceiving the presence of pathogen-derived molecules, innate immune cells actively perform phagocytosis to engulf pathogens themselves or pathogen-derived substances. Engulfed substances are further digested by lytic enzymes within a specific organelle called phagosome. In addition to phagocytosis, innate immune cells secrete lytic enzymes or toxic substances into their surrounding environments and kill pathogens (2, 3).

The main responders of adaptive immune systems are B cells and T cells. B cells produce soluble forms of immunoglobulins (antibodies) that directly bind to pathogen-derived molecules (antigens). The binding of antibodies not only neutralizes the toxicity of antigens but also enhances phagocytosis of antigen by phagocytes. On the other hand, T cells utilize membrane-bound T cell receptors (TCRs) to recognize antigens. Instead of interacting with antigens themselves, TCRs interact with complexes of antigens and major histocompatibility complex (MHC) molecules (4).

T cells are divided into two groups: $CD4^+$ and $CD8^+$ T cells, according to the types of coreceptor (CD4 or CD8) expressed on their surfaces. Upon antigen recognition, $CD4^+$ T cells secrete various cytokines, which can regulate various immune cells. On the other hand, activated $CD8^+$ T cells release cytotoxic substances to kill pathogen-infected cells.

Innate and adaptive immune systems are deeply intertwined. In the process of phagocytosis, pathogen-derived peptide antigens are bound with MHC molecules. The antigen:MHC complexes are subsequently presented on the surface of innate immune cells and exposed to T cells – a process is called antigen presentation. Naïve T cells activated by antigen presentation differentiate into effector T cells. A subset of effector T cells, follicular T helper cells, can help naïve B cell activation and germinal center

reactions. These adaptive immune responses reciprocally promote efficient activation of innate immune cells. This synergism between adaptive and innate immune cells is the basis in maintaining host health.

Innate immune cells

When pathogens break physical and chemical barriers formed by tissues, innate immune cells perform phagocytosis, digestion, and lysis of invading agents. Innate immune cells are a group of white blood cells, including basophils, neutrophils, eosinophils, dendritic cells, monocytes, macrophages, mast cells, and NK cells (Fig.1) (1). By utilizing their pattern recognize receptors (PRR), innate immune cells sense the presence of common pathogen-associated molecular patterns and execute pathogen clearance. The binding between PRR and pathogen molecules initiate a series of innate immune responses, including activation of complement molecules, phagocytosis, and secretion of inflammatory cytokines. In contrast, natural killer (NK) cells can sense alteration of surface molecule expression of pathogen-infected cells using various NK receptors and trigger apoptosis of the infected cells (Fig. 1) (3).

Secreted PRRs, including Mannan-binding lectin (MBL), C-reactive protein (CRP), and serum amyloid protein (SAP) can activate complement system (3). MBL binds to mannose residue of bacterial cell surface and activates MBL-associated serine proteases, MASP-1, and MASP-2, which can trigger the formation of C3 convertase. Once the C3 convertase is activated, it leads a series of protein cleavage events and assembles of membrane attack complex (MAC). The MAC forms pores on the membrane and induce cell lysis of pathogens (Fig. 1) (5). Similarly, CRP and SAP respond to different types of bacterial surface components and lead the activation of C3 convertase (3).

Another innate effector mechanism is phagocytosis, by which innate immune cells engulf and digest pathogens with lytic enzymes. Asubset of innate immune cells, including macrophages, dendritic cells, monocytes and neutrophils, performs phagocytosis with high efficiency and is considered as phagocytes (Fig. 1) (6). The efficiency of phagocytosis could be further enhanced if pathogen-derived molecules:PRR complexes are co-bound with host-derived proteins such as complement molecules or antibodies. This group of protein is called opsonins, which helps phagocytosis (6).

Phagocytosis is also an important step for processing and exposing pathogen-derived peptide antigens – a process called antigen presentation. Because of their high efficiency in phagocytosis and antigen processing abilities, macrophages, dendritic cell, and B cells are called antigen presenting cells (APC) (Fig. 1) (1). During antigen presentation, pathogen-derived peptide antigens are firstly released into phagosomes

and fused with other organelles that are originated from endoplasmic reticulum. In these fused vesicles, peptide antigens are loaded into Major Histocompatibility Complex (MHC) proteins and transported to the plasma membrane. The exposed antigen:MHC complexes can interact with TCR of T cells and induce T cell differentiation. B cells can also present antigens and interact with T cells. In this way, B cells then respond to cytokines released by T cells and subsequently produce antibodies (Fig. 1). This reciprocal activation of B and T cells is called T-cell-dependent B cell response and is an indispensable process for antibody production (7).

To summarize, innate immune cells are not only the actual executor in pathogen clearance but are also essential for activation of adaptive immune response. Antigen presentation performed by phagocytes serves as an important pivot in linking innate and adaptive immune systems (Fig. 1) (8).

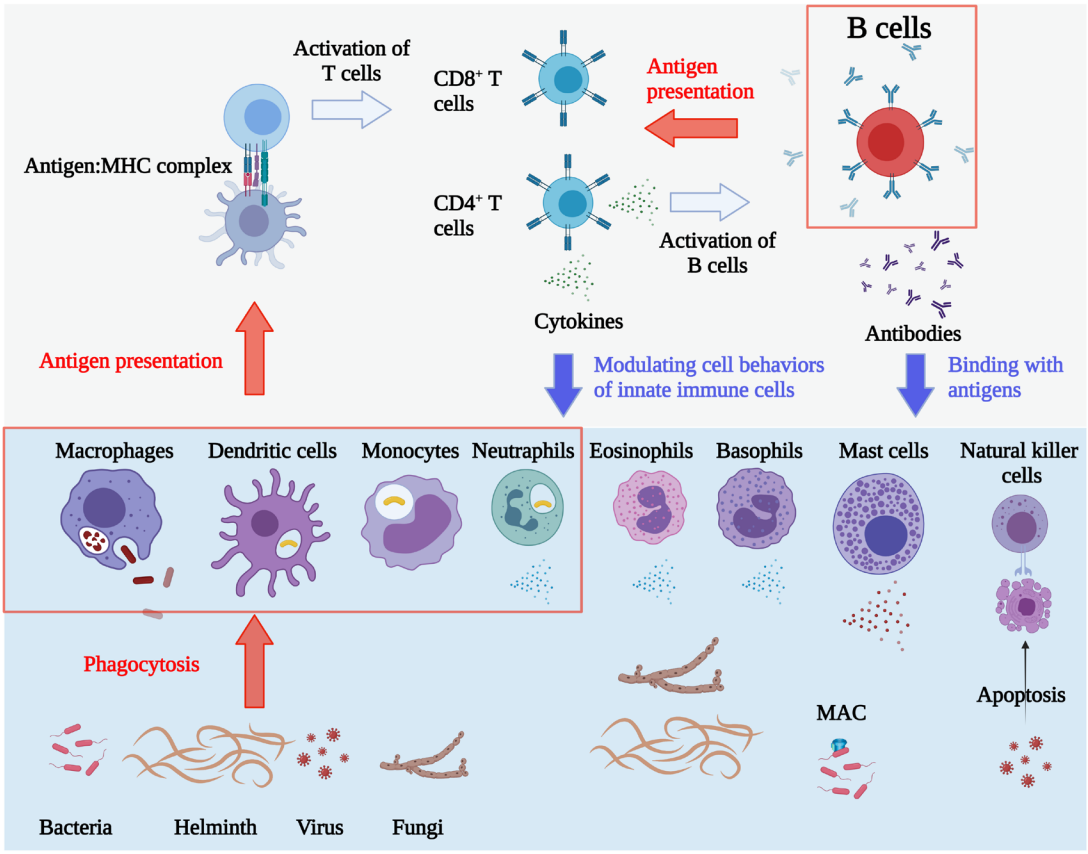

Fig. 1. An overview of immune system and the integration between innate and adaptive immune cells.

Innate immune cells are the first line of immune system. They perform phagocytosis and release cytotoxic substances to clear pathogens. Innate immune cells also secrete pattern recognition receptors to initiate the formation of membrane attack complexes (MAC) and cause lysis of bacteria. A subset of innate immune cells, natural killer cells, induces apoptosis of cells infected by intracellular pathogens such as virus. Innate immune cells specializing in phagocytosis are called phagocytes, including macrophages, dendritic cells, monocytes, and neutrophils. Those cells also dedicate to perform antigen presentation (Red arrows and rectangle) to load pathogen-derived peptide antigens with major histocompatibility complex (MHC) and activate both $CD4^+$ and $CD8^+$ T cells. In addition to innate immune cells, B cells could also present antigens to T cells. Antigen presentation of B cells to $CD4^+$ T cells also activates B cells itself and produce antibodies. Activated $CD4^+$ T and B cells secrete cytokines and antibodies, respectively, which further promotes antigen clearance of innate immune cells (Blue arrows).

Adaptive immune cells

The main players in adaptive immune system, B and T cells, need to undergo primary and secondary differentiation to have antigen-removal functions. In the primary differentiation, precursor B and T cells become mature naïve B and T cells in bone marrow and thymus, respectively (Fig. 2A). Naive B and T cell then enter circulatory system and travel to lymphatic organs such as spleens and lymph nodes, where naïve T cells receive antigen signals from antigen presenting cells (APCs) and undergo the secondary differentiation into effector T cells. Naïve B cells are activated by antigen directly with help from $CD4^+$ effector T cells. Both effector B and effector T cells can reenter circulatory system and migrate toward peripheral tissues under inflammatory conditions (Fig. 2B) (4).

B and T cells express a specialized subset of proteins to recognize a specific portion of target antigens during pathogen clearance. Naïve B cells express membrane-bound immunoglobulins to interact with antigens themselves, whereas effector B cells produce soluble forms of immunoglobulins (antibodies) to directly bind to antigen-bearing pathogens. On the other hand, both naïve and effector T cells utilize membrane-bound T cell receptors (TCRs) for recognizing antigens. Instead of interacting with antigens themselves, TCRs interact with complexes of antigens and major histocompatibility complex (MHC) molecules expressed on APC (4).

T cells are further divided into $CD4^+$ T and $CD8^+$ T cells, depending on which types of co-receptors (CD4 or CD8) of TCRs are expressed. $CD4^+$ T cells utilize CD4 and TCRs to interact with specific antigens presented with MHC class II proteins on a variety of APC. Upon antigen stimulation, effector $CD4^+$ T cells secrete small soluble proteins – cytokines. Cytokines largely modulate behaviors of both innate immune cells and B cells. On the other hand, $CD8^+$ T cells utilize CD8 and TCRs to bind to specific antigens presented with MHC class I proteins on pathogen-infected cells or tumor cells and release cytotoxic substances to kill target cells. $CD8^+$ T cells also release cytokines to induce apoptosis in cells infected by pathogens (4).

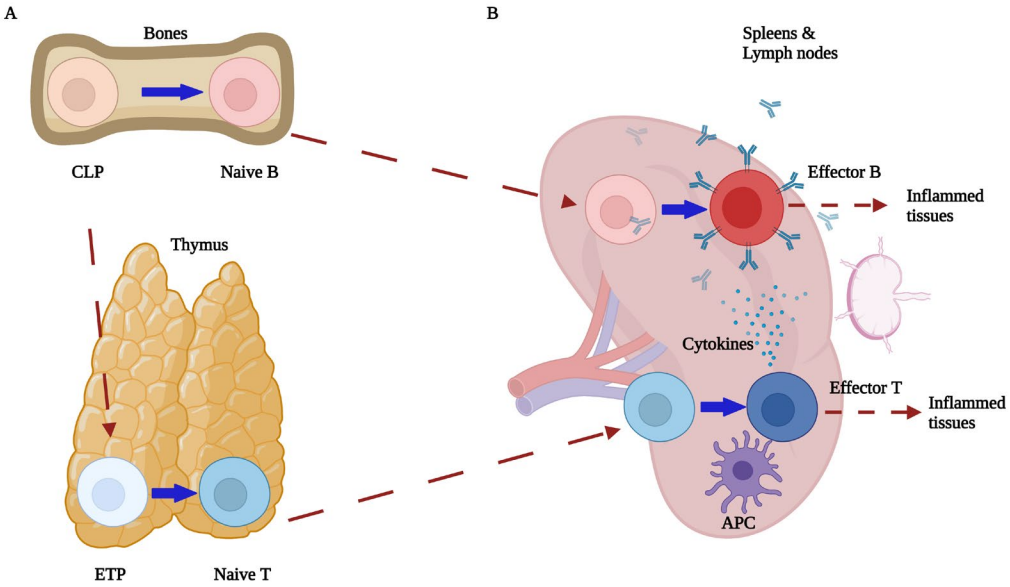

Fig. 2. The development of B and T cells.

(A) The common lymphoid progenitors (CLP) differentiate to naïve B cells and early thymocyte progenitor (ETP) in bone marrow. ETP then migrate to thymus and differentiate into naïve T cells. (B) Both naïve B and T cells enter circulatory system and move to lymphatic organs such as spleen and lymph nodes, where T cells are activated by antigen presenting cells (APC) and become effector T cells. B cells are activated either by antigens directly with help from T cells and become effector B cells. Effector B and T cells can travel to tissues under inflammation. (A-B) Red dashed lines indicate the cell migration is through circulatory system.

CD4$^+$ T cells: integrator of innate and immune system

CD4$^+$ T cells orchestrate the immune system and integrate innate and adaptive immune responses against pathogen infection in a systematic manner.by releasing different types of cytokines that modulate behaviors of a variety of cells (3, 4). Dependent on the ability causing inflammation, cytokines are divided into proinflammatory and anti-inflammatory cytokines. Proinflammatory cytokines such as IL-6 and IFN-γ enhance proliferation, phagocytosis, production of free radicals and apoptosis of innate immune cells. IFN-γ also promotes antigen presentation of APC by upregulating expression of MHC molecules (9). In contrast, anti-inflammatory cytokines such as IL-10 and TGF-β inhibit the growth of innate immune cells by induces expression of inhibitor proteins of cyclin-dependent kinases (CDK) activities (Fig. 3) (10, 11).

Cytokines secreted by CD4$^+$ T cells also help B cells to switch the production of immunoglobulins from membrane-bound immunoglobulin M (IgM) and IgD to various soluble forms of antibodies, including IgA, IgG, and IgE – a process called class switch (12). Class switch changes the constant regions of antibody without affecting its specificity against antigens, enabling B cells to produce antibodies interacting with different effector molecules. For example, binding between antigens and IgG activates complement molecules, similar as the mechanism of mannose binding proteins, lead the formation of membrane attack complex on bacteria cell wall. Each antibody class exhibits unique distribution to various host tissues (Fig. 3)(12).

Although CD4$^+$ effector T cells only have a little effect on the generation of CD8$^+$ effector T cells, cytokines released by CD4$^+$ effector T cells such as IL-2 are required for long-term survival and proliferation of a subset of CD8$^+$ T cells – memory CD8$^+$ T cells (Fig. 3). When naïve CD8$^+$ T cells are primed by antigens and become CD8$^+$ effector T cells at the first time, most of them undergo cell death very quickly after antigens clearance. However, some CD8$^+$ effector T cells enter a different transcriptional status and become memory CD8$^+$ T cells, which persist in tissues for a long time, sometimes decades (13). When memory CD8 T cells encounter the target antigens, they proliferate rapidly and exhibit cytotoxicity. The long-term proliferation and survival of memory CD8$^+$ T cells during the secondary exposure to antigens is highly dependent on IL-2 secreted by CD4$^+$ effector T cells (14, 15).

As CD4 T cells play pivotal roles in linking innate and adaptive immune systems, loss or dysfunction of CD4$^+$ T cells can result in a fatal immunodeficiency in humans. For example, patients with patients with a very rare mutation in the start-codon of *CD4* gene that abrogates the expression of CD4 protein and thus CD4$^+$ T cells exhibit recurrent pneumonia and cannot develop a long-lived antibody response against pathogens. Cytotoxicity and response of innate immune cells to bacterial components were also dysfunctional in these patients (16). Viral infection-induced CD4$^+$ T cell

depletion can also lead to fatal immunodeficiency in humans. The most well-known example is human immunodeficiency viruses (HIV), which infect and kill both naïve $CD4^+$ T and $CD4^+$ effector T cells over the course of years. Without actively controlling HIV progression by antiviral therapy, HIV infection results in higher susceptibility to opportunistic infection due to defective adaptive immune responses (17).

The importance of $CD4^+$ T cells in regulating systematic immune response is also shown on the recent global pandemic of coronavirus disease 2019 (COVID-19). A longitudinal analysis showed that patients with severe COVID-19 symptoms exhibited a higher degree of reduction in both $CD4^+$ and $CD8^+$ T cell number – a phenomenon called lymphopenia, than patients with moderate COVID-19 (18). A possible explanation is severe acute respiratory syndrome corona virus 2 (SARS-Cov2), the virus causing COVID-19, could directly infect and kill $CD4^+$ T cells. SARS-CoV-2 mainly uses its Spike protein (S protein), which binds to Angiotensin-Converting Enzyme 2 (ACE2), for viral entry into cells. Before binding with ACE2, S proteins need to be primed by protease activity from Transmembrane Protease Serine 2 (TMPRSS2) (19). Given that both ACE2 and TMPRSS2 are also expressed in T cells, SARS-CoV-2 might also infect $CD4^+$ T cells. Indeed, recent studies showed that around 50% of lymphocytes in circulation are infected by SARS-CoV-2 during infection (20). A recent study also demonstrated that SARS-CoV-2 could infect $CD4^+$ T cells through CD4 molecules (21). The pathological relevance and mechanism of SARS-CoV2-mediated killing of $CD4^+$ T cells remain unclear and need to be further investigated.

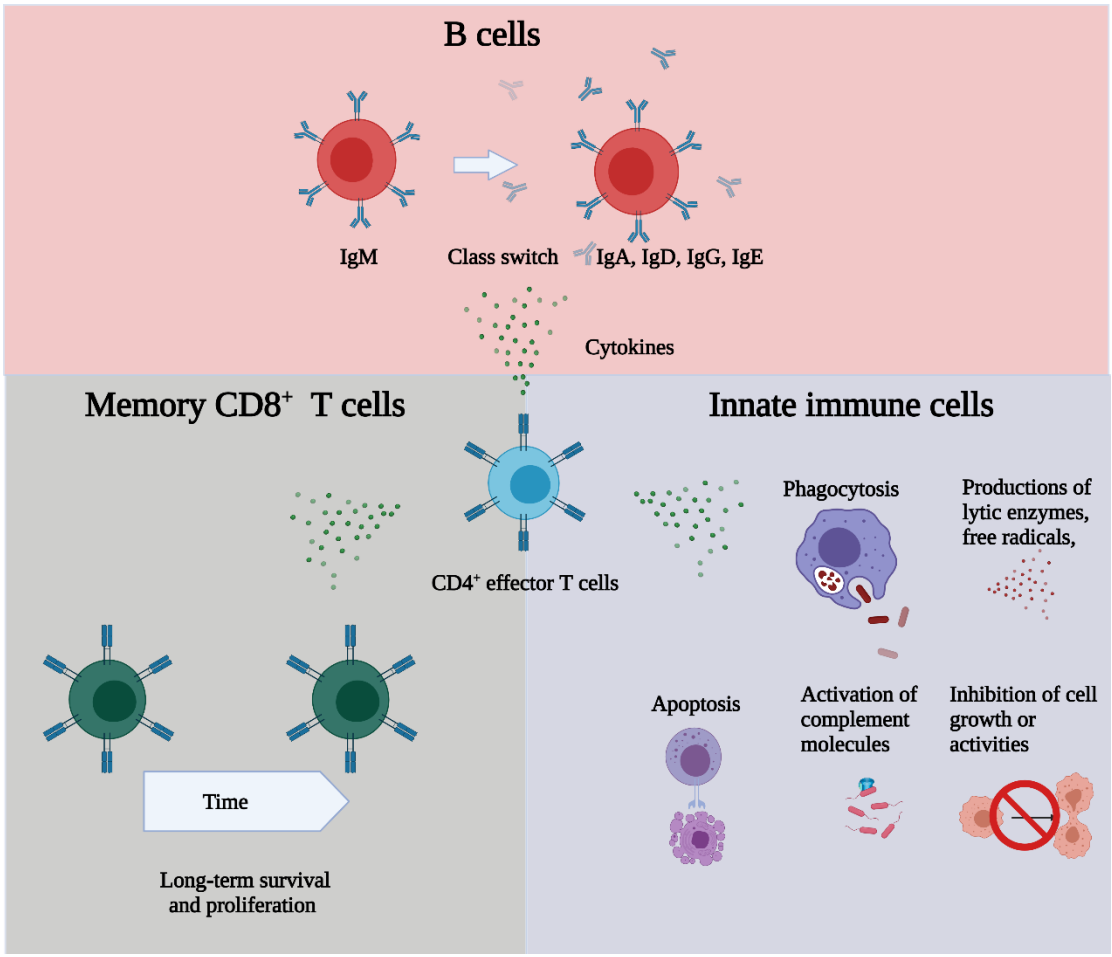

Fig. 3. CD4$^+$ effector T cells is the pivot of immune system.

CD4$^+$ effector T cells secrete cytokines to help class switch of B cells (top), long-term survival of memory CD8$^+$ T cells (left bottom) and modulate behaviors of innate immune cells (right bottom). Ig: immunoglobulin.

Transcriptional regulation in $CD4^+$ T cell differentiation

Because of the pivotal roles of $CD4^+$ effector T cells in immunity, the differentiation of naïve $CD4^+$ T cells to effector T cells in lymphatic tissues can be seen as the initiation of systematic immune response. The differentiation process of $CD4^+$ T cells is regulated by three signals provided from APC. The primary signal is mediated by the interaction between antigen:MHC II complexes and TCR on APC surfaces and naïve $CD4^+$ T cells, respectively. The secondary signal, also called co-stimulatory signal, is activated by the interaction between CD80/86 and CD28. T The tertiary signal is derived from cytokines released by APC and activates Signal Transducers and Activator Transcription (STAT) proteins. STATs in turn induce expression of distinct lineage-specific transcription factors and direct naïve $CD4^+$ T cell differentiation into six functionally distinct $CD4^+$ effector T cell subsets: T helper 1 (Th1), Th2, Th9, Th17, follicular T helper (Tfh) and regulatory T (Treg) cells (22–24). This process, also called lineage specification, drives the formation of different $CD4^+$ effector T cell lineages expressing unique transcriptional programs and effector molecules (25). Antigen, co-stimulatory, and cytokine signals also regulate metabolic reprogramming and apoptosis during $CD4^+$ T cell differentiation.

$CD4^+$ T cell differentiation is regulated by various transcription factors. In addition to STATs and lineage-specifying transcription factors, Interferon Regulatory Factor 4 (IRF4) and its associated Activator Protein 1 (AP-1) proteins play a critical role. In this section, I will introduce the role and function of these transcription factors in $CD4^+$ T cell differentiation. I will then discuss how these transcription factors regulate lineage specification, metabolic reprogramming, and apoptosis.

Transcriptional regulation in lineage specification:

STAT proteins and lineage-specifying transcription factors

The lineage specification is initiated by both antigen and cytokine signals. Upon recognition of pathogen-associated molecules, APC secrete various cytokines into surrounding environment and create a tissue milieu. Depending on cytokines, diverse STAT proteins are activated and in turn induce expression of distinct lineage specific transcription factors, which work together with STAT proteins in the induction of unique transcriptional programs in diverse T helper cell subsets (Fig.4) (25).

Th1 and Th2 cells are the first characterized T helper subsets (26). Molecules derived from intracellular bacteria, virus and protozoa activate APC to secrete IL-12 and IFN-γ, which subsequently activate STAT1 and STAT4 and thereby induce T-bet expression (27–29). T-bet then induces the expression of IFN-γ and TNF-α to activate innate immune cells and $CD8^+$ T cells as well as causing apoptosis in pathogen-infected cell (30, 31). T-bet also induces expression of IL-12Rβ2 – a subunit of IL-12 receptor with high-affinity IL-12 binding sites – which further amplifies the IFN-γ production and stabilizes Th1 phenotypes (32, 33). Th2-stimulating cytokines such as IL-4 are induced by molecules derived from helminth, debris from house dust mite (HDM) and fungal proteases. IL-4 activates STAT6 and thereby induces GATA3 expression in antigen-primed $CD4^+$ T cells. GATA3 then direct the expression of IL-4, IL-5, and IL-13 in Th2 cells. Th2 cytokines are required for anti-helminth immunity, however, unharnessed production of Th2 cytokines also lead to allergy, airway inflammation and hypersensitivity (34, 35).

Th9 cells are a specialized group of $CD4^+$ effector T cells in expressing IL-9, playing important roles in enhancing both host anti-helminth immunity and airway hypersensitivity (36). The differentiation of Th9 cells requires IL-4 and TGF-β signals as well as STAT6 activation (37). Linage-specifying transcription factors required for Th9 is Ets family transcription factor PU.1 (Fig. 4) (38). IL-9 was first thought to be associated with Th2 cells because IL-9 was required for anti-helminth immunity and IgG and IgE production – typical Th2 characteristics (39). However, later studies proved that when IL-4-primed $CD4^+$ T cells are stimulated with TGF-β, they can start producing IL-9 and stop expressing IL-4 and GATA3 (37). Hence, IL-9-producing cells are also considered as a lineage of $CD4^+$ effector T cells.

Th17 cells can be further divided into two subtypes, based on their cytokine expression profiles and association with autoimmunity diseases: homeostatic and pathogenic Th17 cells (40, 41). homeostatic Th17 cells are induced by IL-6 and TGF-β stimulation and secrete IL-17 and IL-10 to regulate activities of gut-resident immune cells (Fig. 4) (42–44). Cytokines secreted by homeostatic Th17 cells also strengthen tissue barriers in small intestines and help B cells to produce IgA, which is required for

controlling commensal microbiota in small intestines (43). On the other hand, pathogenic Th17 cells respond to IL-6, IL-1β, and IL-23 and secret IL-17 as well as proinflammatory cytokines, including IL-22, IFN-γ, and Granulocyte-Macrophage Colony-Stimulating Factor (GM-CSF) (45, 46). Pathogenic Th17 cells contribute to tissue-specific autoimmunity such as inflammation in small intestines and skin as well as systematic autoimmunity (45, 47, 48). In both types of Th17 cells, expression of STAT3 and RORγt are induced to maintain Th17 differentiation and Th17-specific cytokines production (49, 50).

Tfh cells are a T helper subset specializing to help B cell development, class switch, and antibody affinity maturation in a transiently formed structure in lymphatic organs –germinal centers (51). Responding to IL-6 and IL-21, STAT3 is activated and induces expression of Bcl6 in antigen-primed naïve $CD4^+$ T cells staying in germinal centers. Bcl6 subsequently induces expression of Tfh signature molecules, including IL-21, IL-21 receptor (IL-21R), C-X-C chemokine Receptor type 5 (CXCR5) and Programmed cell Death protein 1 (PD-1) (Fig. 4). IL-21 promotes Tfh lineage stability and B cell development in germinal centers in autocrine and paracrine manners, respectively (52–54). Tfh cells utilize CXCR5 to sense the chemokine CXCL13 and stay in T-B cell interface of germinal centers, where they continuously interact with and help B cell development (55). The interaction between PD-1 of Tfh cells and PD-L1/2 of B cells prevents the expression of CXCR3 in Tfh cells, limiting the response of Tfh cells to CXCL9/10 – chemokines bringing Tfh cells to leave germinal centers. Thus, CXCR5 and PD-1 cooperatively provides signals confining the localization of Tfh cells in germinal centers (56).

Unlike other T helper cell subsets, Treg cells inhibit immune responses (57). The differentiation of Treg cells is dependent on IL-2 and TGF-β, which activate STAT5 and induce Foxp3 expression (58). Treg expresses anti-inflammatory cytokines such as IL-10 and TGF-β to inhibit activities of innate immune cells and $CD4^+$ effector T cells. Treg cells also utilize their surface effector molecules CTLA-4 to interact with CD80/86, which interrupts the interaction of CD28 and CD80/86 and blocks the costimulatory signal required for activation of naïve $CD4^+$ T cells (Fig. 4) (57, 59). In thymus, $CD4^+$ T cells recognizing self-antigen with low to medium avidity can differentiate into thymus Treg (tTreg) cells. After maturation, tTreg cells enter circulatory system and peripheral lymphoid tissues as central Treg (cTreg) cells. cTreg cells exhibit a naïve-like phenotypes, such as expressing low and high levels of CD44 and CD62L ($CD44^{lo}CD62L^{hi}$), respectively. Once encountering their target self-antigens in peripheral tissues, cTreg become activated and differentiate into effector Treg (eTreg) with an effector phenotype: $CD44^{hi}CD62L^{lo}$. eTreg expresses higher level of anti-inflammatory cytokines and effector molecules such as IL-10 and CTLA-4 than cTreg.

eTreg are the main cell types of harnessing excessive immune activity in peripheral tissues (57). In addition, with the presence of TGF-β, naïve $CD4^+$ T cells can differentiate into peripheral Treg (pTreg) and provide immunosuppressive functions in peripheral tissues (60).

Recent evidence has suggested that effector $CD4^+$ T cells exhibit a high plasticity. As we have discussed in the conversion from Th2 to Th9 cells (37), similar fate conversion can occur in Th17 cells (transdifferentiate into Th1 and Treg cells) (61, 62) and Treg (transdifferentiate into Th1) (63, 64). Multiple lineage specific transcription factors can also be expressed simultaneously. For example, when Tfh cells are stimulated in the presence of not only IL-21 but also other cytokines such as IL-12, IL-4, IL-6 or TGF-β, in addition to Bcl6, transcription of *Tbx21* (encoding T-bet), *Gata3*, *Rorc* (encoding RORγt), and *Foxp3* can also be induced. As a result, these "Tfh-like cells" not only express IL-21, but also effector cytokines of other T helper lineages such as IFN-γ, IL-4, IL-17A and IL-10. The reciprocal plasticity also exists – when Th1, Th2, Th17 and Treg cells are cultured under IL-21, all T helper cell subsets express Bcl6 and Tfh effector molecules such as IL-21, PD-1 and CXCR5 (65). The flexibility allows $CD4^+$ effector T cells to adjust its transcriptional program in response to rapid changes of extrinsic environment.

Transcriptional regulation in lineage specification:
IRF4, BATF and JunB

In addition to the lineage-specifying transcription factors and STAT proteins, the heterodimer formed by BATF and JunB and their associate proteins IRF4 also play important roles in regulating $CD4^+$ T cell differentiation. These transcription factors are induced by TCR and co-stimulatory signals in all the T helper subsets and act as critical regulators in directing lineage specification. Mice deficient with IRF4, BATF or JunB exhibit various impaired adaptive immunity under *in vivo* immunization conditions (Table 1).

IRF4 was firstly cloned from B cells and later found to be also induced in both $CD4^+$ and $CD8^+$ T cells (54, 66–75). IRF4 regulates transcription of target genes through directly binding to Interferon-Stimulated Response Element (ISRE) of the proximal DNA regions. Without interacting with other proteins, however, IRF4 binds to ISRE only with low affinity (76, 77). This is because the DNA binding activities of N-terminal DNA binding domain (DBD) in IRF4 is repressed by C-terminal repression domain. Binding with other proteins through C-terminal repression domain could "release" the DNA binding ability of DBD (76, 77). Previous studies have demonstrated that in B cells, an ETS family protein PU.1 interacts with IRF4 to release the DBD domain (77). The binding sites for PU.1 and IRF4 is called as ETS-IRF4 composite

element (EICE) (78). In T cells, AP-1 family proteins such as BATF and Jun family proteins play this releasing role to help IRF4 binding to its target sites, called AP-1-IRF4 composite element (AICE) (78, 79).

IRF4 regulates the formation and functions of Th1, Th2, Th9, Th17, Tfh and effector Treg (eTreg) (Fig. 4) (54, 67, 69, 71–75, 80, 81). IRF4-deficient $CD4^+$ T cells showed decreased capacity to differentiate into Th1, Th2, Th9, Th17, Tfh under *in vitro* polarizing conditions (69, 71, 73–75, 80). Accordingly, *Irf4*$^{-/-}$ mice showed impaired adaptive immune response mediated by Th1, Th2, Th9, Th17, and Tfh cells (Table 1). $CD4^+$ T cells expressing IFN-γ and IL-4 were decreased in *Irf4*$^{-/-}$ mice infected with *L. monocytogenes* and *L. major*, respectively (54, 74). *Irf4*$^{-/-}$ mice also exhibited ablated Tfh formation in lymph nodes during *L. major* infection and developed resistance to Th17-mediated pathogenicity during EAE induction (54, 69, 70). Although Foxp3 can be normally induced in IRF4-deficient $CD4^+$ T cells (69), these cells cannot express effector molecules such as CTLA-4 to suppress excessive immune activation in peripheral tissues. Severe autoimmune syndrome and high levels of serum IgG, and IgE were observed in mice with *Irf4* deletion in Treg cells (72, 73, 82).

AP-1 proteins were first identified as a heterodimer formed by Jun and Fos proteins, which promotes growth and oncogenic transformation of mammalian cells (83). Since then, many AP-1 proteins belonging to different subfamilies have been identified: Jun (Jun, JunB, and JunD), BATF (BATF, BATF-2, BATF-3), Fos (Fos, Fos-B, Fra1, and Fra2), Maf (c-Maf, Maf-B/G/A/F/K, and Nrl), ATF and JDP subfamilies. All AP-1 proteins contain a basic leucine zipper (bZIP) domain, and interaction between bZIP domains allows two AP-1 proteins to form homodimers or heterodimers (84). DNA elements bound by AP-1 proteins include 12-O-tetradecanoylphorbol-12-acetate (TPA) response elements (TRE: TGA(C/G)TCA) and cAMP response elements (CRE: TGACGTCA). In addition to forming heterodimers with other AP-1 proteins, many AP-1 proteins have a C-terminal transactivation domain that enables them to interact with non-AP-1 family proteins (85).

So far, the most well documented AP-1 protein in regulating differentiation of $CD4^+$ T cells is BATF (76, 86). Structural analysis of BATF proteins reveals the lack of a transactivation domain (TAD) (84). Without TAD, BATF cannot activate transcription through recruiting RNA polymerase like many other AP-1 family transcription factors. Studies suggest that specific BATF transcriptional activity comes from its interaction with other transcription factors. For example, mutations in the BATF leucine zipper domain, which is required for interacting with other proteins such as IRF4, impaired Th17 differentiation (87). BATF also interacts with chromatin remodeling proteins such as Ets, and CTCF (87, 88). In Th17 cell, BATF works together with chromosome-restructuring proteins such as Ets1 and CTCF to promote chromatin accessibilities and

the formation of three-dimensional chromatin loops in a genome-wide scale including gene loci for *Il17a*, *Il17f* and *Il21*. The BATF-dependent chromatin opening exposes the promoter regions of genes for $CD4^+$ T cells differentiation to STAT3. (88).

Another feature of the BATF is the strong tendency of forming heterodimer with other AP-1 family proteins such as Jun family proteins (84). Although all Jun family proteins are able to form heterodimer with BATF, experimental evidence from electrophoretic mobility shifting assay (EMSA) and chromatin immunoprecipitation with PCR (ChIP-PCR) have demonstrated that BATF-JunB complex is the dominant heterodimer in Th2 and Th17 cells, suggesting that JunB is the major partner of BATF during CD4 T cell differentiation (89, 90).

BATF regulates Th2, Th9, Th17, Tfh and eTreg differentiation (Fig. 4) (72, 89–92). $CD4^+$ T cells isolated from *Batf*$^{-/-}$ mice can develop into Th1, but not Th2, Th17 and Tfh cells under *in vitro* polarizing conditions (89–91, 93). Consistent with those findings, $CD4^+$ T cells expressing IFN-γ are not altered but IL-4-expressing $CD4^+$ T cells largely decrease in *Batf*$^{-/-}$ mice infected with *N. brasiliensis* (90). *Batf*$^{-/-}$ mice are also resistant to asthma induction and have impaired generation of IL-9 production *in vivo* (94). EAE induction and the generation of IL-17-producing $CD4^+$ T cells are severely inhibited in *Batf*$^{-/-}$ mice (89). Tfh-mediated immune response, such as germinal center formation in draining lymph nodes and class switch of B cells, are completely diminished in *Batf*$^{-/-}$ mice during *in vivo* immunization (91, 95). Foxp3 can be induced in BATF-deficient $CD4^+$ T cells, but the proportion of total Treg cells in spleen are mildly reduced in *Batf*$^{-/-}$ mice (72, 89). However, in *Batf*$^{-/-}$ mice, the formation and development of eTreg are totally impaired in peripheral tissues such as visceral adipose (Table 1) (72). In mechanism, BATF promotes glyceride metabolism and increases the fitness of eTreg cells, which enables eTreg cells inhibits the production of IgE during allergic inflammation (96). Moreover, a mutation in Foxp3, which decreases expression of BATF in Treg cells, diminishes the generation of eTreg in peripheral tissues and causes unharnessed activation of Th1, Th2 and Th17 cells (97).

JunB is a major heterodimeric partner for BATF in antigen-primed naïve $CD4^+$ T cells (78, 79, 98). We and others have reported that JunB is required for generation of pathogenic Th17 cells that cause autoimmunity, but not for gut-resident homeostatic Th17 cells (99–101). JunB also controls effector Treg homeostasis and immune suppressive functions (102–104). Furthermore, JunB reportedly promotes expression of cytokines specific to Th2 and Th9 cells (98, 105). Thus, JunB likely contributes to differentiation and function of various $CD4^+$ effector T subsets. However, *in vivo* roles and transcriptional targets for JunB in diverse T helper subsets are not fully understood.

Our previous experiments have demonstrated that under pathogenic Th17 culturing conditions in the presence of IL-6, IL-23, and IL-1β, the generation of Th-17

cells is impaired in JunB-deficient $CD4^+$ T cells. On the other hand, under non-pathogenic Th17 culturing conditions in the presence of TGF-β and IL-6, the differentiation of Th17 cells is moderately affected. Accordingly, mice with *Junb* deletion in $CD4^+$ T cells are resistant to EAE and colitis induction, both of which are mediated by pathogenic Th17 cells. However, the generation of gut-resident homeostatic Th17 cells are not affected in *Junb*-deficient mice (Table 1) (100)(101). As with BATF and IRF4, JunB is required for eTreg but not for total Treg. Foxp3 can be induced in JunB-deficient $CD4^+$ T cells, but the frequency of total Treg cells is not affected in T cell-specific *Junb*-deficient mice (Table1) (104). However, JunB-deficient Treg cells lose its ability to inhibit cytokine production from Th1, Th2 and Th17 *in vitro* (102).

The role of JunB in Th1 differentiation remains unclear and even controversial. Two independent studies have demonstrated inconsistent results that expression of IFN-γ was either not altered or upregulated in JunB-deficient Th1 cells. Mice with different genetic backgrounds in these studies may account for this inconsistency. Whether JunB deletion affects *in vivo* Th1-mediated response has not been studied (99, 101).

A previous study has demonstrated the requirement of JunB in production of Th2 effector cytokine such as IL-4 and promoting airway inflammation (105). However, mice used in this study are a systematic knockdown strain, not the commonly-used conditional knockout mice strains (Table1) (105). Thus, the artificial effects of this systematic knockdown technique on Th2 effector cytokines production could not be verified. Moreover, this study could not exclude the possibility that the attenuated airway inflammation could be due to reduced JunB expressions in innate immune cells but not in $CD4^+$ T cells.

In summary, compared to the well documented roles of BATF and IRF4 in lineage specification, the functions of JunB in Th1 and Th2 differentiation and corresponding *in vivo* immune responses are less understood.

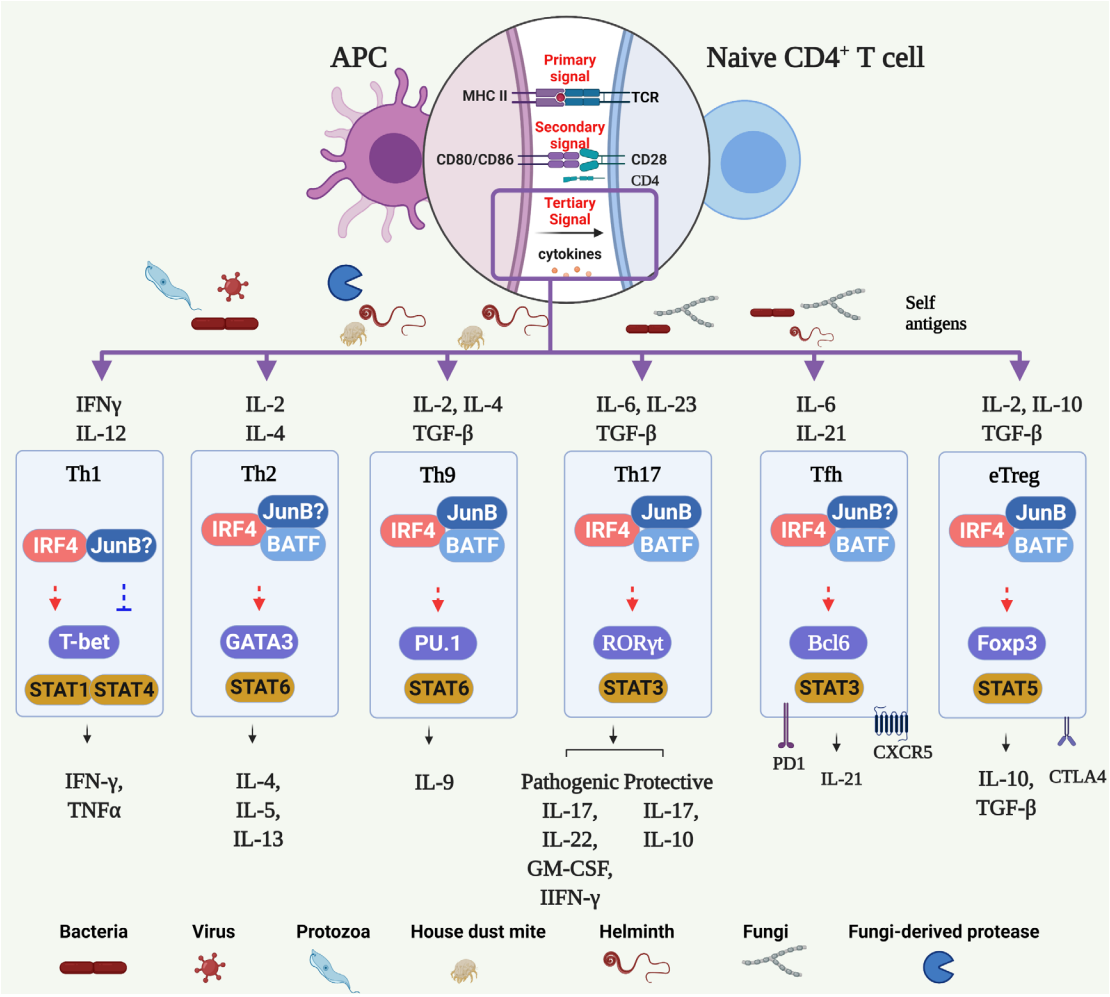

Fig. 4. Transcriptional regulation in lineage specification

Antigens derived from different sources activate antigen presenting cells (APC) to secrete various cytokines, creating specific cytokine milieu and direct the lineage specification of $CD4^+$ effector T cells. Depending on cytokines, distinct signaling transducer and activator of transcription (STAT) family proteins are activated, which subsequently induce the expression of lineage specifying transcription factors. In addition, IRF4, BATF and JunB, which are induced by TCR and costimulatory signals, work together with STAT proteins and lineage specifying transcription factors to induce expression of lineage-specific effector molecules in each T helper cell subset. Compared to IRF4 and BATF, the roles of JunB in lineage specification of Th1, Th2 and Tfh cells remain unclear or controversial. TGF-β: transforming growth factor β; IFN-γ: interferon gamma; CTLA-4: cytotoxic T lymphocyte-associated protein 4; CXCR5: C-X-C motif chemokine receptor 5; T-bet: T-box expressed in T cells; GATA3: GATA-binding protein 3; RORγt: RAR-related orphan receptor gamma.

Table 1. A summary of impaired adaptive immunity in mice deficient with IRF4, BATF and JunB

Protein	Phenotypes related to each T helper cell subset	References
IRF4	**Th1:** Impaired expression of IFN-γ and TNF-α in $CD4^+$ T cells during bacterial infection (*L. monocytogenes*) [a]. **Th2:** Impaired expression of IL-4 in $CD4^+$ T cells and susceptible to helminth infection (*L. major*) [a]. **Th9:** Impaired expression of IL-9 in $CD4^+$ T cells and increased resistance to asthma induction [a]. **Th17:** Impaired expression of IL-17 in $CD4^+$ T cells and increased resistance to EAE induction [a]. **Tfh:** Deficiency in generating germinal center in draining lymph nodes during helminth infection (*L. major*) [a]. **eTreg:** Impaired generation of eTreg, abnormally increased serum antibodies, and developed in autoimmune disease [d].	(54, 69–72, 74, 75, 80, 81)
BATF	**Th1:** Unaltered expression of IFN-γ in $CD4^+$ T cells during bacterial helminth infection (*L. major*) [a]. **Th2:** Impaired expression of IL-4 in $CD4^+$ T cells and higher susceptibility to helminth infection (*N. brasiliensis*) [b]. **Th9:** Impaired expression of IL-9 in $CD4^+$ T cells and increased resistance to airway inflammation [b]. **Th17:** Impaired expression of IL-17 in $CD4^+$ T cells and increased resistance to EAE induction [b]. **Tfh:** Deficiency in $CD4^+$ T cell-dependent class switch and deficiency in generating germinal center in draining lymph nodes during *in vivo* immunization [b]. **eTreg:** Impaired generation of eTreg, abnormally increased serum antibodies, and developed in autoimmune disease [b].	(72, 90, 91, 94, 96, 106, 107)
JunB	**Th1:** No report. **Th2:** Impaired expression of IL-4 in $CD4^+$ T cells and increased resistance to airway allergy induction [f]. **Th9:** Decreased expression of IL-9 in $CD4^+$ T cells [g]. **Th17:** Impaired expression of IL-4 in $CD4^+$ T cells and increased resistance to EAE induction. No influence of gut-resident $CD4^+$ T cells expressing IL-17 [h, i]. **Tfh:** No report. **eTreg:** Impaired generation of eTreg, abnormally increased serum antibodies, and developed in autoimmune disease [h].	(98–103, 105)

a. *Irf4*$^{-/-}$ mice (54, 69–71, 74).
b. *Batf*$^{-/-}$ mice (89–91).
c. *Batf*$^{\Delta Z/\Delta Z}$ mice (94).
d. *Foxp3*^{cre}*Irf4*$^{fl/fl}$ mice (72).
e. *Foxp3*^{cre}*Batf*$^{fl/fl}$ mice (72).
f. Ubi-JunB / *Junb*$^{-/-}$ mice, a transgenic *Junb*$^{-/-}$ mice strain expressing JunB under the control of human ubiquitin C promoter, which causes a systematic JunB knockdown in mice (105).
g. siRNA targeting *Junb* in mouse CD4^{+} T cells (98).
h. *Cd4*^{cre}*Junb*$^{fl/fl}$ mice (100, 101).
i. *Meox2*^{cre}*Junb*$^{fl/fl}$ mice (99).
j. *Foxp3*^{cre}*Junb*$^{fl/fl}$ mice (102).

Transcriptional regulation in metabolic reprogramming

Cells utilize several metabolic pathways to obtain bioenergy and metabolites for building blocks. When cells are in the resting state, glycolysis, β-oxidation, and glutaminolysis pathways converge to Tricarboxylic Acid (TCA) cycles, in which a series of redox reactions occur to transfer electrons from metabolites to electron acceptors such as Nicotinamide Adenine Dinucleotide (NAD^+). The electron transfer process couples with the transfer of protons in the inner membrane space of mitochondria, generating the gradient of protons across mitochondrial membranes and driving the synthesis of Adenosine Triphosphate (ATP) – the major source of bioenergy (Fig. 5). Because the terminal acceptor of this electron transfer process is oxygen, the process of obtaining energy in mitochondria is also called oxidative phosphorylation (OXPHOS). In contrast, the energy generation from glycolysis in cytoplasm does not require oxygen and is sometimes called anaerobic respiration (108).

Although OXPHOS is an efficient pathway for cells to obtain energy, it requires a longer time than glycolysis. Hence, to meet the high demands for bioenergy in activated T cells, cellular metabolism is usually shifted from OXPHOS to glycolysis (Fig. 4) (109, 110). In fact, recent studies also suggested that this metabolic reprogramming to glycolysis is used for immediate supply of energy and building materials. For examples, Th17 cells obtain acetyl-CoA as precursors for fatty acid synthesis through glycolysis during its rapid differentiation and proliferation (Fig. 5) (111).

Transcriptional regulation underlying the metabolic reprogramming in activated T cells is controlled by Hypoxia-Inducible Factor 1 (HIF1) (Fig. 5). In the resting state, oxygen molecules are sufficient and easily diffuse across cell membrane. Inside the cell, oxygen molecules bind to prolyl-4-hydroxylase (PHD) protein, which further hydroxylate HIF1α and results in its degradation. During infection, however, tissues are under hypoxia conditions, allowing HIF1α becomes stabilized and dimerizes with HIF1β to form HIF-1. HIF-1 can translocate into nucleus and act as a transcription factor that upregulates many genes required for glycolysis (112).

The expression of HIF1α and metabolic reprogramming in $CD8^+$ T cells is controlled by IRF4 (Fig. 4B). Deletion of IRF4 in $CD8^+$ effector T cells decreased expression of HIF1α and glycolysis activities but increased OXPHOS activities, suggesting that IRF4 is essential for metabolic reprogramming toward glycolysis. IRF4 upregulates expression of genes for glycolysis such as glucose transporter GLUT4 and glycolytic enzymes Hexokinase 2 (HK2) in CD8 effector T cells (68). Similarly, IRF4 plays essential roles in maintaining Th1 effector function through upregulating expression of Hk2 and Glucose Transporter 3 (GLUT3) but not HIF1α. Accordingly, glycolysis is completely diminished in IRF4-deficient Th1 cells, and IRF4-deficient mice exhibit impaired expression of Th1 signature cytokines such as IFN-γ and TNF-α

in CD4 T cells during *L. monocytogenes* infection. Although IRF4-deficient Th1 cells also showed impaired OXPHOS activities, the mechanism of IRF4 -dependent regulation of OXPHOS is still unclear (74).

Similar to IRF4, BATF promotes both glycolysis and OXPHOS activities in $CD8^+$ effector T cells through directly upregulating the expression of HK2 and HIF1α (Fig. 5B) (106, 113). Moreover, BATF also increases cellular NAD^+ through inhibiting expression of NAD^+-dependent deacetylase Sirt1 (106). The increased NAD^+ could serve as electron acceptors and boost both glycolysis and OXPHOS activities during T cell activation (106).

Critical roles of IRF4 and BATF in regulation of metabolic activities during T cell activation suggest the involvement of JunB in this regulation; however, whether JunB deletion affects glycolysis and OXPHOS activities in diverse T helper cell subsets remain to be determined

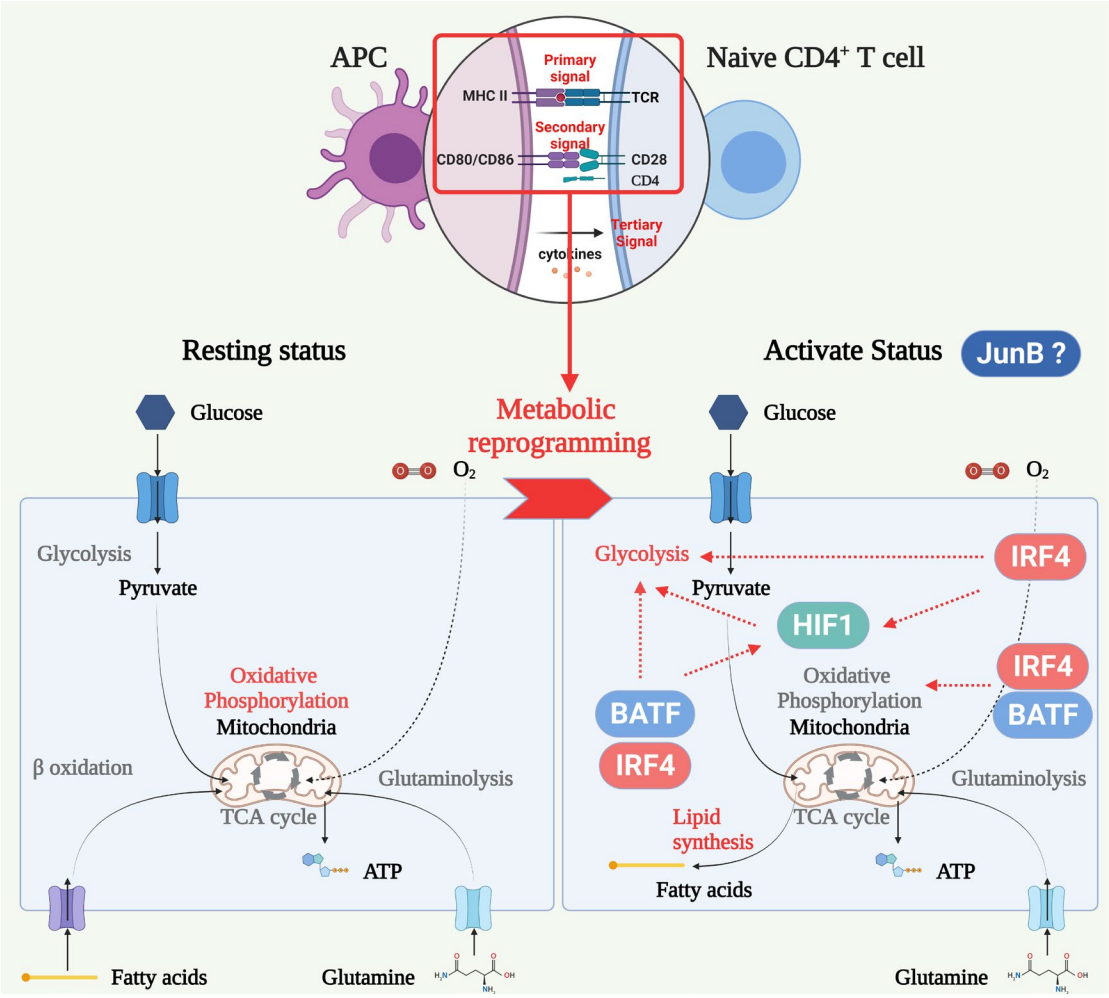

Fig. 5. The transcriptional regulation in metabolic reprogramming during CD4+ T cell differentiation.

During differentiation, $CD4^+$ T cells need to proliferate and produce effector molecules within a short time window. To meet the high demands of bioenergy and building molecules, the metabolic activities in activated $CD4^+$ T cells shift from oxidative phosphorylation to glycolysis. This metabolic reprogramming process is transcriptionally regulated by Hypoxia Inducible Factor 1 (HIF1) as well as by IRF4 and BATF. Compared to IRF4 and BATF, whether JunB regulates metabolic activities during T cell activation has not been reported yet. Pathways activated in each stage are highlighted as red. The gene encoding HIF1α subunit of HIF1 protein is transcriptionally regulated by IRF4 and BATF and is shown as red dashed lines. Genes involved in each pathway and transcriptionally regulated by indicated transcription factors are also shown as red dash lines. APC: antigen presenting cells; CD: Cluster of Differentiation; TCA cycle: Tricarboxylic cycle; ATP: Adenosine Triphosphate.

Transcription regulation in apoptosis

In response to antigen signal a single naïve $CD4^+$ T cell can proliferate and generate thousands of effector CD4 T cells to elicit immune response (114). The frequency of effector $CD4^+$ T cells should be under extensive regulation during immune responses to minimize the damages to tissues, especially when antigens are removed. In vertebrates, hosts have evolved a mechanism called Activation-Induced Cell Death (AICD) by which most of activated T cells undergo apoptosis after antigen clearance (115).

Two apoptosis pathways are activated in AICD – extrinsic and intrinsic pathways, which are mediated by FS-7-Associated Surface antigens (Fas) and proapoptotic molecules Bcl-2-interacting mediator of cell death (Bim), respectively (Fig. 6). The extrinsic pathway is initiated by the interaction between Fas and its ligand FasL on surface of activated T cells, which recruits the adaptor FAS-associated death domain protein (FADD) and procaspase 8. Cleavage of procaspase 8 generates active caspase 8 which triggers a downstream caspase cascade that involves caspase 3 (Fig.6) (116). On the other hand, intrinsic signals activated by various stimuli such as oxidative stress, calcium flux, and IL-2 deprivation stabilize Bim proteins or trigger the degradation of B Cell Lymphoma 2 (Bcl2) – a protein that can bind with Bim and neutralize its proapoptotic activities (117). Bim then induces oligomerization of Bak/Bax proteins and pore formation on the outer membrane of mitochondria, causing release of cytochrome c into cytoplasm. Cytochrome c subsequently activates the cleavage of procaspase 9 which converge into a downstream caspase 3 cascade (118).

Apoptosis pathways are transcriptionally regulated by IRF4 and BATF. Both IRF4 and BATF inhibit transcription of *Fasl*, *Bcl2l11* (encoding Bim) and *Casp3* (encoding Caspase 3) (68, 79, 113, 119). Deletion of either IRF4 or BATF increase apoptotic cell population in CD8 effector T cells (68, 113). Moreover, overexpression of BATF in both $CD4^+$ and $CD8^+$ T cells inhibit apoptosis and induce lymphoproliferative disorders in mice (120). Taking these together, expression of IRF4 and BATF in activated T cells is required for repressing expression of apoptosis initiators to control apoptosis before antigen clearance.

The cytoplasmic abundance of Bim is not only regulated by IRF4 and BATF, but also by Forkhead box O3 (Foxo3). In healthy cells, growth factors such as cytokines stimulate Akt to phosphorylate Foxo3 and to inhibit its activity. Once IL-2 are deprived, Foxo3 is activated and promotes the transcription of *Bcl2l11* (121, 122). Deprivation of cytokines also prevents Erk1/2-mediated phosphorylation of Bim on its serine 69 residue, which promotes ubiquitylation and degradation of Bim through proteosome pathway (118, 123).

However, little is known about whether JunB is involved in regulating apoptosis in activated $CD4^+$ T cells. Our lab has demonstrated that JunB deletion in Treg cells increased the accumulation of apoptotic effector Treg in peripheral tissues (102). Hence, it is possible that JunB may promote cell survival in $CD4^+$ T cells during TCR stimulation across diverse T helper cell subsets. Whether JunB, like BATF and IRF4, could directly bind and inhibit transcription of apoptosis initiators such as FasL and Bim, remains unknown.

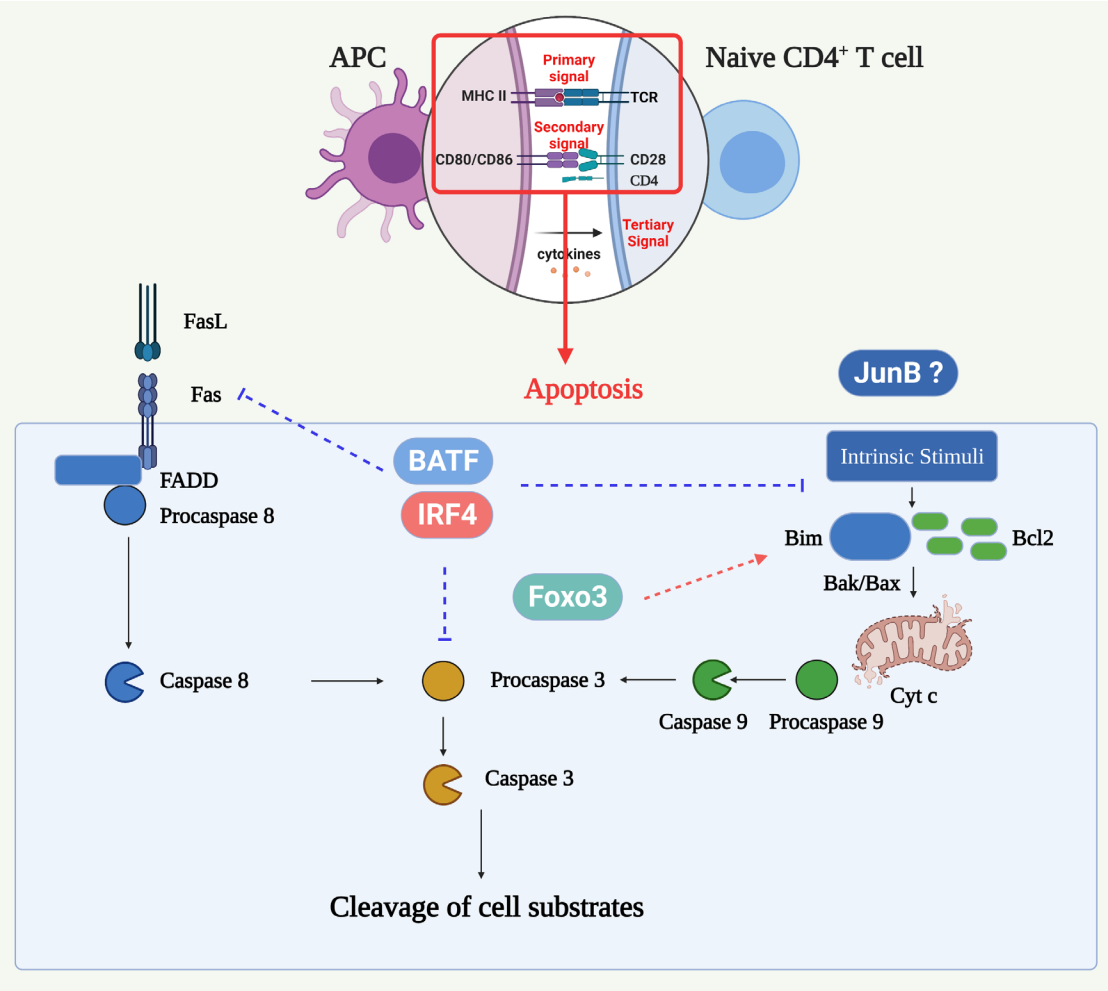

Fig. 6. The transcriptional regulation of apoptosis during CD4+ T cell differentiation.

Extrinsic and intrinsic apoptosis pathways are induced to ensure most of activated $CD4^+$ T cells undergo cell death after antigen clearance. The extrinsic pathway is induced by interaction of FS-7-Associated Surface antigens (Fas) and its ligand FasL. Fas then recruits the adaptor FAS-associated death domain protein (FADD) and induces the cleavage of procaspase 8. The intrinsic pathway is triggered by intrinsic stimuli such as oxidative stress or IL-2 deprivation, which subsequently either facilitate the degradation of B Cell Lymphoma 2 (Bcl-2) or stabilize proapoptotic molecules Bcl-2-interacting mediator of cell death (Bim). Bim then induces oligomerization of Bak/Bax proteins and pore formation on the outer membrane of mitochondria, causing release of Cytochrome c (Cyt c). Both pathways converge into activation of caspase 3. Caspase 3 then induces cleavages of cellular substrates and apoptosis. These two pathways are transcriptionally regulated by IRF4, BATF and Forkhead box O3 (Foxo3). Whether JunB regulates apoptosis during T cell activation has not been reported yet. Apoptotic molecules positively and negatively regulated by indicated transcription factors are highlighted as red and blue lines, respectively.

Problem statement

IRF4 and BATF play critical roles in regulating a broad spectrum of biological functions together with STAT proteins and lineage specifying transcription factors. The major BATF partner, JunB, is critical for Th17 and eTreg differentiation and functions, but its role in other effector CD4 T subsets is not fully understood. The aim of this thesis is to reveal roles and function of JunB in Th1 andTh2 cells and to understand common and cell-type-specific JunB-dependent transcriptional program in effector CD4 T subsets.

Chapter 2: Method and materials

Mice.

Floxed *Junb* (*Junb*$^{fl/fl}$) mice have been described previously (100). *Cd4*^{cre} (stock# 017336), OT-II (stock# 004194), *Rag1*$^{-/-}$ (stock# 002216), and B6SJL (stock# 002014) mice were obtained from the Jackson Laboratory. All mice were maintained on a C57BL/6 background under specific pathogen-free conditions. Sex-matched, 6–12-week-old mice were used for experiments. All animal experimental protocols were approved by the Animal Care and Use Committee at Okinawa Institute of Science and Technology Graduate University.

Isolation of naïve CD4$^+$ T cells.

Murine naïve CD4$^+$ T cells were purified from pooled spleens by negative selection using MojoSort mouse naïve CD4$^+$ T cell selection kit (480039; Biolegend), in accordance with manufacturer's instructions. Flow cytometry analysis confirmed that the purity of CD4$^+$CD25$^-$CD62L^{hi}CD44^{lo} cells ranged from 90% to 95% (Fig. 7A).

Cell culture.

Murine naïve CD4$^+$ T cells were purified with MojoSort mouse naïve CD4$^+$ T cell selection kit as described in previous section. Purified naïve CD4$^+$ T cells were cultured in 24-well (4 x 10^5 cells per well), 48-well (2 x 10^5 cells per well) or 96-well (1 x 10^5 cells per well) plates coated with 5 μg/mL anti-CD3ε antibody (145-2C11; Biolegend) in IMDM medium (12440-061; Invitrogen) containing 1 μg/mL anti-CD28 antibody (37.51; Biolegend), 10% FBS, 1x streptomycin-penicillin (containing 100 U/ml penicillin and 100 mg/mL streptomycin, P4333; Sigma), and 55 mM β-mercaptoethanol (20985-023; Invitrogen). In addition, the following cytokines were added in each polarizing condition: 20 ng/mL IL-2 (570402; Biolegend), 1 μg/mL anti-IFN-γ (XMG1.2; Biolegend), and 1 μg/mL anti-IL-4 (11B11; Biolegend) for Th0; 20 ng/mL IL-2, 20 ng/mL IL-12 (577002; Biolegend), and 1 mg/mL anti-IL-4 for Th1; 20 ng/mL IL-2, 100 ng/mL IL-4 (574306; Biolegend), and 1 mg/mL anti-IFN-g for Th2; 20 ng/mL IL-6 (575706; Biolegend), and 3 ng/mL TGF-β1 (100-21C; PeproTech) for Th17. Polarized cells were harvested for further analysis at the indicated time points.

Adoptive transfer.

Naïve CD4$^+$ T cells isolated from *Junb*$^{fl/fl}$ OT-II or *Junb*$^{fl/fl}$*Cd4*^{cre} OT-II mice (CD45.2$^+$) were mixed with naïve CD4$^+$ T cells isolated from congenic OT-II mice

($CD45.1^+CD45.2^+$) at a ratio of 2:1. Cells (3 x 10^6 cells per mouse) were intravenously injected into congenic recipient B6SJL mice ($CD45.1^+$).

Immunization.

One day after adoptive transfer, mice were anesthetized with isoflurane and immunized with 20 mg of OVA peptide 323-339 (ISQAVHAAHAEINEAGR, GL Biochem) emulsified in 100 mL complete Freund's adjuvant (CFA) or mixed with 10 mg of lipopolysaccharides (LPS) from *Escherichia coli* O111 (L4391; Sigma;) or 40 mg papain (P5306; Sigma). CFA was prepared from 100 mL incomplete Freund's adjuvant (263910; BD) and 1 mg desiccated *Mycobacterium tuberculosis* H37 Ra (231141; BD) according to the manufacturer's instructions and emulsified with OVA peptide using an ultrasonic homogenizer (VP-050; TAITEC) on ice for 30-45 min. LPS and papain were dissolved in PBS and mixed with OVA peptide at room temperature before immunization. For immunization with CFA or LPS, mice were injected subcutaneously on each side close to the base of tail. For immunization with papain, mice were injected intranasally with 40 ug papain each time for two consecutive days. Analysis was conducted at indicated number of days post immunization (dpi).

Lymphopenia induced cell proliferation assay.

Naïve $CD4^+$ T cells isolated from $Junb^{fl/fl}$ or $Junb^{fl/fl}Cd4^{cre}$ mice ($CD45.2^+$) were mixed with naïve CD4 T cells isolated from congenic mice ($CD45.1^+CD45.2^+$) at a ratio of 1:1. Cells (1 x 10^6 cells per mouse) were intraperitoneally injected into congenic recipient B6SJL mice ($CD45.1^+$). 14 days post transfer, single cell suspension from spleens and inguinal lymph nodes of $Rag1^{-/-}$ mice were made by mildly pushing spleens through 70 μm cell strainers (352350; BD) and suspended in PBS containing 0.5% of FBS.

Antibodies.

For flow cytometry analysis, the following antibodies were used with a 1:100 dilution: anti-CD3 (17A2; Biolegend), anti-CD4 (GK1.5; Biolegend), anti-CD25 (PC61; Biolegend), anti-CD44 (IM7; Biolegend), anti-CD62L (MEL-14; Biolegend), anti-CD45.1 (A20; Biolegend), anti-CD45.2 (104; Biolegend), anti-FasL (MFL3; Biolegend), anti-IL-17A (TC11-18H10.1; Biolegend), anti-IFN-γ (XMG1.2; Biolegend), anti-JunB (C-11; Santa Cruz Biotechnology), anti-GATA3 (16E10A23; Biolegend), anti-ROR-γt (Q31-378; BD), anti-T-bet (4B10; Biolegend), and anti-rabbit IgG (Poly4064; Biolegend). For ChIP analyses, anti-JunB (2 μg per ChIP, 210; Santa

Cruz), anti-BATF (2 μg per ChIP, WW8; Santa Cruz), and anti-IRF4 (2 μg per ChIP, M-17; Santa Cruz) were used.

Flow cytometry.

For analysis of cell surface molecules, cells were stained with their antibodies and Zomibe-NIR (1:400, 423106; Biolegend) in PBS containing 2% FBS for 30 min on ice. For analysis of intracellular molecules, cells were stained with a Foxp3 Staining Buffer Set (00-5253-00; eBioscience) according to the manufacturer's protocol. For analysis of intracellular cytokines, cells were re-stimulated with 100 ng/mL phorbol 12-myristate 13-acetate (P8139; Sigma) and 1 mg/mL ionomycin (I0634; Sigma) in the presence of 10 μg/mL brefeldin A (420601; Biolegend) for 4 h, and then stained with a Foxp3 Staining Buffer Set. For analysis of cells isolated from spleens and lymph nodes (Fig. 16-19), cells were incubated with anti-CD16/CD32 (1:100, 93; Biolegend) before antibody staining. The gating strategy for flow cytometry analysis and fluorescence minus one (FMO) control data are described in Fig. 7 and Fig. 8.

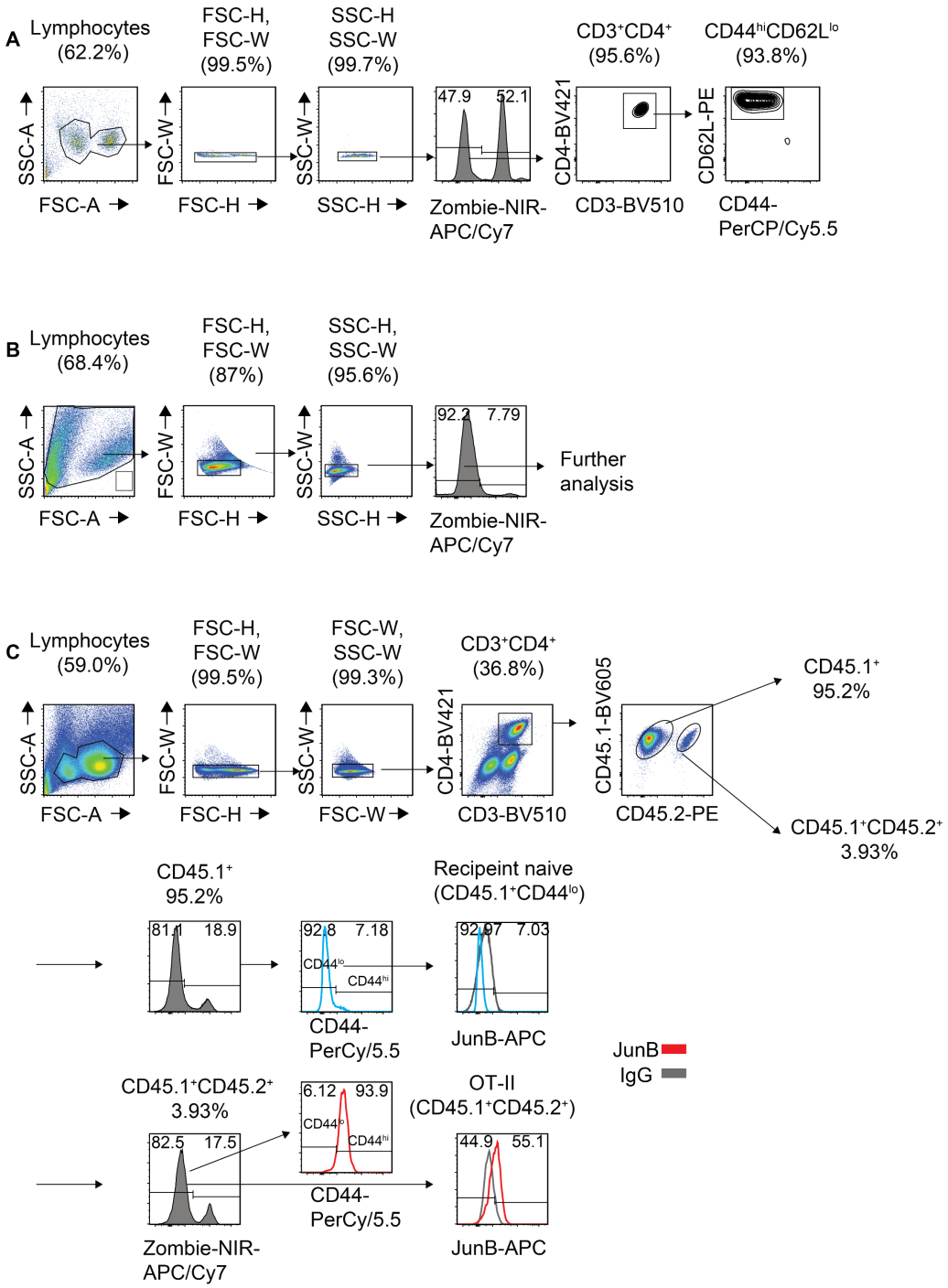

Fig. 7. Purity of naïve CD4+ T cells and gating strategies for flow cytometry analysis of CD4+ T cells cultured under in vitro polarizing conditions.

(A) Flow cytometry purity analysis of murine naïve $CD4^+$ T ($CD4^+CD25^-CD62L^{hi}CD44^{lo}$) cells. **(B)** Gating strategies for all *in vitro* polarizing cultures (related to Fig. 12 -14). **(C)** Gating strategies for flow cytometry analysis of transferred OT-II cells ($CD45.1^+45.2^+$) and recipient $CD4^+$ T cells ($CD45.1^+$). Flow cytometry analysis of the fluorescence minus one (FMO) control group for JunB in transferred OT-II cell is shown (related to Fig. 15, 17).

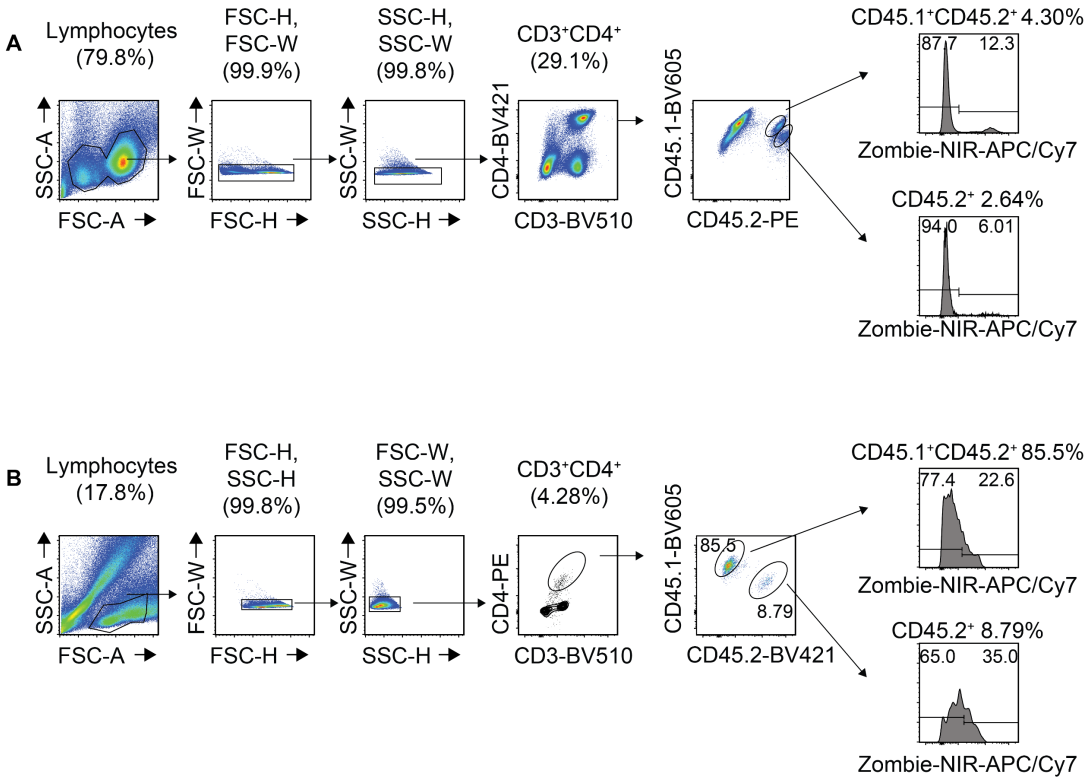

Fig. 8. Gating strategies for flow cytometry analysis

(**A**) Gating strategies for flow cytometry analysis of transferred control OT-II (*Junb*$^{fl/fl}$) or JunB-deficient OT-II (*Junb*$^{fl/fl}$*Cd4*^{cre}) (45.2$^+$) and co-transferred congenic OT-II CD4$^+$ T cells (CD45.1$^+$45.2$^+$) (related to Fig. 16). (**B**) Gating strategies for flow cytometry analysis of CD4$^+$ T cells of transferred control CD4$^+$ T cells (*Junb*$^{fl/fl}$) or *Junb*-deficient CD4$^+$ T cells (*Junb*$^{fl/fl}$*Cd4*^{cre}) (CD45.2$^+$) and co-transferred congenic CD4$^+$ T cells (CD45.1$^+$) from *Rag1*$^{-/-}$ mice (related to Fig. 18).

Preparation of ribonucleoprotein (RNP) complex.

The ribonucleoprotein (RNP) complex was prepared as described in detail previously (124). Guide RNA targeting *Junb* (gJunB) or negative control guide RNA (gNTC, 1072544) were purchased from Integrated DNA Technology. In short, guide RNA was first mixed with tracrRNA (1072535; Integrated DNA Technology) in equal molar concertation at room temperature for 10 min. RNA mix was then annealed by heating at 95°C for 5 min in a thermocycler (TP600; Takara) and slowly cooled to 25°C. For one nucleofection reaction, the RNP complex was prepared by mixing 150 nmol gRNA:tracRNA duplex with 60 nmol Cas9 protein (A36498; Invitrogen) at room temperature for 10 min right before nucleofection.

Table 2. List of guide RNA

gRNA ID	Sequence	Starting positions
gJunB	GACCCCGATAGGGATCCGCC	Chr8: 84978282

Nucleofection of naïve CD4$^+$ T cells.

Nucleofection of naïve CD4$^+$ T cells was performed with P4 primary cell nucleofector kit (V4XP-4024; Lonza) following the manufacturer's protocol (124). Up to 1 x 10^7 purified naïve CD4$^+$ T cells from C57BL/6 mice were washed with PBS, suspended with 20 mL P4 primary cell nucleofector solution and mixed with 5 mL of RNP complex at room temperature for 2 min in a round-bottom 96-well plate. The cell/RNP mix was transferred to nucleofection cuvette strips, and CD4$^+$ T cells were electroporated using Lonza 4D Nucleofector X unit (program code: DS137). After nucleofection, 200 mL prewarmed RPMI was added to a cuvette to transfer cells into flat-bottom 96-well plates. 1 x 10^6 cells were then rested in RPMI containing 5 ng/mL IL-7 (577802; Biolegend), 10% FBS, 1 x streptomycin-penicillin, and 55 μM β-mercaptoethanol for 72 h before polarization.

Seahorse assay.

To determine the metabolic activities, Oxygen consumption rate (OCR) and extracellular acidification rate (ECAR) were measured by using mito stress (103015-100; Agilent Technologies) and glycolysis stress kits (103020-100; Agilent Technologies), respectively. These two assays first measured the basal level of metabolic activities and then measured the altered metabolic rates when cells were sequentially treated with various reagents (Fig. 10). Naïve CD4$^+$ T cells were cultured

under Th1-, Th2- and Th17-polarizing conditions for 48 h and transferred to the analysis plate (2 x 10^5 cells per well). The analysis plate was first coated with 50 mL of 2% gelatin (G1890; Sigma) and pre-incubated at 37 ^oC for 1 h. To measure basal OCR, cells were incubated with XF base medium supplemented with 1 mM pyruvate (11360070; Gibco), 2 mM glutamine (A2916801; Gibco) and 10 mM glucose (A2494001; Gibco) for the first 20 minutes. Cells were then subsequently treated with 1.5 μM oligomycin, 1 μM fluorocarbonyl cyanide phenylhydrazone (FCCP) and 0.5 μM rotenone/antimycin A mix (103015-100; Agilent Technologies). To measure basal ECAR, cells were incubated with XF base medium supplemented with 2 mM glutamine for the first 20minutes. Cells were then treated with 10 mM glucose, 1 μM oligomycin, and 50 mM 2-deoxyglucose (2-DG) (103020-100; Agilent Technologies). The OCR and ECAR were analyzed using a Seahorse XFe96 analyzer (Seahorse Bioscience), according to the manufacturer's instructions.

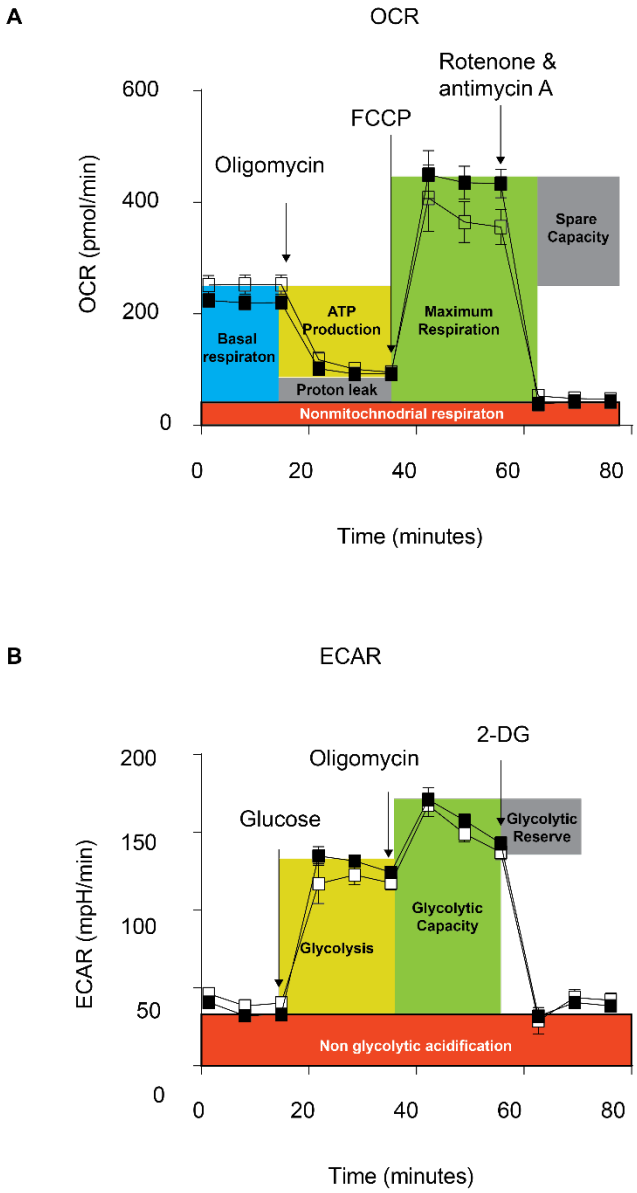

Fig. 9. Metabolic rates measured by seahorse assay.

Oxygen consumption rate (OCR) and Extracellular acidification rate (ECAR) were measured by seahorse in *in-vitro* differentiated T helper cells. (A) In OCR analysis, basal respiration is measured first, and respiration activities in each phase are measured from cells sequentially treated with oligomycin, fluorocarbonyl cyanide phenylhydrazone (FCCP), rotenone and antimycin A. (B) In ECAR analysis, basal glycolysis activity is fist measured from cells treated with glucose, and then glycolytic activities in each phase are measured from cells sequentially treated with oligomycin and 2-Deoxy-D-Glucose (2-DG).

Enzyme-Linked Immunosorbent Assay (ELISA)

Concentrations of IFN-γ and IL-13 in supernatant from *in-vitro* differentiated T helper cell culture were determined by ELISA using Mouse IFN-γ (430801; Biolegend) ELISA MAX Standard kit and Mouse IL-13 Uncoated ELISA kit (88-7137; Invitrogen), respectively, following manufacturers' instructions. Flat-bottom, 96-well plates (Greiner, 655061) were coated with anti-mouse IFN-γ (1:200, Biolegend) and anti-mouse IL-13 (1:250, Invitrogen) capture antibodies overnight at 4ºC. Plates were washed with 0.05% Tween20 (9005-64-5; Sigma) in PBS (PBST) and blocked with PBS containing 1% bovine serum albumin (BSA, 018-15154; Wako) for 1 h at room temperature. Samples were diluted with PBS containing 1% BSA (no dilution or 1:100 for IFN-γ and 1: 100 for IL-13) and incubated for 3 h at room temperature. Plates were then washed and incubated with the following biotin-conjugated antibodies for 1 h at room temperature: anti-mouse IFN-γ (1:200) and anti-mouse IL-13 (1:250). Plates were incubated with streptavidin conjugated with horse-radish peroxidase for 30 min at room temperature and incubated with TMB (T0440; Sigma) for another 15 min. The reaction was stopped by adding 50 µl of 2N sulfuric acid, and absorbance at 450 nm and 570 nm was read using ELISA plate reader (iMark; Bio-rad).

RT-qPCR.

Total RNA were isolated from cells using RNeasy Plus Mini Kit (74136; Qiagen). The amounts of RNA was determined by spectrophotometer (Nanodrop 2000; Thermo) and 200 ng of RNA were subsequently used for cDNA synthesis with Revertra Ace qPCR Kit (FSQ-101; Toyobo). The resulting cDNA was used as a template for qPCR performed with Faststart SYBR master mix (4673484; Roche) and thermal cycler (Thermal Cycler Dice Real Time system III; Takara). Primers used for qPCR are listed below.

Table 3. Lists of RT-qPCR primers

Primer ID	Sequence	Length of amplicons (bp)
Junb_F	GACCTGCACAAGATGAACCACG	129
Junb_R	ACTGCTGAGGTTGGTGTAGACG	
Actb_F	CATTGCTGACAGGATGCAGAAGG	138
Actb_R	TGCTGGAAGGTGGACAGTGAGG	

RNA-Seq.

Naïve $CD4^+$ T cells were cultured under Th0-, Th1- and Th2-polarizing conditions for 48 h. Then, cells were stained with Zombie-NIR (1:400, 423105; Biolegend), and viable

cells were sorted with FACS. RNA samples were prepared using Trizol (Invitrogen) with a Qiagen RNAeasy kit (Qiagen). Before sequencing, *Junb* mRNA level was first confirmed by RT-qPCR, as described in previous section. Total RNA was provided to the OIST DNA sequencing section for library preparation and sequencing. cDNA libraries for RNA-Seq were prepared with an NEBNext Ultra II Directional RNA Library Prep Kit for Illumina (E7760L; New England BioLabs) and purified using Agencourt AMPure XP beads (A63880; Beckman Coulter) following the manufacturer's instructions. Adapter dimers in cDNA libraries were removed with a LabChip NGS 3K reagent kit (CLS960013; PerkinElmer) and confirmed using a TapeStation (Agilent). Purified cDNA libraries were quantified with droplet digital PCR (BioRad QX-200 system). Sequencing was performed on an Illumina NovaSeq 6000 to generate 150-nucleotide paired-end reads at a read depth of at least 20 million reads per sample.

Differential gene expression analysis.

Raw reads from RNA-Seq were first trimmed with Cutadapt 2.10 (125). Trimmed reads were then directly mapped to the UCSC mouse genome *mm10,* and transcripts were quantified with Salmon 1.3.0 using default settings. To provide gene annotation, a mouse genome index was used during transcript quantification with a k value of 31 (126). After transcript quantification, raw feature counts of each transcript were first normalized within and between samples to obtain TPM (Transcripts Per kilobase Million). Differential gene expression analysis was conducted with DeSeq2 (127). Three or four independent biological samples were used for the analysis. Genes that were differentially expressed in *Junb*-deficient vs control cells (log2 Fold change < -0.5 or > 0.5, p value < 0.05, base mean > 100) were selected for pathway analysis using Enrichr (128, 129).

ChIP-Seq.

ChIP-Seq samples were prepared using a SimpleChIP Plus Enzymatic Chromatin IP Kit (9005S; Cell Signaling) as previously described (100). Naïve $CD4^+$ T cells from $Junb^{fl/fl}$ (WT) mice were cultured under Th1-polarizing conditions. After 48 h, activated cells (0.5-1 x 10^6 per ChIP-seq) were cross-linked in culture medium containing 1% formaldehyde at room temperature for 10 min, and glycine solution was added to stop the reaction. Then fixed cells were lysed and nuclei were isolated and treated with micrococcal nuclease (0.00313 μL/mL) for 20 min at 37°C. The nuclease reaction was stopped by adding 0.05 M ethylenediaminetetraacetic acid (EDTA). Samples were then sonicated to disrupt nuclear membranes and centrifuged to collect supernatants containing chromatin. Chromatin solutions were incubated with 1 μg of antibodies

overnight at 4°C with rotation, and complexes of antibodies and chromatin were collected with Dynabeads Protein G (10004D; Invitrogen). Beads were washed with low-salt and high-salt solutions five times and three times, respectively, and incubated 5 min for each washing at 4°C. Chromatin was eluted, de-cross-linked following the manufacturer's instructions, purified by phenol/chloroform extraction, and used for ChIP-sequencing. To generate DNA sequencing libraries, DNA was blunt-ended and ligated with adaptors using a KAPA Hyper Prep Kit (KK8500; KAPA Biosystems). Adaptor-ligated DNA was then cleaned up with an Agencort AMPure XP (A63880; Beckman Coulter) at a 1.8 x DNA ratio, amplified by PCR, and purified using the AMPure XP at a 1.2 x DNA ratio. Library DNA was size-selected using a 2% agarose gel cassette of Blue Pippin (Sage Science) for a target size range 150-300 bp and quantified with droplet digital PCR (BioRad QX-200). Sequencing was performed on an Illumina HiSeq 4000 to generate 150-nucleotide single-end reads at a read depth of at least 20 million reads per sample.

ChIP-Seq peak calling, annotation, and visualization.

Raw reads of ChIP-Seq were obtained as described above (for Th1) or from GSE86535 (for Th17) and GSE121295 (for Treg) (100, 102). Raw reads from Th1, Th17 and Treg were trimmed using Cutadapt 2.10 (125). Trimmed reads were then mapped to mouse genome *mm10* by calling Bowtie2 2.3.4.3 in TopHat2 2.1.1 (126, 130). Peaks were called for each sample replicate using Homer 4.11 with default parameters (FDR < 0.001) and a combined peak dataset was obtained from the union of Th1, Th17, and Treg dataset. To annotate peaks, they were assigned to the nearest genes using the annotatePeaks function in Homer v4.11. To visualize peaks, in Homer v4.11, a mapped read tag directory was first created by calling the makeTagDirectory function and a bed graph file was generated based on this Tag directory (130). Overlapping ChIP-Seq peaks for JunB, BATF and IRF4 were identified using bedtools functions with the following parameters, f=0.5 and -r (131).

Motif scan.

JunB-binding motifs across the mouse genome were identified using the scanMotifGenomeWide.pl function in Homer v4.11 (mm10). The AP-1-binding motif, RATGASTCAT, was used for this motif scan. Genomic regions containing AP-1 motifs were assigned to their nearest genes using the annotatePeaks function in Homer v4.11 (130).

Prediction of direct and indirect JunB responsive genes with BETA analysis.

Using RNA-seq data, I first defined genes that were differentially expressed in *Junb*-deficient vs control cells (log2 Fold change < -0.5 or > 0.5, p value < 0.05, base mean > 100) as JunB responsive genes. Next, I associated JunB responsive genes with ChIP-seq peaks for JunB and overlapping ChIP-seq peaks for JunB, BATF, and IRF4, as well as AP-1 motifs. I calculated the regulatory potential (RP) of each gene with the following equation (132): $\text{RP score} = \sum_{i=1}^{k} e^{-(0.5+4\Delta i)}$, where k equals the number of all binding peaks/motif within ± 10 kbp of the gene (132). Δ is distance to transcription starting site (TSS) of the gene, normalized to 100 kb. For example, Δ = 0.1 means the ChIP-seq peak or AP-1 motif is within 10 kb from TSS of the gene. A higher RP score indicates a greater density of ChIP-Seq peaks or AP-1-binding motifs within 100 kb of the TSS of the nearest gene. I then calculated the BETA score with the following equation (133): BETA = (R_{gb} / n) * (R_{ge} / n), where Rgb = 1 for the gene with the largest regulatory potential, and the other is based on the increasing of P value. Similarity, R_{ge} = 1 for the gene with the largest absolute value of log2 Fold change, and the other is based on the increasing of P value. n stands for the number of differentially expressed genes. Genes with BETA scores greater than 0 are considered direct JunB responsive targets.

BETA activating and repressive function prediction of JunB responsive genes.

Activating/repressive function prediction to determine the activator or repressor role of JunB was performed with BETA software (133). Differential expression of genes in *Junb*-deficient $CD4^+$ T cells vs control cells was obtained from RNA-seq data. A consensus JunB ChIP-seq peak dataset was obtained from the union of JunB ChIP-seq data for Th1 cells and Th17 subsets (GSE86535), as described in previous section. Genes were first categorized as non-differential (NON), up- (UP) and down-regulated (DOWN), based on their expression profiles. For a given gene, the regulatory potential score was calculated with JunB ChIP-seq peaks felling within 10 kb upstream of TSS or within this gene body. A higher regulatory potential score represents a greater JunB ChIP-seq occupancy near this given gene. Genes are cumulated by the rank based on the regulatory potential score from low to high. The distributions of UP and DOWN genes were compared to the NON gene distribution. The significance of activating or repressive function, as represented by P values, were obtained by Kolmogorov-Smirnov test (134).

Differential motifs enrichment in direct JunB responsive genes

Motif scan of targets for known transcription factors around JunB ChIP-seq peaks (200 bp regions centered on JunB ChIP-seq peak summits) in genomic regions containing JunB responsive genes (10 kbp upstream of TSS or within the gene bodies of JunB responsive genes) was performed with BETA software (133). Genes were first categorized as non-differentially expressed (NON), up- (UP), and down-regulated (DOWN) genes, based on their expression profiles. To identify motifs differentially enriched in JunB ChIP-seq peaks near JunB responsive genes, the occurring frequency of a given motif found in ChIP-seq peaks near up- (UP) or down-regulated (DOWN) genes was obtained and compared to the occurring frequency of non-differentially expressed (NON) genes. The significance of a differentially enriched motif, represented by P value, was measured by the one-tailed t test (133).

Code availability.

All command lines and scripts used in this research are available on https://github.com/oistishikawa/ChIP_Seq
https://github.com/oistishikawa/RNA_Seq

Data availability.

RNA-Seq and ChIP-Seq data have been uploaded to the Gene Expression Omnibus with primary accession number GSE172490.

Statistical analysis.

Unpaired two-tailed Student's t tests were performed using Prism software (GraphPad). P values < 0.05 were considered statistically significant.

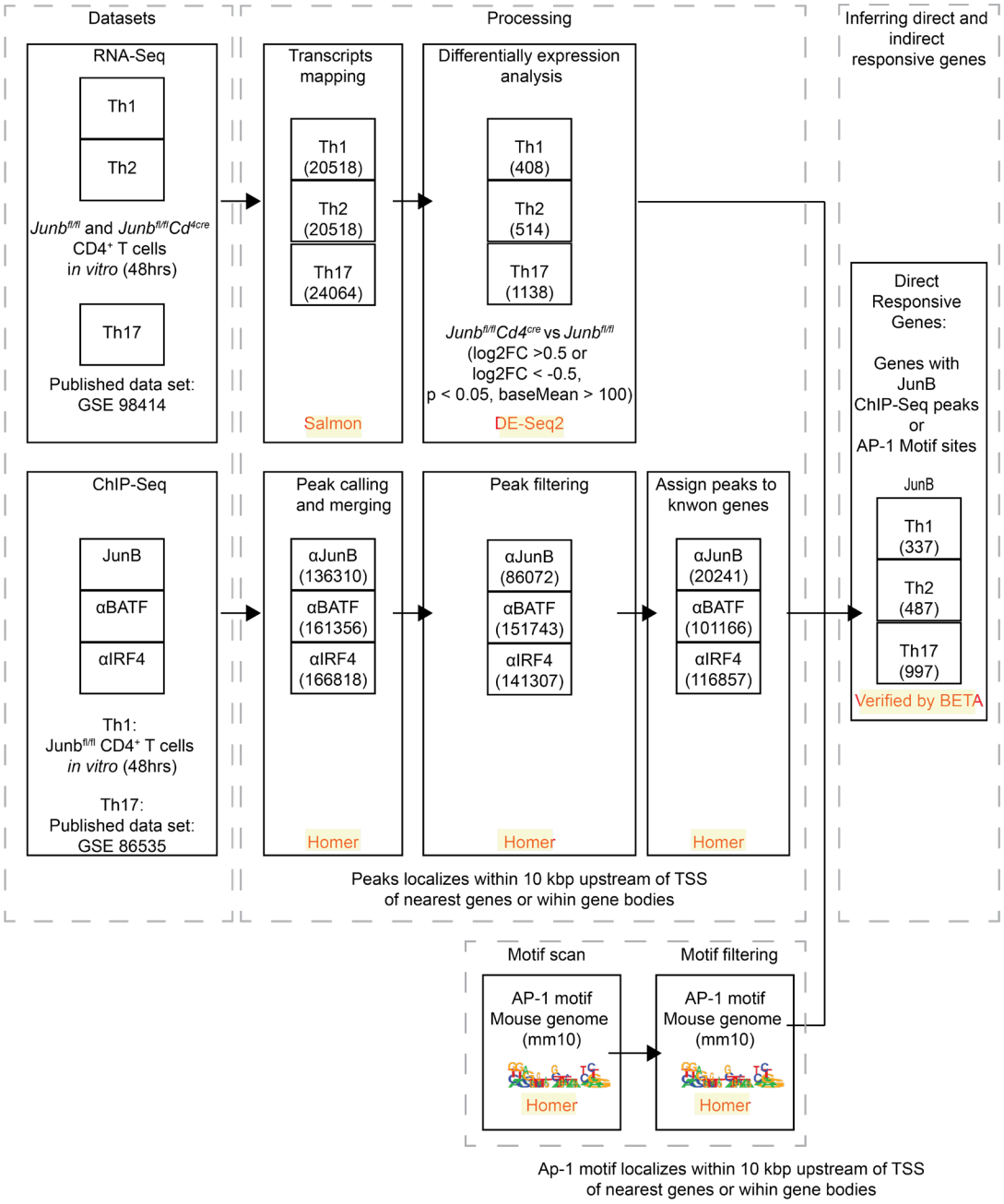

Fig. 10. Framework schematic for bioinformatics analysis and prediction of direct/indirect JunB target genes.

Bioinformatics software used in each process step were highlighted. Detailed parameters and command lines were explained in method and materials section. This framework schematic is related to Fig. 22.

Chapter 3: Result

Part I. JunB promotes cell survival in CD4+ effector T cells in vitro

We and others have demonstrated that JunB contributes to differentiation and functions of Th2, Th9, Th17 and effector Treg (eTreg) cell subsets (97–103,104). Whether JunB regulates common biological functions in diverse $CD4^+$ effector T cell subsets, however, is still unclear. Previous studies have shown that deletion of IRF4 and BATF upregulated expression of key apoptosis initiators such as Bim and Fas, suggesting that IRF4 and BATF may promote cell survival through regulating apoptosis in both $CD4^+$ and $CD8^+$ T cells (66, 68, 106, 113, 120, 135). As a major partner of BATF and IRF4, JunB may also possess similar biological functions in regulating T cell survival. Indeed, our recent study demonstrated that the percentage of apoptotic cells increased in *Junb*-deficient eTreg cells in peripheral tissues (102). Thus, JunB might promote cell survival when $CD4^+$ T cells are activated by TCR stimulation, regardless of cell subsets.

To test this hypothesis, I activated naïve $CD4^+$ T cells isolated from $Junb^{fl/fl}$ (control) or $Junb^{fl/fl}Cd4^{cre}$ (*Junb*-deficient) mice with anti-CD3 and anti-CD28 antibodies in the presence of cytokines that promote differentiation of Th0, Th1, Th2, or Th17 subsets. 96 h after activation, I observed that *Junb*-deficient $CD4^+$ T cells exhibited a significant decrease in the percentage and absolute number of living cells under Th1-, Th2- and Th17-polarizing conditions. As in Th0-polarizing conditions, most cells died, regardless of the presence or absence of JunB (Fig. 11A). To determine whether JunB affects apoptosis, I used two markers for apoptosis - Annexin V and Bim. Annexin V staining at 72 h after activation demonstrated an increase of apoptotic cells (Annexin V^+ Zombie-NIR^-) in *Junb*-deficient $CD4^+$ T cells under Th1-, Th2- and Th17-polarizing conditions (Fig. 11B). Furthermore, JunB deficiency upregulated Bim under all Th-polarizing conditions (Fig. 11C).

Previous studies have shown that Cre/loxP-mediated gene deletion may result in decreased cell viability and abnormal metabolic activity in mammalian cells (136, 137). To exclude the possibility that the impaired cell survival in *Junb*-deficient $CD4^+$ T cells may be caused by artificial effects of our Cre/loxP *Junb* knockout model, I evaluated the effects of JunB knockout in activated $CD4^+$ T cells with CRISPR/Cas9-mediated gene deletion methods (124). I electroporated naïve $CD4^+$ T cells isolated from wild-type mice (C57BL/6) with Cas9 proteins and guide RNAs targeting *Junb*. 72h later, I activated cells under Th1-, Th2- and Th17-polarizing conditions. Transduction of a guide RNA targeting *Junb* resulted in an increase of cells deficient for JunB expression under all differentiation conditions tested (Fig 12A). Cells exhibiting deficient JunB expression also showed significant decreases of cell survival (Fig 12B). These data indicate the requirement for JunB in promoting survival in TCR-stimulated $CD4^+$ T

cells was not caused by the artificial effects of Cre/loxP knockout model. These results indicate that JunB promotes cell survival probably by repressing expression of apoptosis initiator Bim across diverse T helper cell subsets *in vitro*.

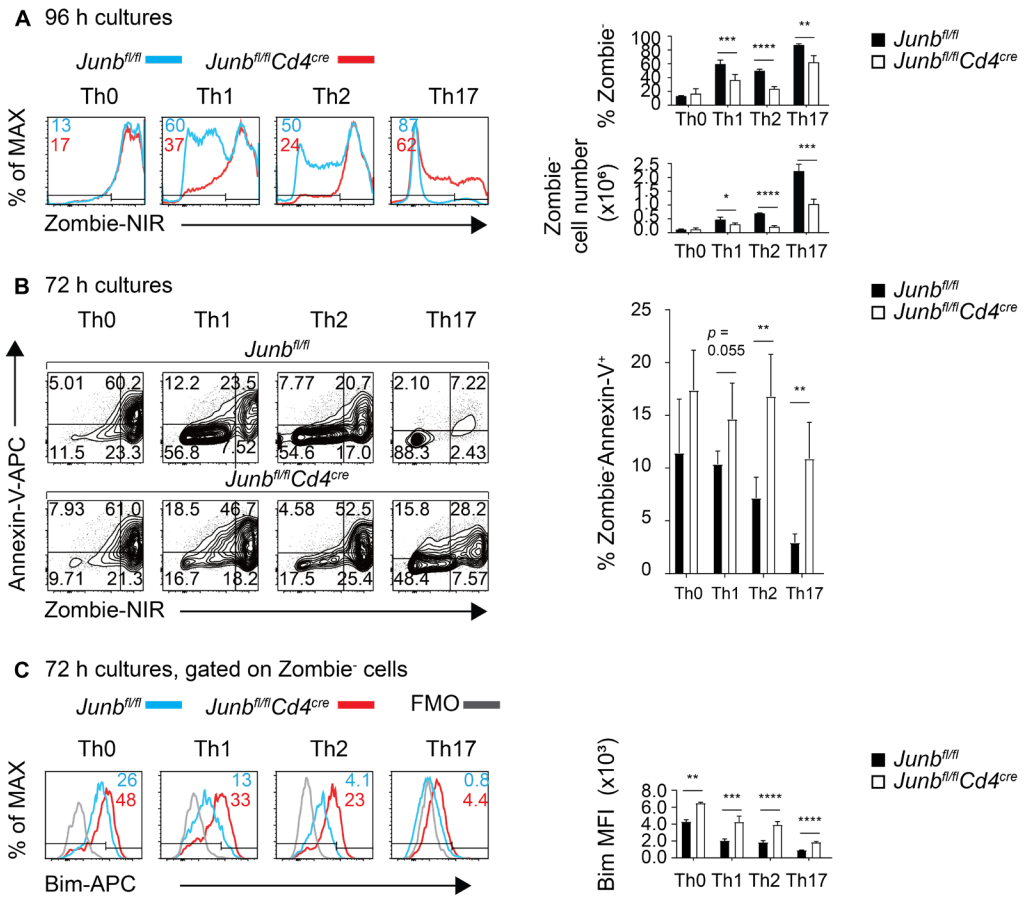

Fig. 11. JunB is required for survival of TCR-stimulated CD4$^+$ T cells.
Naïve CD4$^+$ T cells isolated from *Junb$^{fl/fl}$* or *Junb$^{fl/fl}$Cd4^{cre}* mice were cultured in differentiation conditions for Th0, Th1, Th2, and Th17 cells and were analyzed by flow cytometry at indicated time points. **(A)** Zombie-NIR staining of cells cultured for 96 h. Numbers in histograms (left) indicate average percentages of Zombie-NIR$^-$ cells. Bar graphs show percentages (top right) and absolute numbers (bottom right) of Zombie-NIR$^-$ cells. **(B)** Zombie-NIR and Annexin-V staining of cells cultured for 72 h. Counter plots (left) and the bar graph (right) indicating percentages of Zombie-NIR$^-$ Annexin-V$^+$ cells are shown. **(C)** Analysis of Bim expression in cells cultured for 72 h. Numbers in histograms (left) indicate average percentages of Bim$^+$ cells. Bar graphs (right) show median fluorescence intensity (MFI). (A-C) Error bars indicate s.d. (n = 4-6 wells per group). * $p < 0.05$, ** $p < 0.01$, *** $p < 0.001$, **** $p < 0.0001$, (unpaired two-tailed Student's test). Data represent two independent experiments.

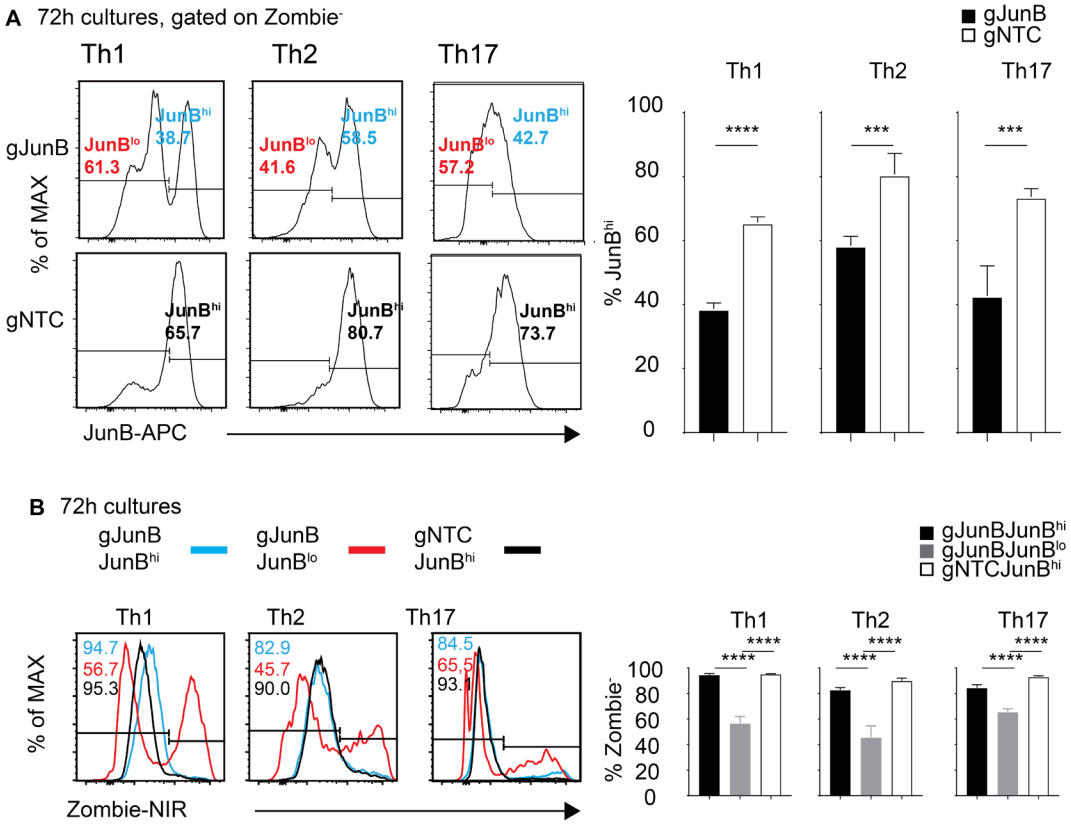

Fig. 12. CRISPR-mediated JunB knockout impaired survival of TCR-stimulated CD4$^+$ T cells.

Naïve CD4$^+$ T cells isolated from C57BL/6 mice were electroporated with Cas9 protein together with guide RNA targeting *Junb* (gJunB) or negative control guide RNA (gNTC). After nucleofection, cells were rested in RPMI containing IL-7 for 72 h and cultured under Th1-, Th2- and Th17-polarizing conditions. After resting, JunB and Zombie-NIR were analyzed by flow cytometry. (**A**) Flow cytometry analysis of JunB. Numbers in histogram plots indicate average percentages of cells exhibiting high or low JunB expression levels (JunB^{hi}, JunB^{lo}). (**B**) Flow cytometry analysis of Zombie-NIR. Error bars indicate s.d. (n = 4-6 wells per group). * $p < 0.05$, ** $p < 0.01$, *** $p < 0.001$, **** $p < 0.0001$, (unpaired two-tailed Student's test).

Part II. JunB regulates expression of a subset of lineage-specific genes *in vitro*

The role of JunB in Th1 and Th2 differentiation remains unclear and even controversial. Two independent studies reported that expression of IFN-γ was upregulated or unaltered in *Junb*-deficient Th1 cells (99, 101). Similarly, expression of IL-4 was reportedly downregulated or unaltered in *Junb*-deficient Th2 cells (99, 101).

To re-investigate the role of JunB in Th1 and Th2 differentiation, I activated naïve $CD4^+$ T cells isolated from control and *Junb*-deficient mice under Th1-, Th2-, and Th17-polarizing conditions and examined the expression of lineage-specifying transcription factors and signature cytokines by flow cytometry analysis. Consistent with previous studies, expression of T-bet and IFN-γ was significantly up-regulated in *Junb*-deficient cells under Th1- and Th17-polarizing conditions (Fig. 13A, B). On the other hand, the concentration of IFN-γ in culture medium from *Junb*-deficient cells was not altered in Th1-polarizing conditions, but it was increased in Th17-polarizing conditions (Fig. 13C). It is likely that the frequency of IFN-γ-expressing cells was increased, but the absolute number was not altered due to defective survival of JunB-deficient cells under Th1-polarizing conditions.

Under Th2-polarizing conditions, flow cytometry analysis showed that expression of Th2-lineage-specifying transcription factor, GATA3, was not affected, but expression of Th2 signature cytokines IL-4 and IL-13 was down-regulated in *Junb*-deficient Th2 cells (Fig. 13A, B). Furthermore, concentration of IL-13 was significantly lower in culture medium from *Junb*-deficient Th2 cells (Fig. 13C). Thus, JunB deletion in $CD4^+$ T cells upregulated and downregulated the expression of Th1- and Th2-lineage specific cytokine expression, respectively.

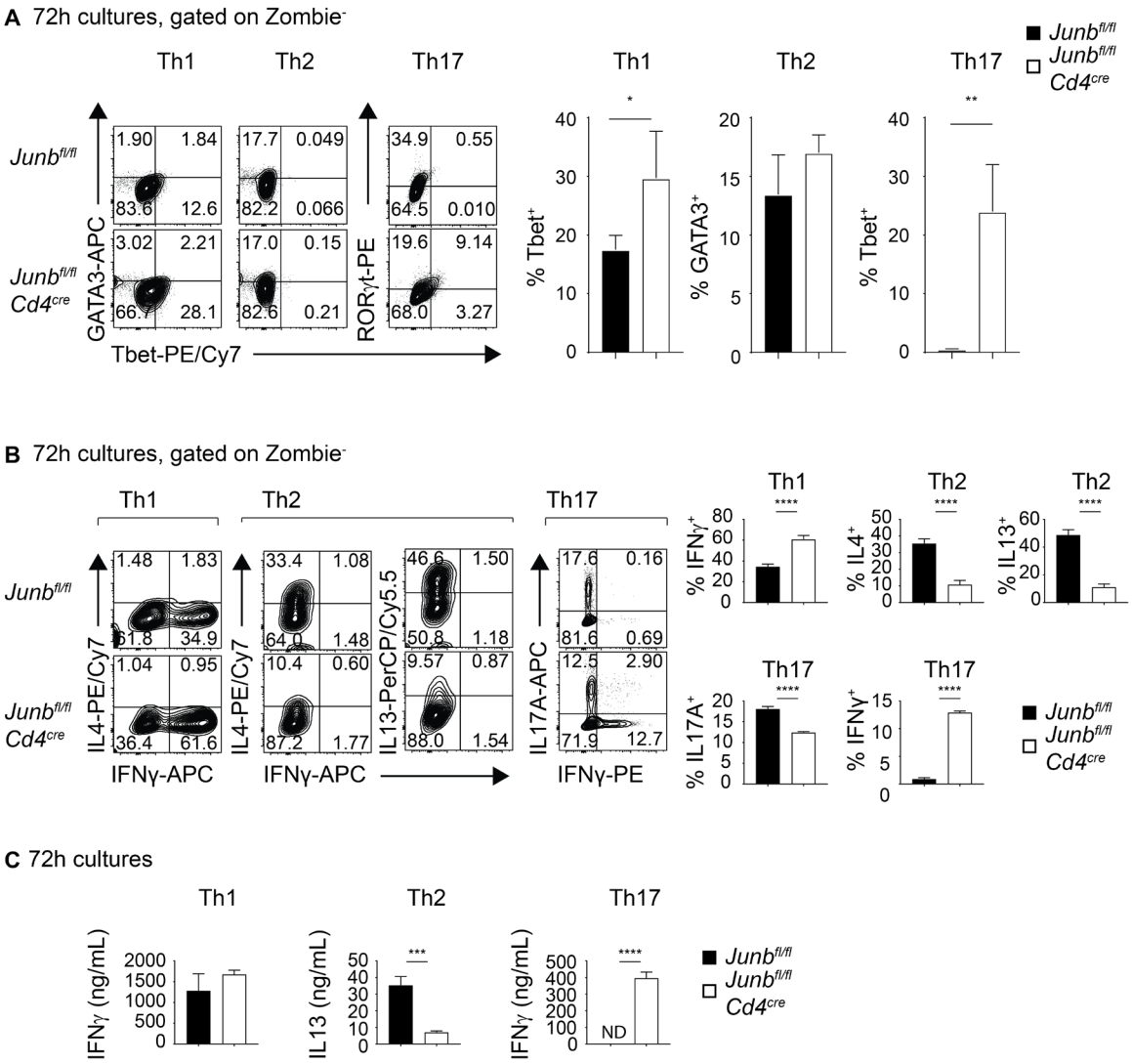

Fig. 13. JunB-dependent regulation of the lineage-specifying transcription factor and signature cytokines in CD4$^+$ effector T cells.

Naïve CD4$^+$ T cells isolated from *Junb*$^{fl/fl}$ or *Junb*$^{fl/fl}$*Cd4*^{cre} mice were cultured under the indicated polarizing conditions for 72 h. Flow cytometry analysis of expression of lineage-specifying transcription factors (A) and cytokines (B) for Th1, Th2, and Th17 cells. Enzyme-linked immunosorbent assay (ELISA) analysis (C) of concentrations of cytokines for medium of Th1, Th2, and Th17 cells. ND, not detectable. (A-C) Error bars indicate s.d. (n = 4-6 wells per group). * $p < 0.05$, ** $p < 0.01$, *** $p < 0.001$, **** $p < 0.0001$, (unpaired two-tailed Student's test). Data represent two independent experiments.

Part III: JunB modulates metabolic programs only in Th2, but not in Th1 and Th17

JunB-interacting partners, BATF and IRF4, regulate metabolic activities in both $CD4^+$ and $CD8^+$ T cells (68, 74, 106, 113). Moreover, a recent study further demonstrated that IRF4 directs the metabolic programs shifting from oxidative phosphorylation (OXPHOS) toward glycolysis in $CD8^+$ effector T cells during immune response (68). To investigate the role of JunB in regulating metabolic programs of $CD4^+$ T cells, I activated control and *Junb*-deficient $CD4^+$ T cells under differentiation conditions for Th1, Th2, and Th17 cells and analyzed oxidative phosphorylation and aerobic glycolysis activity using a seahorse analyzer. Under both Th1- and Th17-polarizing conditions, extracellular acidification rates (ECAR) and oxygen consumption rates (OCR) were not affected by loss of JunB (Fig. 14A, B). However, under Th2-polarizing conditions, basal ECAR were significantly lower in *Junb*-deficient $CD4^+$ T cells than in controls, although the maximum glycolytic capacity (ECAR in the presence of oligomycin) was comparable (Fig. 14A). As OCR were not affected (Fig. 14B), the OCR/ECAR ratio in *Junb*-deficient $CD4^+$ T cells increased under Th2-polarizing conditions, suggesting a metabolic program shifting from glycolysis activity to oxidative phosphorylation in *Junb*-deficient Th2 cells. These results indicate that JunB is required for promoting glycolysis and metabolic reprogramming of Th2 cells, but not of Th1 or Th17 cells.

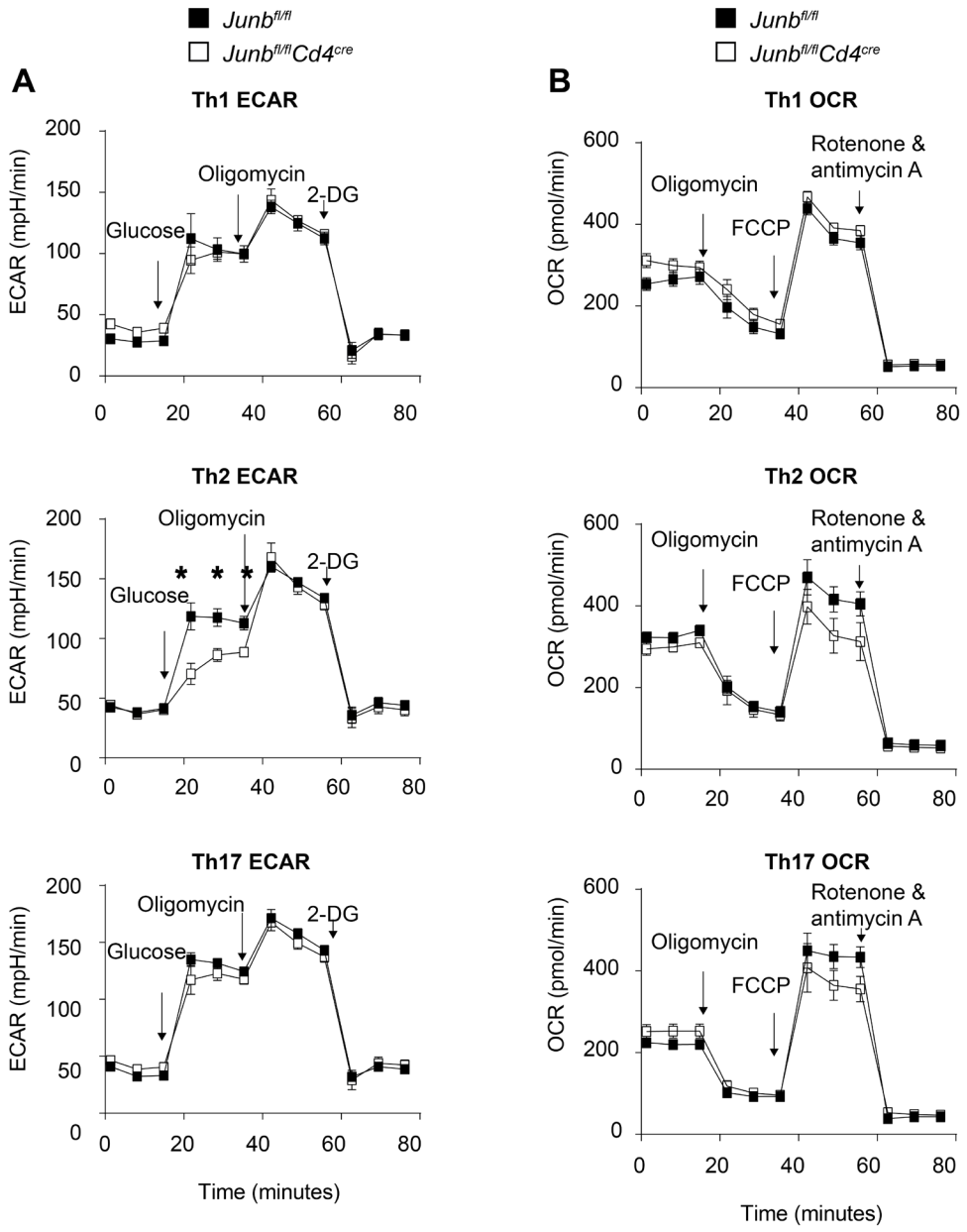

Fig. 14. Metabolic reprogramming in *Junb*-deficient CD4$^+$ T cells.

Naïve CD4$^+$ T cells isolated from *Junb*$^{fl/fl}$ or *Junb*$^{fl/fl}$*Cd4*^{cre} mice were cultured under Th1-, Th2-, and Th17-polarizing conditions. After 48 h, metabolic activity was measured using a seahorse analyzer. (A) Extracellular acidification rate (ECAR) in cells cultured under differentiation conditions for Th1, Th2, and Th17 cells. During ECAR measurement, cells were sequentially treated with glucose, oligomycin, and 2-Deoxy-D-glucose (2-DG). (B) Oxygen consumption rate (OCR) in cells cultured under differentiation conditions for Th1, Th2, and Th17 cells. During OCR measurement, cells were sequentially treated with oligomycin, fluorocarbonyl cyanide phenylhydrazone (FCCP), rotenone and antimycin A. (A, B) Error bars indicate s.e.m (n = 6 wells per group). * $p < 0.05$, (unpaired two-tailed Student's test). Data represent two independent experiments.

Part IV. JunB promotes cell survival of CD4$^+$ effector T cells *in vivo*.

My *in vitro* data demonstrated that JunB is not only required for survival of various CD4$^+$ effector T subsets under TCR stimulation but also required for expression of a subset of genes encoding effector molecules such as IL-4 and IL-13. Next, I sought to determine the *in vivo* role of JunB in CD4$^+$ effector T cells using the adoptive transfer technique, which allows us to track TCR transgenic CD4$^+$ T cells specific to a single antigen at different time points throughout the course of an immune response (138).

First, to analyze expression of JunB in CD4$^+$ T cells activated *in vivo*, I isolated naïve CD4$^+$ T cells from OT-II transgenic mice (hereafter referred to as OT-II cells), in which all T cells harbor a allele of TCR and specifically respond to peptide derived from ovalbumin 323 – 339 epitope ($OVA_{323-339}$) (139, 140). I then transferred OT-II cells into congenic mice on a CD45.1$^+$ background and immunized the recipient with $OVA_{323-339}$ peptide in Complete Freund's Adjuvants (CFA) 1 day later (Fig. 15A). At 3, 5, and 7 days post immunization (dpi), I analyzed expression levels of CD44 and JunB in CD4$^+$ T cells isolated from inguinal lymph nodes. Almost all transferred OT-II cells (>99%) became activated (CD44 high, CD44^{hi}) at 5 dpi (Fig. 15B), and expression of JunB was induced in more than half of activated OT-II cells and was maintained until 7 dpi (Fig. 15C).

I next sought to determine the effects of JunB deletion on the differentiation of CD4$^+$ T cell in mice immunized with various adjuvants. To this end, I co-transferred naïve OT-II cells isolated from *Junb*$^{fl/fl}$ OT-II (control OT-II) or *Junb*$^{fl/fl}$*Cd4*^{cre} OT-II (*Junb*-deficient OT-II) mice (CD45.2$^+$) together with congenic OT-II cells (CD45.1$^+$ 45.2$^+$) at a 2:1 ratio into congenic recipient mice (CD45.1$^+$). One day later, I immunized mice with $OVA_{323-339}$ peptides together with either CFA, LPS, or papain (Fig. 16A) (114, 141, 142). In all immunization conditions tested, accumulation of *Junb*-deficient OT-II cells at 5 dpi was severely impaired (Fig. 16B-D). Furthermore, the frequency of apoptotic cells (Annexin V$^+$ Zombie-NIR$^-$) tended to be higher in *Junb*-deficient OT-II cells than controls, although the difference was not statistically significant (Figure. 17B). Percentages of cells expressing a pro-apoptotic molecule, Bim, were significantly higher in *Junb*-deficient OT-II cells (Figure. 17C). I also analyzed the effect of JunB deletion on the frequency of cytokine-expressing cells. CFA, LPS, and papain mainly induced accumulation of OT-II cells expressing cytokines for Th17 (IL-17A), Th1 (IFN-γ), and Th2 cells (IL-4/13), respectively (Fig. 16E-G). Consistent with previous reports (99–101), the percentage of IL-17-expressing cells in mice immunized with CFA was significantly lower in *Junb*-deficient OT-II cells than in controls (Fig. 16E). In contrast, the percentage of IFNγ-expressing cells in *Junb*-deficient OT-II cells was increased in mice immunized with LPS (Fig. 16F). Both the percentages of IL-4- and IL-13-expressing cells and the expression level of IL-4 and IL-13 were comparable

between *Junb*-deficient and control OT-II cells (Fig. 16G). These data indicate that JunB promotes accumulation of antigen-primed $CD4^+$ T cells, regardless of the context of inflammation and that JunB has a repressive effect on IFN-γ under LPS-induced inflammation, which is consistent with our *in-vitro* findings.

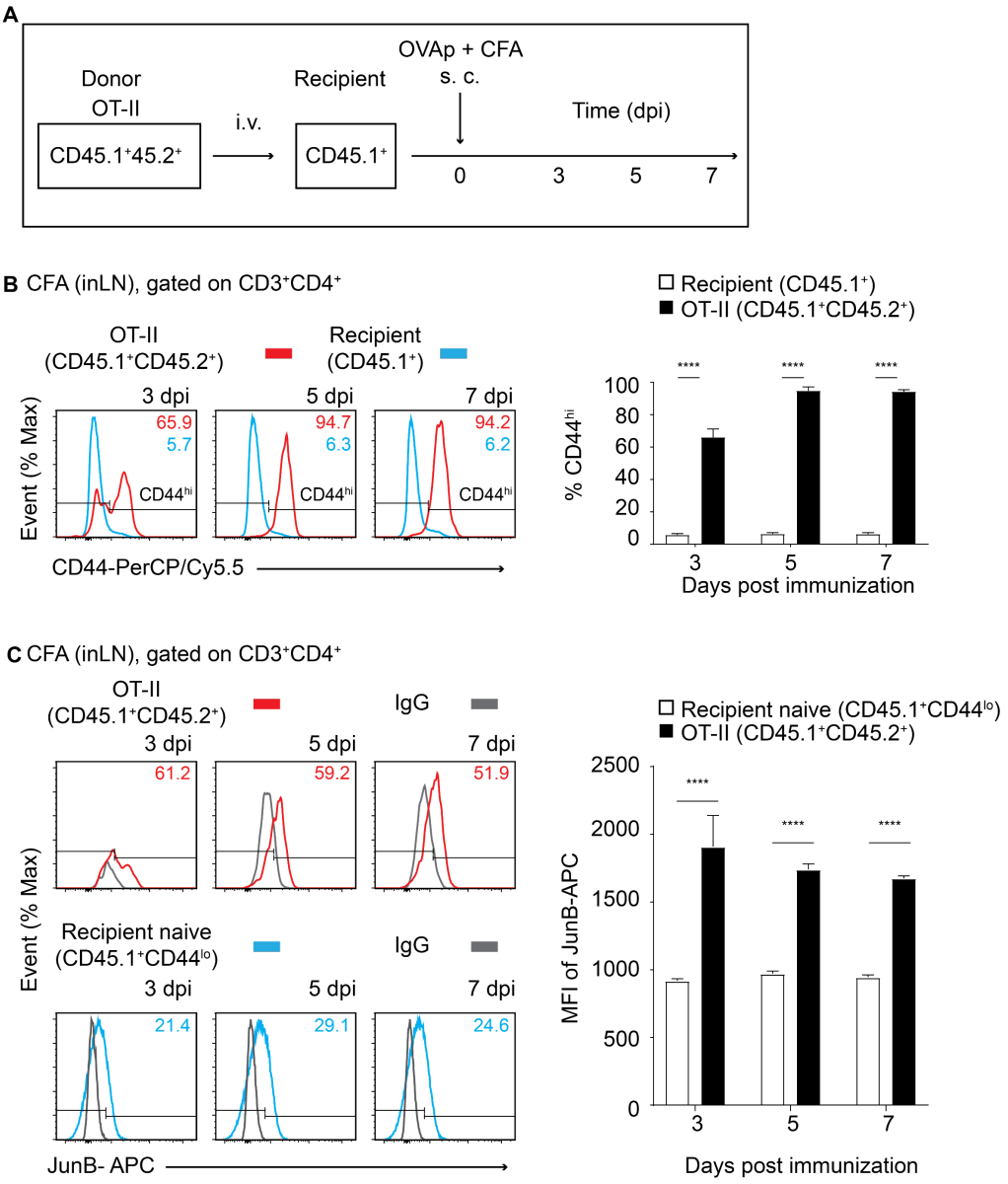
A
Donor
OT-II
CD45.1+45.2+
i.v.
Recipient
CD45.1+
OVAp + CFA
s. c.
Time (dpi)
0
3
5
7
B CFA (inLN), gated on CD3+CD4+
OT-II
(CD45.1+CD45.2+)
Recipient
(CD45.1+)
3 dpi
5 dpi
7 dpi
65.9
5.7
94.7
6.3
94.2
6.2
CD44hi
Event (% Max)
CD44-PerCP/Cy5.5
Recipient (CD45.1+)
OT-II (CD45.1+CD45.2+)
% CD44hi
****
Days post immunization
C CFA (inLN), gated on CD3+CD4+
OT-II
(CD45.1+CD45.2+)
IgG
61.2
59.2
51.9
Recipient naive
(CD45.1+CD44lo)
21.4
29.1
24.6
JunB- APC
Recipient naive (CD45.1+CD44lo)
OT-II (CD45.1+CD45.2+)
MFI of JunB-APC

Fig. 15. JunB is homogeneously expressed in antigen-primed CD4+ T cells in vivo.

2 x 10^6 naïve OT-II cells ($CD45.1^+CD45.2^+$) were transferred to congenic recipient mice ($CD45.1^+$), followed by immunization with $OVA_{323-339}$ peptides emulsified in CFA. At the indicated days post-immunization (dpi), cells were harvested from inguinal lymph nodes and analyzed. **(A)** Immunization scheme. i.v. intravenous injection, s.c. subcutaneous injection. **(B)** Flow cytometry analysis of CD44 in transferred ($CD45.1^+CD45.2^+$) OT-II cells and recipient ($CD45.1^+$) $CD3^+CD4^+$ T cells isolated from inguinal lymph nodes at indicated days post-immunization (dpi). Representative histograms (left) are shown (transferred OT-II cells: red lines, host $CD4^+$ T cells: blue lines). Numbers in histograms (left) indicate average percentages of $CD44^{hi}$ cells. Bar graphs (right) indicate the percentage of $CD44^{hi}$ cells in transferred OT-II cells and recipient $CD3^+CD4^+$ T cells. **(C)** Flow cytometry analysis of JunB expression in transferred OT-II cells ($CD3^+CD4^+CD45.1^+CD45.2^+$) and recipient naïve $CD4^+$ T cells ($CD3^+CD4^+CD45.1^+CD44^{lo}$) at the indicated dpi. Representative histograms (left) are shown (OT-II: red lines, host naïve CD4 T cells: blue lines, mouse IgG control: grey lines). Numbers in histograms (left) indicate average percentages of $JunB^+$ cells. Bar graphs (right) indicate the median florescence intensity (MFI) of JunB in transferred OT-II cells and recipient $CD3^+CD4^+$ T cells. (B-C) Error bars indicate s.d. (n =4). Error bars indicate s.d. (n =3). **** $p < 0.0001$, (unpaired two-tailed Student's test).

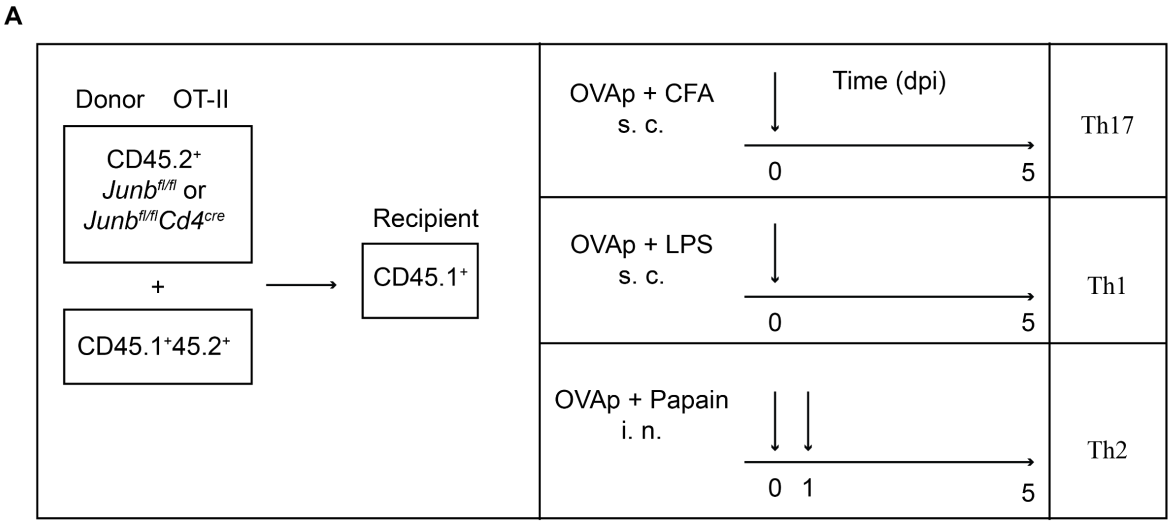
A
Donor OT-II
CD45.2+
Junbfl/fl or
Junbfl/flCd4cre
+
CD45.1+45.2+
Recipient
CD45.1+
OVAp + CFA
s. c.
Time (dpi)
0
5
Th17
OVAp + LPS
s. c.
0
5
Th1
OVAp + Papain
i. n.
0 1
5
Th2

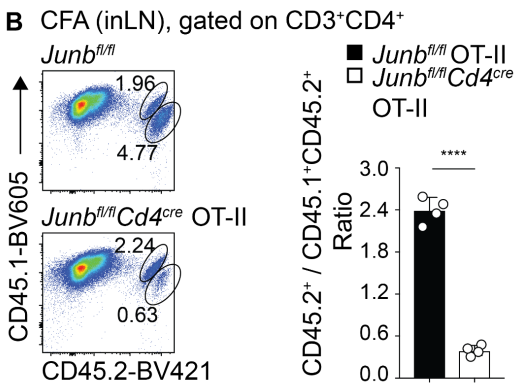
B CFA (inLN), gated on CD3+CD4+
Junbfl/fl
1.96
4.77
Junbfl/flCd4cre OT-II
2.24
0.63
CD45.1-BV605
CD45.2-BV421
Junbfl/fl OT-II
Junbfl/flCd4cre OT-II
CD45.2+ / CD45.1+CD45.2+ Ratio
****

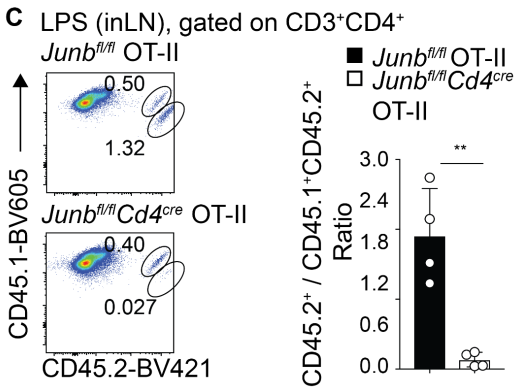
C LPS (inLN), gated on CD3+CD4+
Junbfl/fl OT-II
0.50
1.32
Junbfl/flCd4cre OT-II
0.40
0.027
CD45.1-BV605
CD45.2-BV421
Junbfl/fl OT-II
Junbfl/flCd4cre OT-II
CD45.2+ / CD45.1+CD45.2+ Ratio
**

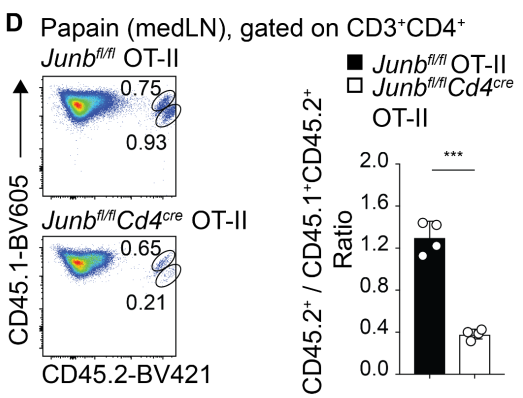
D Papain (medLN), gated on CD3+CD4+
Junbfl/fl OT-II
0.75
0.93
Junbfl/flCd4cre OT-II
0.65
0.21
CD45.1-BV605
CD45.2-BV421
Junbfl/fl OT-II
Junbfl/flCd4cre OT-II
CD45.2+ / CD45.1+CD45.2+ Ratio
***

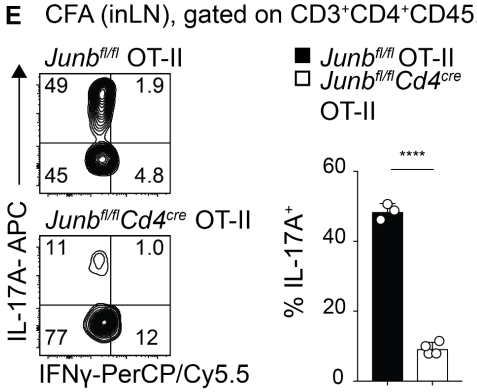
E CFA (inLN), gated on CD3+CD4+CD45.2+
Junbfl/fl OT-II
49
1.9
45
4.8
Junbfl/flCd4cre OT-II
11
1.0
77
12
IL-17A- APC
IFNγ-PerCP/Cy5.5
Junbfl/fl OT-II
Junbfl/flCd4cre OT-II
% IL-17A+
****

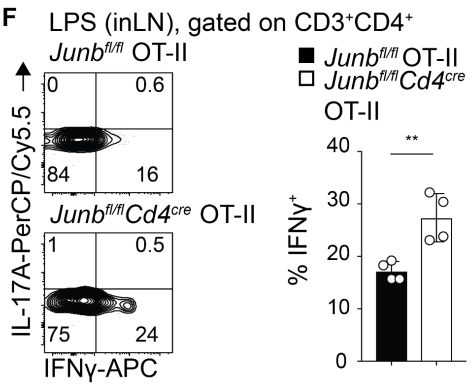
F LPS (inLN), gated on CD3+CD4+
Junbfl/fl OT-II
0
0.6
84
16
Junbfl/flCd4cre OT-II
1
0.5
75
24
IL-17A-PerCP/Cy5.5
IFNγ-APC
Junbfl/fl OT-II
Junbfl/flCd4cre OT-II
% IFNγ+
**

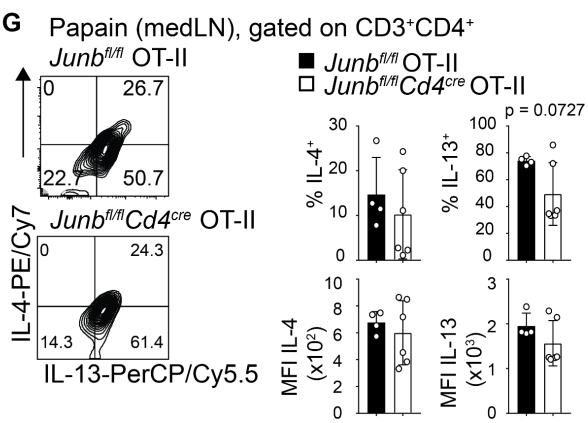
G Papain (medLN), gated on CD3+CD4+
Junbfl/fl OT-II
0
26.7
22.7
50.7
Junbfl/flCd4cre OT-II
0
24.3
14.3
61.4
IL-4-PE/Cy7
IL-13-PerCP/Cy5.5
Junbfl/fl OT-II
Junbfl/flCd4cre OT-II
% IL-4+
% IL-13+
p = 0.0727
MFI IL-4 (x10²)
MFI IL-13 (x10³)

Fig. 16. JunB promotes accumulation of antigen-primed CD4+ T cells in vivo.
Naïve *Junb*$^{fl/fl}$ OT-II or *Junb*$^{fl/fl}$*Cd4*^{cre} OT-II cells (CD45.2^{+}) were co-transferred with congenic wild-type OT-II cells (CD45.1^{+}CD45.2^{+}) at a 2:1 ratio into congenic recipient mice (CD45.1^{+}). One day later, mice were immunized with $OVA_{323-339}$ peptides emulsified in CFA or mixed with LPS or papain. At 5 dpi, cells were isolated from draining lymph nodes and analyzed by flow cytometry. (**A**) Immunization scheme. *i.v.* intravenous injection, *s.c.* subcutaneous injection, *i.n.* intranasal injection. (**B-D**) Expression of CD45.1 and CD45.2 in CD3^{+}CD4^{+} T cells isolated from mice immunized with CFA (B), LPS (C), and papain (D). Representative dot plots are shown (left). Bar graphs (right) show the ratio of *Junb*$^{fl/fl}$ OT-II or *Junb*$^{fl/fl}$*Cd4*^{cre} OT-II cells (CD45.2^{+}) vs co-transferred OT-II cells (CD45.1^{+}CD45.2^{+}). inLN, inguinal lymph nodes, medLN, mediastinal lymph nodes. (**E-G**) Flow cytometry analysis of IL-17A and (E), IFN-γ (F) and IL-4/13 expression (G) in OT-II cells (CD3^{+}CD4^{+}CD45.2^{+}) isolated from mice immunized with CFA (A), LPS (B), and papain (C). Representative dot plots are shown (left). Bar graphs (right) indicate the percentage of cells expressing IL-17A (E), IFN-γ (F), IL-4/13 and the MFI of IL-4/13 (G) in *Junb*$^{fl/fl}$ OT-II or *Junb*$^{fl/fl}$*Cd4*^{cre} OT-II cells. MFI. Median fluoresce intensity. (B-G) Error bars indicate s.d. (n = 4-6 mice per group). * $p < 0.05$, ** $p < 0.01$, *** $p < 0.001$, **** $p < 0.0001$, (unpaired two-tailed Student's test). Data represent two independent experiments.

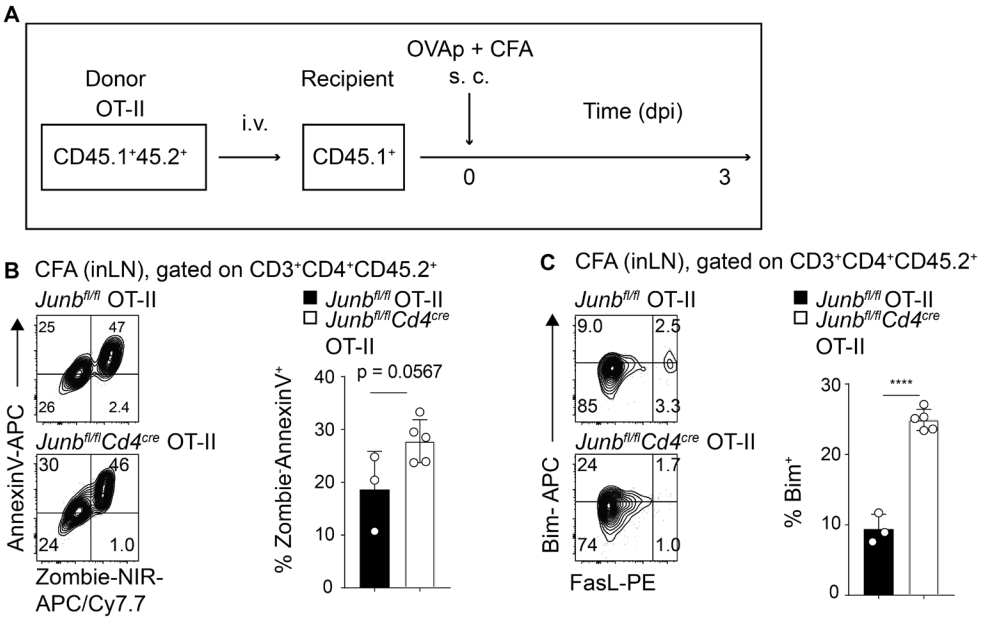

Fig. 17. JunB is essential for inhibition of apoptosis as well as Bim expression in antigen-primed CD4+ T cells in vivo.

2 x 10^6 *Junb*$^{fl/fl}$ OT-II or *Junb*$^{fl/fl}$*Cd4*^{cre} OT-II cells (CD45.2$^+$) were transferred to congenic recipient mice (CD45.1$^+$), followed by immunization with $OVA_{323-339}$ peptides emulsified in CFA. At the 3 days post-immunization (dpi), cells were harvested from inguinal lymph nodes and analyzed. (**A**) Immunization scheme. *i.v.* intravenous injection, *s.c.* subcutaneous injection. (**B-C**) Expression of Zombie-NIR and AnnexinV (B), and Bim and FasL (C) in total CD3$^+$CD4$^+$CD45.2$^+$ cells isolated from draining lymph nodes, analyzed by flow cytometry. inLN, inguinal lymph nodes. (B-C) Representative dot plots (left) and bar graphs (right). Error bars indicate s.d. (n =4-6 mice per group). * $p < 0.05$, ** $p < 0.01$, *** $p < 0.001$, **** $p < 0.0001$, (unpaired two-tailed Student's test). (B-C) Data represent two independent experiments.

Part V. JunB promotes lymphopenia-induced $CD4^+$ T cell homeostatic proliferation *in vivo*

My data suggested that JunB is required for the accumulation of $CD4^+$ effector T cells induced upon immunization in an antigen-dependent manner. Next, I investigated whether JunB is also required for accumulation of $CD4^+$ effector T cells induced in an antigen-independent manner using a lymphopenia-induced homeostatic proliferation model (143). In mouse or human, lymphopenia is a low-T-cell number symptom that is usually caused by genetic disorder or HIV infection. When hosts recover from lymphopenic conditions, excessive nutrients, antigen:MHC complex, and cytokines create a special signal niche that drive naïve $CD4^+$ T cells undergo a rapid proliferation to reconstitute the T cell compartment, which results in activation of naïve CD4 T cells in an antigen-independent manner (144). To test whether JunB is required for lymphopenia-induced $CD4^+$ T cell proliferation, I co-transferred naïve $CD4^+$ T cells isolated from $Junb^{fl/fl}$ (control) or $Junb^{fl/fl}Cd4^{cre}$ (*Junb*-deficient) mice ($CD45.2^+$) together with congenic naïve $CD4^+$ T cells ($CD45.1^+$) at a 1:1 ratio into congenic $Rag1^{-/-}$ recipient mice (Fig. 18A). At 14 days post transfer, the accumulation of *Junb*-deficient $CD3^+CD4^+$ T cells was severely impaired in spleens and mesenteric lymph nodes – where transferred naïve $CD4^+$ T cells receive antigen stimulation and proliferate (Fig.18B, C). This data indicates that JunB is required for accumulation of lymphopenia-induced $CD4^+$ effector T cells.

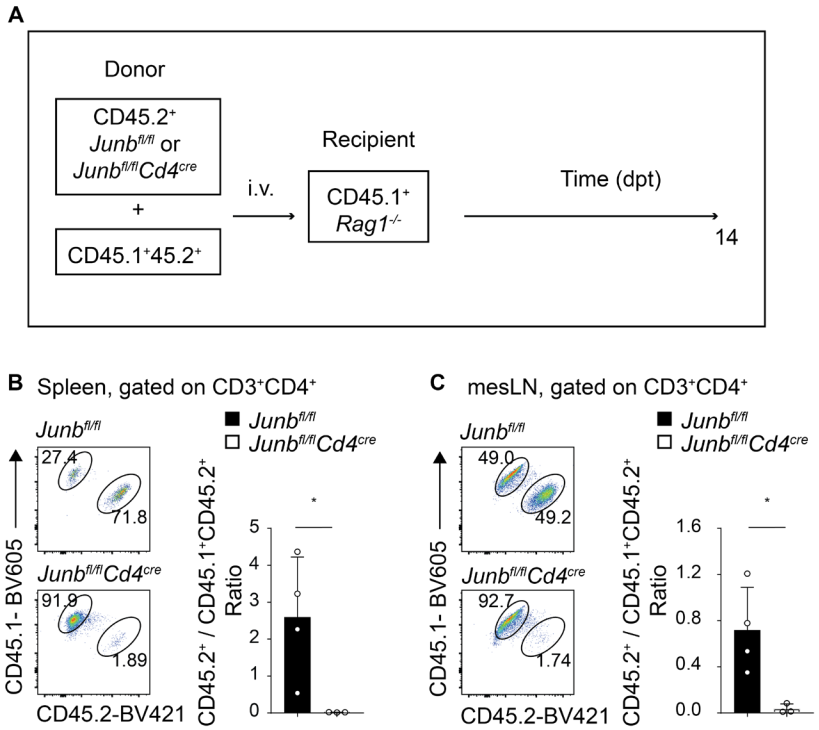

Fig. 18. JunB promotes lymphopenia-induced accumulation of CD4+ effector T cells in vivo.

Naïve CD4$^+$ T cells from *Junb*$^{fl/fl}$ or *Junb*$^{fl/fl}$*Cd4*^{cre} mice (CD45.2$^+$) were co-transferred with naïve CD4$^+$ T cells from congenic wild-type mice (CD45.1$^+$CD45.2$^+$) at a 1:1 ratio into congenic recipient *Rag1*$^{-/-}$ mice (CD45.1$^+$). 14 days later, cells were isolated from spleens and mesenteric lymph nodes and analyzed by flow cytometry. (**A**) Adoptive transfer scheme. *i.v.* intravenous injection. (**B-C**) Expression of CD45.1 and CD45.2 in CD3$^+$CD4$^+$ T cells isolated from spleen (B) and mesenteric lymph nodes (C) of *Rag1*$^{-/-}$ mice received adoptive transfer were analyzed by flow cytometry. Representative dot plots are shown (left). Bar graphs (right) show the ratio of *Junb*$^{fl/fl}$ or *Junb*$^{fl/fl}$*Cd4*^{cre} CD3$^+$CD4$^+$ T cells (CD45.2$^+$) vs co-transferred CD3$^+$CD4$^+$ T cells (CD45.1$^+$). (B-C) Error bars indicate s.d. (n = 4-6 mice per group). * $p < 0.05$, ** $p < 0.01$, *** $p < 0.001$, **** $p < 0.0001$, (unpaired two-tailed Student's test).

Part VI. Bioinformatics study: JunB-dependent transcriptional regulation in CD4$^+$ effector T cells

JunB regulates common and lineage specific transcriptional programs among distinct CD4$^+$ effector T cell subsets

We and others have identified that JunB regulates many effector genes during Th17 differentiation such as *Il17a*, *Il17f*, *Il23r* and *Il21* (99–101). My data further demonstrated that JunB regulates expression of IFN-γ and IL-4/13 during Th1 and Th2 cell differentiation, respectively. To further understand JunB-dependent transcriptional regulation in various CD4$^+$ effector T cell subsets, I performed RNA-seq analysis of CD4$^+$ T cells activated *in vitro* for 48 h under Th0-, Th1-, and Th2-poralizing conditions. Expression of 266 genes in Th0 cells, 355 genes in Th1 cells, and 514 genes in Th2 cells was significantly affected by the loss of JunB (Fig. 19 A-C).

In *Junb*-deficient Th1 cells, *Ifng*, *Il12rb2*, *Il2ra,* and *Eomes* were upregulated, but *Ifngr2* was downregulated (Fig. 19B). In *Junb*-deficient Th2 cells, *Il4ra* and *Il13* were upregulated and downregulated, respectively (Fig. 19C). Loss of JunB did not affect expression of the lineage-specifying transcription factors, *Tbx21* and *Gata3*, in Th1 and Th2 cells, respectively (Fig. 19B, 19C). Combined with 1,138 differentially expressed genes identified in the previously reported RNA-seq data of *Junb*-deficient Th17 cells (101), I identified 1,755 genes that were upregulated or downregulated by the loss of JunB in T helper cell differentiation (Fig. 19E). Most of those genes were found in a specific Th subset (85 genes specific to Th0 cells, 157 specific to Th1 cells, 247 specific to Th2 cells, 884 genes to Th17), while only 28 genes were found in all T helper cells tested (Fig. 20 E). Notably, under all Th-polarizing conditions tested, *Bcl2l11* (encoding Bim) and TCR-induced genes (*Sell*, *Ikbke, Thy1*) were upregulated (Fig. 19E).

Enriched pathway analysis revealed that TCR-mediated apoptosis, IL-2, and TCR signaling pathways were significantly affected by loss of JunB (Fig. 20A-D). Pathways involved in cell proliferation and cellular metabolism were not detected in the pathway analysis, but expression of some genes encoding glycolytic enzymes was affected by deletion of JunB. *Eno3* (encoding enolase 3) was upregulated under all Th-polarizing conditions tested (Fig. 19E), while *Pgm2l1* (encoding glucose 1,6-bisphosphate synthase) was downregulated only under Th2 polarizing conditions (Fig. 19B). Thus, JunB is essential for control of a subset of genes induced by TCR and IL-2 signaling, including *Bcl2l11*, and it also regulates various cytokines and cytokine receptors that are expressed in specific CD4$^+$ effector T subsets.

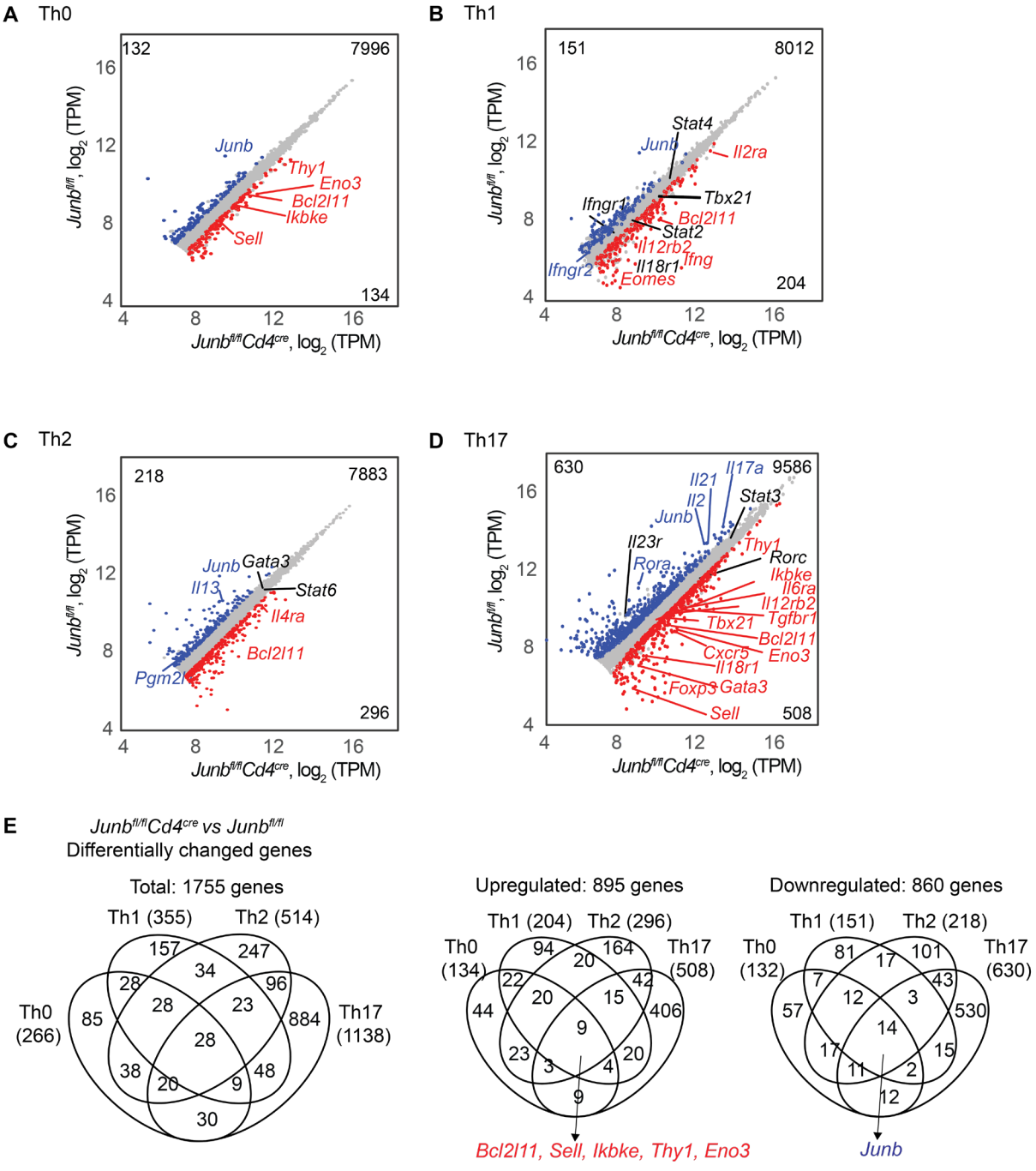

E *Junb*$^{fl/fl}$*Cd4*^{cre} *vs Junb*$^{fl/fl}$
Differentially changed genes

Fig. 19. JunB-dependent transcriptional regulation in T helper cell differentiation. Naïve $CD4^+$ T cells isolated from *Junb*$^{fl/fl}$ or *Junb*$^{fl/fl}$*Cd4*^{cre} mice were cultured under Th0-, Th1- and Th2-polarizing conditions for 48 h and subjected to RNA-seq analysis. Differentially expressed genes in *Junb*-deficient $CD4^+$ T cells vs control cells (log_2 fold change > 0.5, *p* value < 0.05, base mean > 100 TPM (normalized transcript per kilobase million)) were identified in each Th-polarizing condition. (**A-D**) Scatter plots represent genes differentially expressed in *Junb*-deficient $CD4^+$ T cells vs control cells under differentiation conditions for Th0 (A), Th1 (B), and Th2 (C) cells. RNA-seq data for *Junb*-deficient $CD4^+$ T cells cultured under Th17-polarizing conditions were from GSE 98414. (D) Genes considered significantly upregulated or downregulated are highlighted in red and blue, respectively. Genes with insignificant changes are highlighted in grey. On each plot, left top and right bottom numbers indicate numbers of upregulated or downregulated genes, respectively. **(E)** Venn diagrams show the overlap of differentially expressed genes identified in *Junb*-deficient $CD4^+$ T cells vs control cells under different Th-polarizing conditions.

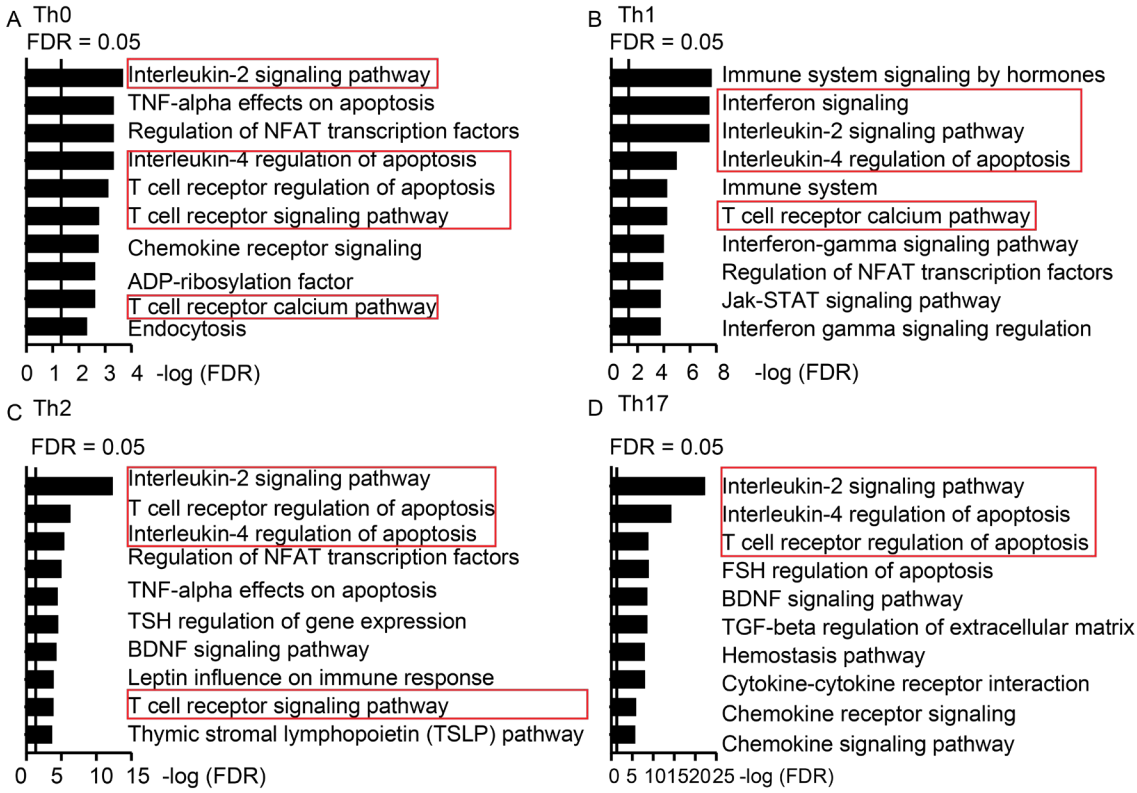

Fig. 20. JunB regulates IL-2 signaling, TCR signaling and apoptosis pathways. EnrichR pathway analysis of genes differentially expressed in *Junb*-deficient $CD4^+$ T cells vs control cells under differentiation conditions for Th0 (A), Th1 (B), and Th2 (C). RNA-seq data for *Junb*-deficient $CD4^+$ T cells cultured under Th17-polarizing conditions were from GSE 98414 (D). Pathways related to IL-2 signaling, TCR signaling, and apoptosis are highlighted.

JunB directly binds and regulates genes involved in differentiation and functions of diverse CD4$^+$ effector T cells

We and others have shown that JunB colocalizes with BATF and IRF4 at various gene loci containing AICE motifs and thereby directly regulates expression of genes important for Th17 cells (78, 79, 100, 101). However, the mechanism of JunB-dependent transcriptional regulation in differentiation of other CD4$^+$ effector T cells remains largely uncharacterized. To address this, I investigated genome-wide JunB-DNA binding in cells activated under Th1-polarizing conditions *in vitro* using chromatin immunoprecipitation sequencing (ChIP-seq) analysis with antibodies to JunB, BATF and IRF4 and compared with ChIP-seq data that we previously obtained from Th17 subsets (100). In both Th1 and Th17 cells, more than 60% of all the three transcription factors (TF) peaks fell in regions within 10kbp upstream of transcription starting sties (TSS) or located in the gene bodies (Fig. 21A, B and Table 4). This suggests that JunB, BATF and IRF4 regulate expression of their target gens largely through binding to regions proximal to their target genes in both Th1 and Th17 cells.

Next, I further integrated ChIP-seq data for JunB, BATF, and IRF4 in Th1 and Th17 (100) and RNA-seq data for *Junb*-deficient Th1, Th2, and Th17 subsets (101). I first combined ChIP-seq data obtained from Th1 and Th17 cells to generate a consensus ChIP-seq peak set for JunB, BATF, and IRF4. I then associated this ChIP-seq peak set or AP-1 binding motif with genomic regions containing "JunB-responsive genes" (genes differentially expressed between *Junb*-deficient and control CD4$^+$ T cells in RNA-seq data). I detected JunB ChIP-seq peaks and AP-1-binding motifs in 10 kbp upstream of transcription starting site or directly within gene bodies of most JunB-responsive genes, regardless of whether they were upregulated or downregulated by deletion of JunB in Th1, Th2 and Th17 subsets. With the analysis using binding and expression target (BETA) software, I identified genes that have a greater likelihood of direct regulation by JunB. These genes I considered "direct JunB responsive genes" (BETA > 0, Fig. 22A). Direct JunB responsive genes include many genes important for differentiation and function of CD4$^+$ effector T subsets, including cytokines, chemokines, their receptors, exhaustion related molecule, and *Bcl2l11*, while indirect JunB responsive genes included *Il6ra*, of which protein products are involved in many CD4$^+$ effector T cell subsets differentiation (Fig. 22A) (145).

I next examined whether the JunB ChIP-seq peaks overlapped with BATF and IRF4 ChIP-seq peaks in genomic regions containing direct JunB responsive genes. Overlapping ChIP-seq peaks for JunB, BATF, and IRF4 were detected in genomic regions for more than 70% of direct JunB responsive genes (Fig. 22B). Thus, JunB cooperatively works with BATF and IRF4 to directly regulate the transcriptional programs in Th1, Th2, and Th17 cells.

Lastly, I performed Enrichr pathway analysis to further reveal the function difference between direct JunB responsive genes that were or were not co-bound by BATF and IRF4. Consistent with the pathway analysis of genes regulated by JunB (Fig. 20), TCR-mediated apoptosis, IL-2, and TCR signaling pathways were significantly enriched in direct JunB responsive genes that were co-bound by BATF and IRF4 (Fig. 23A-C). In the other hand, no specific biological pathway was significantly enriched in genes direct JunB responsive genes that were not bound by BATF and IRF4 (Fig. 23A-C). However, genes with only JunB peaks contain genes required for Th1 differentiation such as *Eomes* and *Ifngr2* (Fig. 23A) (146) or *Myo6* – a gene encoding the actin-based motor proteins that move cargo towards the minus ends of actin filaments (Fig. 23B) (147). Together, this data suggest that JunB may regulate a subset of gene expression and controls different biological functions during Th1 and Th2 differentiation independently of BATF and IRF4.

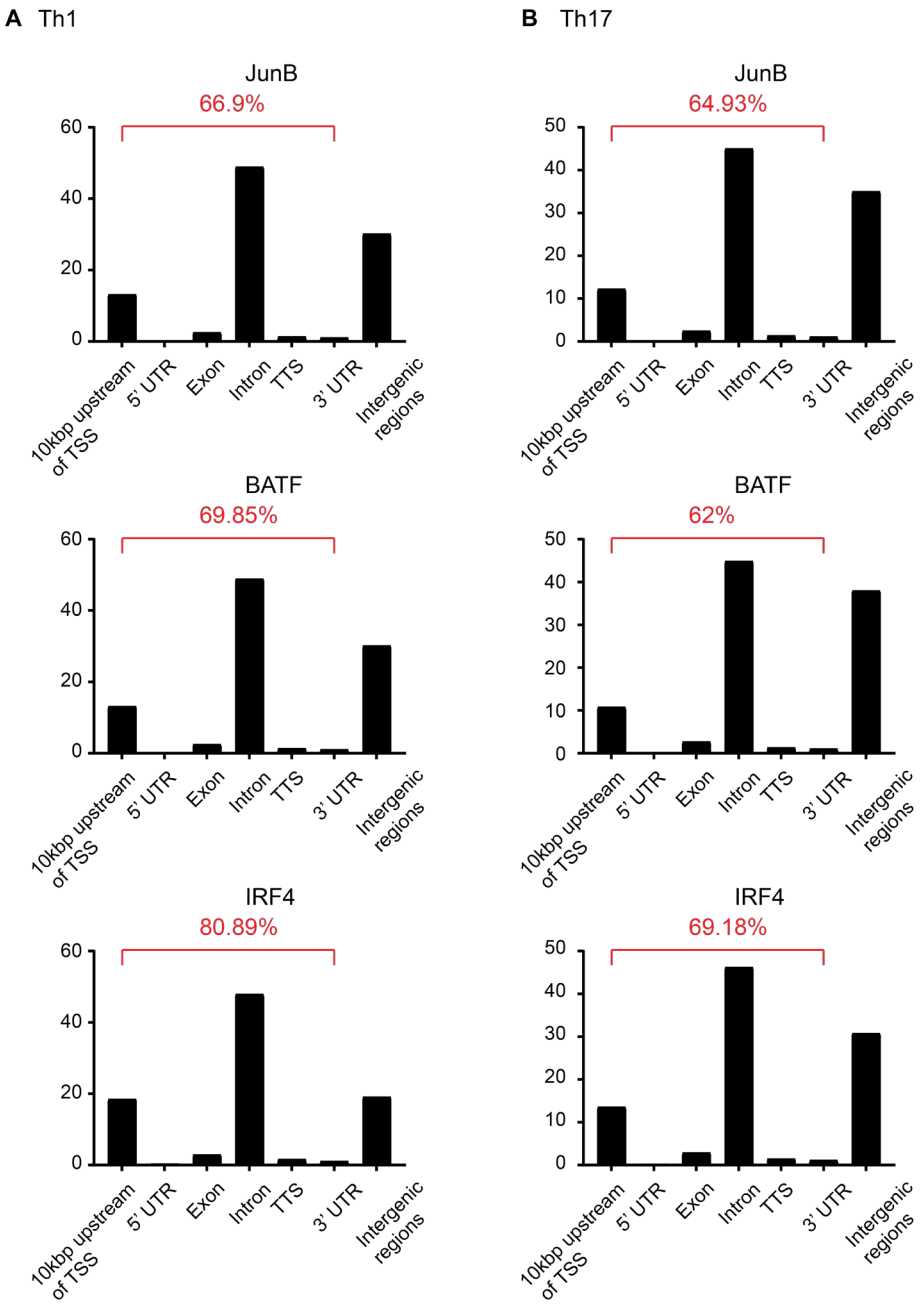

Fig. 21. Profiles of JunB, BATF and IRF4 binding peaks in Th1 and Th17 cells

JunB, BATF and IRF4 ChIP-seq data were obtained from cells cultured under Th1-polarizing conditions for 48h (A) or from Th17 cells (GSE86535) (B). Histograms show frequencies of each transcription factor (TF) binding peaks in different types of DNA regions. Numbers on histogram indicate the total percentages of TF binding peaks felling within 10kbp upstream of transcription starting site or within gene bodies, the boundaries of which of a given gene are defined by transcription starting sites and termination sites. TSS, transcription starting site; UTR, untranslated region; TTS: transcription termination site.

Table 4. A detailed list of profiles of JunB, BATF and IRF4 binding peaks

	Th1			***Th17***		
	JunB	BATF	IRF4	JunB	BATF	IRF4
5-10 kbp upstream of TSS	4.36	4.48	4.72	4.36	4.34	4.51
< 5 Kbp upstream of TSS	8	8.67	13.8	7.9	6.47	9.1
5′ UTR	0.14	0.16	0.36	0.16	0.11	0.24
1st Exon	0.27	0.35	0.59	0.28	0.26	0.45
Other Exon	2.11	2.18	2.32	2.21	2.48	2.49
Intron	47.3	48.93	47.95	45.07	44.9	46.24
TTS	1.3	1.39	1.65	1.38	1.34	1.47
3′ UTR	1.02	1.08	1.14	1.11	1.06	1.19
Intergenic regions	33.1	30.15	19.11	35.07	38.01	30.83

ChIP-Seq analysis for JunB, BATF and IRF4 binding sites in Th1 and Th17 (GSE86535) were further categorized based on their genome annotations. The numbers in the table indicate the percentage of ChIP-seq peaks for each transcription factor that locates within the specified DNA regions. This table is related to Fig. 23. TSS, transcription starting site; UTR, untranslated region; TTS: transcription termination site.

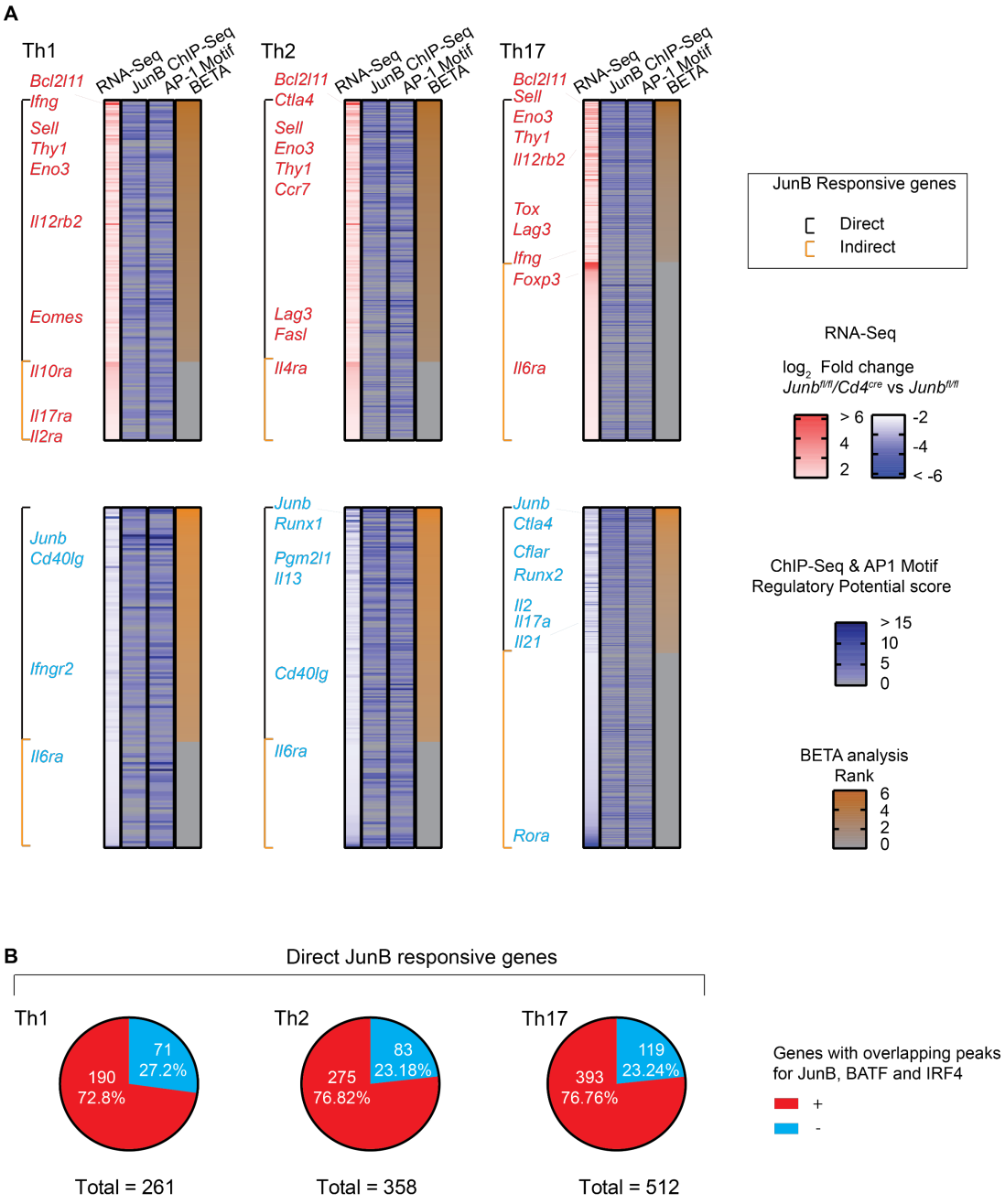
A
Th1
Th2
Th17
RNA-Seq
JunB ChIP-Seq
AP-1 Motif
BETA
Bcl2l11
Ifng
Sell
Thy1
Eno3
Il12rb2
Eomes
Il10ra
Il17ra
Il2ra
Junb
Cd40lg
Ifngr2
Il6ra
Ctla4
Ccr7
Lag3
Fasl
Il4ra
Runx1
Pgm2l1
Il13
Tox
Lag3
Foxp3
Cflar
Runx2
Il2
Il17a
Il21
Rora
JunB Responsive genes
Direct
Indirect
RNA-Seq
log2 Fold change
Junbfl/fl/Cd4cre vs Junbfl/fl
> 6
4
2
-2
-4
< -6
ChIP-Seq & AP1 Motif
Regulatory Potential score
> 15
10
5
0
BETA analysis
Rank
6
4
2
0
B
Direct JunB responsive genes
Th1
71
27.2%
190
72.8%
Total = 261
Th2
83
23.18%
275
76.82%
Total = 358
Th17
119
23.24%
393
76.76%
Total = 512
Genes with overlapping peaks
for JunB, BATF and IRF4
+
-

Fig. 22. JunB directly regulates expression of various genes in CD4$^+$ effector T cell subsets.

Differentially expressed genes (JunB responsive genes) in *Junb*-deficient CD4$^+$ T cells vs control cells were obtained from RNA-seq analysis (as in Fig. 21). A consensus JunB ChIP-seq peak dataset was obtained from the union of JunB ChIP-seq data for Th1 cells and Th17 subsets (GSE86535). AP-1-binding motifs were scanned across the mouse genome (ver. *mm10*). Data of RNA-seq, JunB ChIP-seq, and AP-1-binding motif analyses were merged and are shown in the heatmap. BETA analysis data (a higher BETA rank score represents a greater likelihood of direct regulation by JunB) is also shown in the heatmap. JunB-responsive genes that had BETA scores greater than 0 were defined as "direct JunB responsive genes". In contrast, JunB responsive genes that had BETA score equal to 0 were defined as "indirect JunB responsive genes". **(B)** Pie charts show the percentage of direct JunB responsive genes that did or did not have overlapping peaks for JunB, BATF, and IRF4. Overlapping peaks were obtained by comparing ChIP-seq data of JunB with that of BATF and IRF4. The consensus ChIPseq peak sets for BATF and IRF4 were obtained from the union of ChIP-seq data for Th1 cells and Th17 subsets (GSE86535).

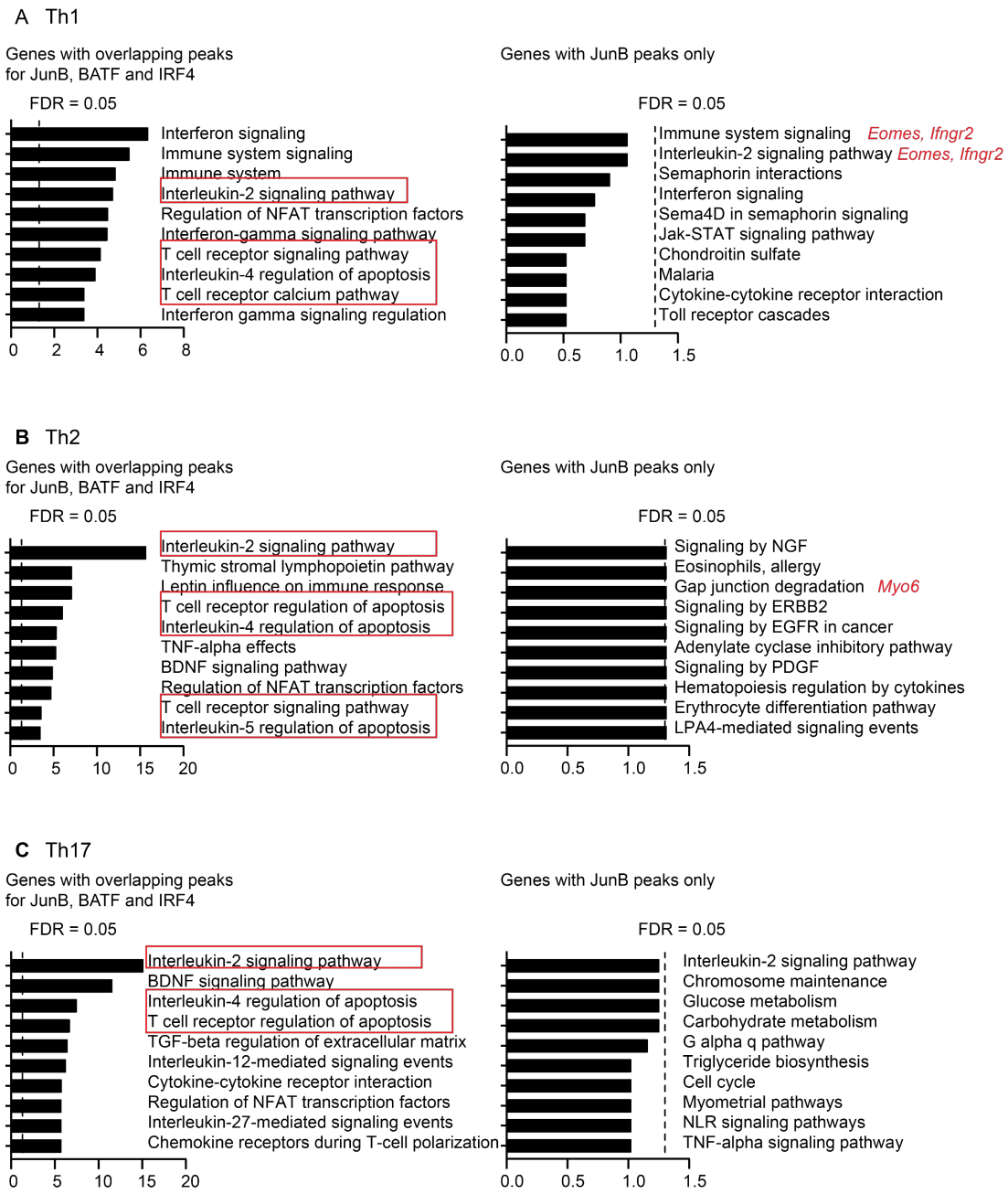

Fig. 23. The function difference between direct JunB responsive genes that co-localized by JunB, BATF and IRF4 and those that are bound with only JunB. EnrichR pathway analysis of direct JunB responsive genes in cells cultured under differentiation conditions for Th1 (A), Th2 (B), and Th17 (C). Histogram graphs show pathways enriched in genes with overlapping peaks for Junb, BATF and IRF4 (left) or pathways enriched in genes with JunB peaks only (right). Pathways related to IL-2 signaling, TCR signaling, and apoptosis are highlighted.

JunB potential interacts with various family proteins to acts as both a repressor and activator in CD4$^+$ effector T cells

My RNA-seq analysis revealed that JunB acts as both an activator and repressor in regulating gene expression in CD4 T cell differentiation. To further address this, I performed activating/repressive function prediction with BETA software (133), which allows us to integrate RNA-seq and ChIP-seq data and examine whether JunB preferably binds to target genes that are up- or down-regulated by JunB. This analysis revealed that although the occupancy of JunB ChIP-seq peaks in genomic regions containing genes that are upregulated by JunB are slightly higher than those containing genes that are down-regulated by JunB, the difference is not statistically significant (Fig. 24). Thus, JunB can bind to various genes in order to promote and repress gene expression.

How JunB performs this "Janus" regulation is still unclear. One hypothesis is JunB interacts with different family proteins to extend its regulatory capacity. Previous studies suggested that AP-1 heterodimer can interact with other transcription factors such as NFAT family proteins with their dimerized leucine zipper domain (148). Recent studies also suggested Ets family proteins interact with BATF and JunB in regulating function and differentiation in Th17 and Th9 cells (88, 98). To identify potential JunB interacting partners, I performed motif scan with BETA software to reveal differentially enriched motifs in JunB ChIP-seq peaks near the genomic regions containing genes regulated by JunB (10kbp upstream of TSS or within the gene bodies of JunB responsive genes). As in line with previous studies, motif of Etv3, a Ets family protein, was significantly enriched in JunB ChIP-seq peaks near JunB up- and down-regulated genes over those that are not regulated by JunB, regardless of cell subsets (Fig. 25). I also obtained motifs of Rsf2 and Osr2, members of Rfx and β-β-α-Zinc finger domain families, respectively, differentially enriched in JunB responsive genes in Th1, Th2, and Th17 cells (Fig. 25). Thus, JunB potentially interacts with various family proteins to perform its activating and repressive regulatory functions in various CD4$^+$ effector T

cells.

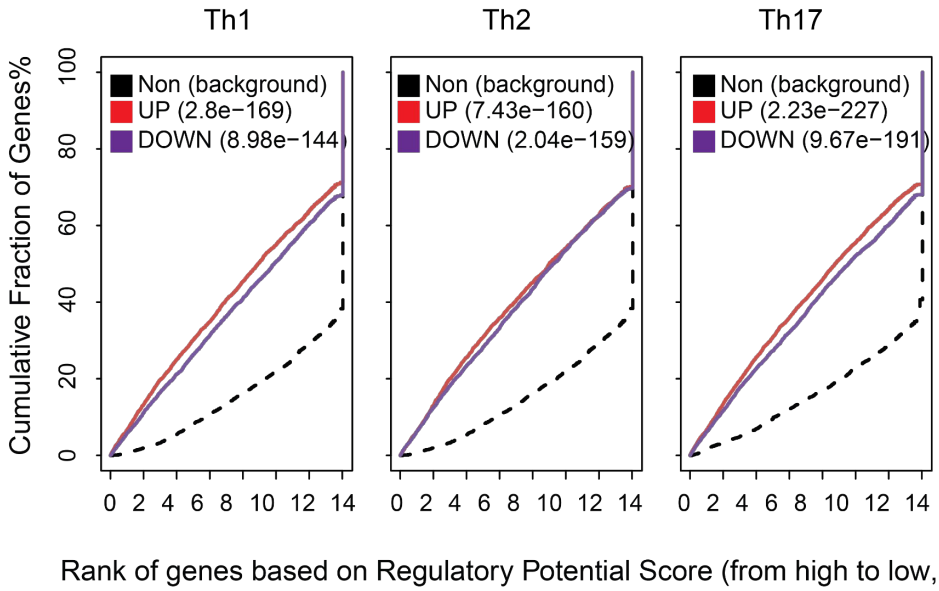

Fig. 24. JunB acts as both an activator and repressor in providing direct transcriptional regulation on gene expression

BETA activating/repressive function prediction of JunB responsive genes in Th1, Th2, and Th17 cells. Differentially expressed genes between *Junb*-deficient $CD4^+$ T cells and control cells was from RNA-seq data (JunB responsive genes, as in Fig. 21). A consensus JunB ChIP-seq peak dataset was obtained from the union of JunB ChIP-seq data for Th1 cells and Th17 subsets (GSE86535). Genes were first categorized as non-differential (NON), up- (UP), and down-regulated (DOWN) genes, based on their expression profiles. For a given gene, the regulatory potential score was calculated based on JunB ChIP-seq peaks felling within 10 kb upstream of TSS or within this gene body. A higher regulatory potential score represents a greater JunB ChIP-seq occupancy near this given gene. Genes are cumulated by the rank based on the regulatory potential score from low to high. Cumulative regulatory potential scores of up- (UP) and down-regulated (DOWN) genes were represented by the red and purple lines, respectively. Cumulative regulatory potential scores of non-differentially regulated (NON) genes was represented as the dashed line, serving as background. P values that represent the significance were obtained by comparing the UP or DOWN group distributions to the NON group with Kolmogorov-Smirnov test.

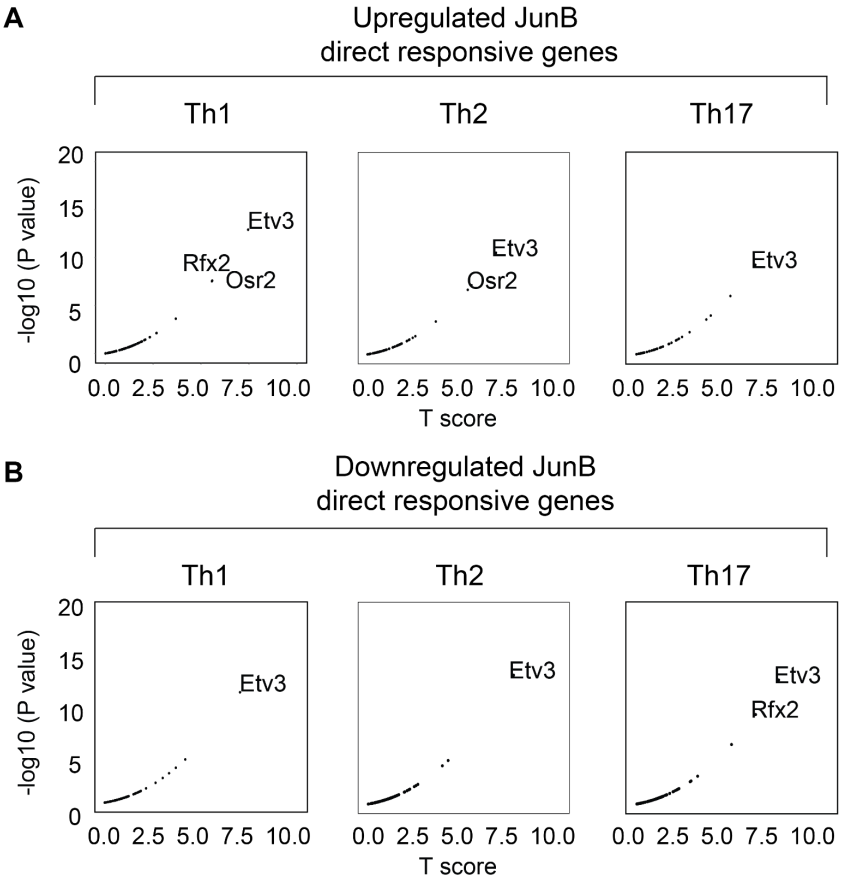

Fig. 25. Motifs are differentially enriched in JunB responsive genes

Motif scan of known transcription factors was performed with BETA software for identifying motifs in genomic regions containing JunB ChIP-seq peaks near JunB responsive genes (10kbp upstream of TSS or within the gene bodies of JunB responsive genes). Only 200bp regions centered on the peak summits were used for motif scan. To identify motifs differentially enriched in genomics regions containing JunB responsive genes, genes were first categorized as non-differentially expressed (NON), up- (UP), and down-regulated (DOWN) genes. The occurring frequency of a given motif found in ChIP-seq peaks near up- (UP) or down-regulated (DOWN) genes was obtained and compared to the occurring frequency of non-differentially expressed (NON) genes. The significance of a differentially enriched motif, represented by P value, was measured by the one-tailed t test.

Chapter 4: Discussion

Part I. Thesis overview

Here I demonstrate that JunB is required for accumulation of various $CD4^+$ effector T cells both *in vitro* and *in vivo*. Accumulation of antigen-primed $CD4^+$ T cells was significantly impaired by deletion of JunB in mice immunized with LPS, papain, or CFA, which predominantly induced Th1, Th2, and Th17 responses, respectively. Commensurate with this, viability of TCR-stimulated naïve $CD4^+$ T cells was decreased by deletion of JunB under *in vitro* differentiation conditions for Th1, Th2, and Th17 cells. One of the key functions of JunB is to inhibit apoptosis in TCR-stimulated naïve $CD4^+$ T cells, as *Junb*-deficient $CD4^+$ T cells are more sensitive to TCR-induced apoptosis with a concomitant increase of expression of a pro-apoptotic molecule, Bim. Common target genes for JunB in differentiation of various $CD4^+$ effector T subsets include genes associated with TCR and IL-2 signaling, such as *Bcl2l11* (encoding Bim), *Sell* (encoding CD62L), *Ikbke* (encoding IκBKε) and *Thy1* (encoding CD90). JunB bound directly to loci of those genes and negatively regulated their expression in Th1, Th2, and Th17 cells. Dysregulation of those genes likely contributes to defective accumulation of TCR-stimulated $CD4^+$ effector T cells. As deletion of *Junb* also greatly sensitizes thymus-derived Treg cells to TCR-induced apoptosis (102), TCR-stimulated $CD4^+$ effector and regulatory T cells share a common requirement for JunB-dependent negative modulation of the TCR-induced apoptosis signal.

JunB also regulates expression of a variety of genes in a context-dependent manner. As our lab and others have reported, JunB promotes expression of *Rorc*, *Il17a* and *Il17f* (100, 101) in Th17 cells and negatively regulates *Ifng* in Th1 and Th17 cells (101). In this study, my RNA-seq analysis further clarified the role of JunB in a transcriptional program for $CD4^+$ effector T differentiation. In Th1-polarizing conditions, expression of Th1 signature genes, not only *Ifng*, but also *Il12rb2*, *Il2ra* and *Eomes*, was promoted by JunB deletion. In Th2-polarizing conditions, *Il4ra* and *Il13* were upregulated and downregulated, respectively, by JunB deletion. However, JunB deletion did not affect induction of the lineage-specifying transcription factors, T-bet and GATA3, in Th1 and Th2 cells, respectively. Thus, JunB is not required for induction of lineage-specifying transcription factors, but it regulates expression of some lineage-specific molecules in Th1 and Th2 differentiation.

In addition to previously identified JunB target genes in Th17 differentiation, I have identified a large number of novel JunB targets in Th1 and Th2 differentiation. Many JunB target genes were identified in a specific $CD4^+$ effector T subset, which might be partly due to subset-specific chromatin landscapes. My integrated analysis of ChIP-seq and RNA-seq data identified direct and indirect targets for JunB in $CD4^+$ effector T subsets. Remarkably, direct JunB targets included molecules that have been

functionally characterized in immune responses, including cytokines, chemokines, and their receptors. BATF and IRF4 co-bound about 70% of those genes, confirming a critical role for JunB in BATF and IRF4-dependent transcriptional control in $CD4^+$ effector T cell differentiation.

Deletion of JunB decreased expression of a glycolysis-related gene, *Pgm2l1*, in Th2-, but not in Th1- and Th17-polarizing conditions. This might account for impaired aerobic glycolysis in *Junb*-deficient cells under Th2-polarizing conditions. In contrast, although another glycolysis-related gene, *Eno3*, was upregulated by deletion of JunB in all Th-polarizing conditions tested, aerobic glycolysis in Th1 and Th17 cells was not significantly affected by deletion of JunB. This is in contrast to the critical function of IRF4 in regulating glycolytic enzyme genes in $CD4^+$ and $CD8^+$ effector T cell differentiation. These data suggest that JunB regulates metabolic reprogramming that is necessary for specific T helper subsets.

My data demonstrate that JunB is required for survival of Th1, Th2, Th17 and probably other $CD4^+$ effector T cells. However, in some situations, $CD4^+$ effector T cells can be generated normally, independently of JunB. For example, loss of JunB does not affect the frequency of gut-resident homeostatic Th17 cells (100, 101). We still do not know what determines the necessity of JunB in $CD4^+$ effector T cell generation, but JunB may not be needed for accumulation of cells that are activated by a weak TCR signal or in a less inflammatory environment.

In conclusion, my thesis provides substantial evidence that JunB plays a critical role not only in Th17, but also in Th1 and Th2 responses both *in vitro* and *in vivo*. My data clarify genome-wide transcriptional targets for JunB in those T helper cells (Fig. 26). Collectively, these data shed light on JunB-dependent transcriptional regulatory mechanisms in differentiation of various $CD4^+$ effector T cells.

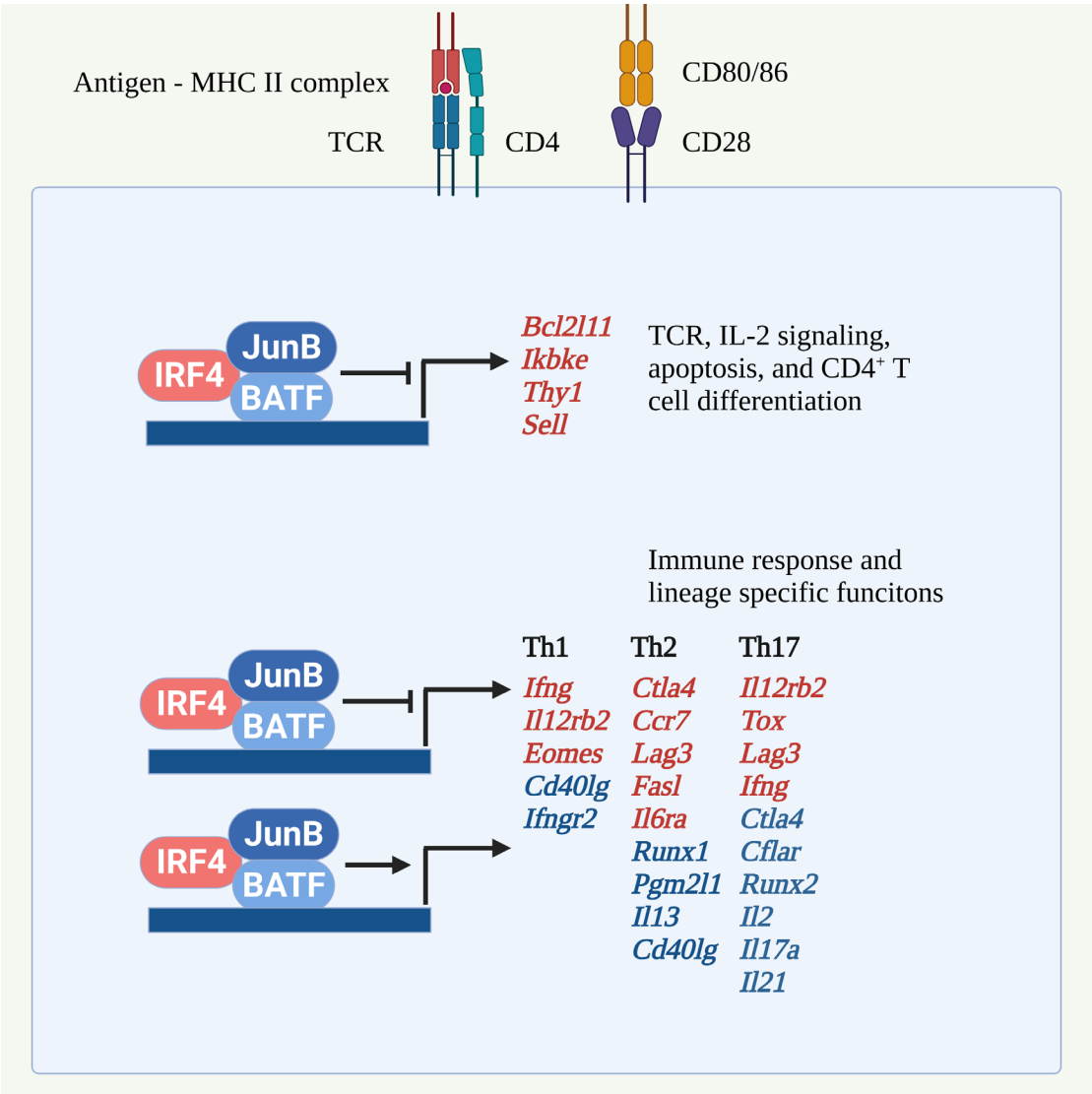

Fig. 26. JunB-dependent regulatory mechanism in CD4$^+$ effector T cells

JunB directly regulates genes involved in TCR, IL-2 signaling and apoptosis across diverse T helper cell subsets. At each cell subset, JunB provides a direct regulation on expression of lineage specific genes. Genes up- and down-regulated by JunB deletion in CD4$^+$ T cells are marked as red and blue, respectively.

Part II. JunB inhibits Th1 differentiation but promotes Th2 cell functions

JunB plays different roles between Th1 and Th2 cells. JunB is not required for Th1 differentiation and seems to act as a repressor for Th1 program, as deletion of JunB upregulates expression of T-bet and IFN-γ (Fig. 13). RNA-seq analysis revealed more Th1-linegae specific genes, including *Eomes*, *Il12rb2*, and *Il2ra*,whose expression was repressed by JunB (Fig. 20) (29, 146). In contrast to this, JunB promotes production of effector cytokine IL-4 and IL13 in Th2 cell (Fig. 13). The promoting activity of JunB in Th2 effector function, however, is context-dependent, as deletion of JunB does not change expression of IL-4 and IL-13 in OT-II cells activated by papain immunization (Fig. 16). In mice immunized with papain, cytokines other than IL-4, which I used in *in-vitro* Th2 differentiation, might induce IL-4 and IL-13 independently of JunB. JunB regulates IFN-γ probably through T-bet regulation, as deletion of JunB upregulates the expression of T-bet in Th1 (Fig. 20). On the other hand, JunB is not required for GATA3 expression in Th2 *in vitro* (Fig. 13).

AP-1 factors likely regulate T helper cell differentiation in a context-dependent manner. For example, BATF is not required for Th1 differentiation but promotes Th2 differentiation (Table 5) (89, 90). Another AP-1 protein, c-Maf, does not regulate the expression of IFN-γ in Th1 but promotes the expression of IL-4 in Th2 (149). This context-dependent regulation of AP-1 proteins could be explained by the difference of opening chromatin profiles between Th1 and Th2 cells. It could also be caused by the flexibility of AP-1 proteins in interacting with a variety of transcription factors through their C-terminal domains. For instance, JunB may interact with a potential IFN-γ inhibitor in Th1 cells but interact with other transcription factors in promoting the expression of IL-4 and IL-13 in Th2 cells. The difference of JunB-mediated protein interactomes should be investigated in future studies.

Part III. The role of JunB in differentiation, proliferation, and cell death

During activation, $CD4^+$ T cells undergo a rapid expansion in responding to both antigen and cytokine stimulation. Meanwhile, antigen stimulation also induces the apoptosis. Until the antigen is removed, the rate of cell proliferation should be faster than the rate of apoptosis. Any disturbance of this balance will result in premature death of $CD4^+$ effector T cells. More importantly, the premature death could also have the secondary effects on the differentiation into $CD4^+$ effector T cells.

JunB inhibits the rate of apoptosis of $CD4^+$ effector T cells by inhibiting Bim expression. On the other hand, JunB does not regulate cellular proliferation, as deletion of JunB does not alter any pathways related to cell proliferation (Fig. 21). However, to further confirm this, CFSE dilution assay should be performed at an earlier time point, e.g., 3 days post immunization, in OVA peptide/adjuvants immunization experiment.

This can help us to understand whether deletion of JunB do affect the proliferation of $CD4^+$ effector T cells or not.

Deletion of JunB upregulates the expression of Bim and subsequently increases the percentages of apoptotic cells in $CD4^+$ effector T cells (Fig. 7) activated *in vivo*. The expression of Bim expression in *Junb*-deficient OT-II cells is 2-fold when compared to control OT-II cells. The difference of percentages of apoptotic cells between *Junb*-deficient and control OT-II cells, however, is modest (Fig. 17). This suggests that although the expression of Bim was upregulated, the onset of apoptosis and the subsequent accumulation of apoptotic cells may require a longer time. Hence, to observe a more significant influence caused by JunB deletion in OT-II cells, it is necessary to examine the percentage the apoptotic cells between control and *Junb*-deficient OT-II cells at a later time point.

JunB deletion further promotes the differentiation of Th1 but impaired the effector functions of Th2 cells. We still do not know whether increased cell death in *Junb*-deficient Th1/Th2 cells is related to this altered differentiation. I can address this by analyzing the effect of CRISPR-Cas9-mediated Bim knock out on Th differentiation in *Junb*-deficient $CD4^+$ effector T cells.

Part IV. Comparisons of roles between JunB and IRF4/BATF in Th1 and Th2 cells

In this thesis, I demonstrate that JunB has both common and different roles during Th1 and Th2 differentiation when compared to IRF4 and BATF. Similar as IRF4 and BATF, JunB also promotes cell survival of $CD4^+$ effector T cells. I further reveal that JunB inhibits Bim expression in both Th1 and Th2 (Table 5) (120, 135). Moreover, deletion of JunB increased the expression of *Thy1* that encodes CD90 – a surface protein expressed among all $CD4^+$ effector T cell subsets. Previous studies have suggested that apoptosis is increased in $CD4^+$ effector T cells when surface CD90 molecules are crosslinked with other proteins or anti-CD90 antibodies (150). Therefore, deletion of JunB not only initiates the apoptosis through upregulating Bim expression, but also increases the susceptibility to apoptosis in both Th1 and Th2 cells.

The role of JunB in Th1 differentiation is opposite to IRF4. As discussed before, JunB may act as a repressor of Th1 differentiation. In contrast to this, IRF4 promotes Th1 differentiation through promoting the expression of T-bet and IFN-γ as well as enzymes required for glycolysis (Table 5) (74).

JunB regulates more biological functions than IRF4 and BATF during Th2 differentiation. Similar as IRF4 and BATF, JunB promotes the expression of Th2 effector cytokines IL-4 and IL-13 (Fig. 13) (75, 80, 90). In addition, JunB regulates metabolic reprogramming in Th2 and the expression of *Pgm2l1* – enzyme required for

glycolysis (Fig. 14). JunB also inhibits the expression of exhaustion marker *Lag3* (Fig. 20) (Table 5). However, the role of IRF4 and BATF among these regulations have not been reported yet.

Table 5. A detailed list of comparisons of role of JunB in Th1 and Th2 with IRF4 and BATF

Cell Types	TFs	Main functions (Key target genes)	Reference
In both Th1 and Th2	JunB	Promotes cell survival through inhibiting expression of apoptosis-related molecules such as Bim and CD90.	This study
	IRF4	Promotes cell survival in $CD4^+$ effector T cells.	(119)
	BATF	Promotes cell survival in $CD4^+$ effector T cells through inhibiting apoptosis.	(120)
Th1	JunB	Inhibits the expression of T-bet and IFN-γ, as well as other lineage-specific genes such as *Il12rb2*, *Eomes,* and *IL2ra*.	This study, (101)
	IRF4	Promotes glycolysis of Th1 (HK2, GLUT3). Promotes the expression of IFN-γ, TNF-α and T-bet.	(74)
	BATF	No specific role has been reported yet.	(89, 90)
Th2	JunB	Promotes the cytokine production of Th2 (IL-4 and IL-13). Promotes glycolysis of Th2 (PGM2L1). Inhibits the expression of gene encoding exhaustion marker such as *Lag3*.	This study, (105)
	IRF4	Promotes the differentiation and functions of Th2 (GATA3, IL-4, and IL-13).	(70, 75, 80, 81)
	BATF	Promotes the differentiation and functions of Th2 (GATA3, IL-4, and IL-13).	(90)

Part V. Improvement of cell culturing conditions

In *in vitro* differentiation experiments, the percentages of living cells of control (*Junb*$^{fl/fl}$) CD4$^+$ T cells is 13%, 60% and 50% when cultured under Th0-, Th1- and Th2-polaring conditions for 96h, respectively (Fig. 11A). These results suggest that the culturing conditions are not suitable for long-term survival of cells, especially under Th0-polarizing conditions. It may be due to the differences of cytokine compositions between Th0- and Th1/2-polarizing conditions. The only cytokine present in Th0 conditions is IL-2. However, in addition to IL-2, IL-12 and IL-4 were added in Th1- and Th2-polarizing conditions, respectively. As both IL-12 and IL-4 can enhance the cell viability as well as stimulating proliferation (151, 152), the survival signal provided in Th0-polarizing conditions may not be comparable to that in Th1 and Th2 conditions. One of the solutions is to increase the amount of IL-2 in Th0 conditions, as IL-2 alone can also provide survival signals and stimulate cell proliferation (153). Moreover, to avoid the possible nutrients and cytokine depletion during long-term culturing, a 1:3 split of cells could be conducted at an earlier time point, e.g., 48h, before the analysis of apoptotic cells.

Part VI. Improvement of *in vivo* immunization assays for observing the role of JunB in CD4$^+$ effector T cell under exhaustion or low TCR stimulation

Previous studies have suggested that JunB is rapidly induced in activated CD4$^+$ T cells once TCR is stimulated. In this study, I further suggested that JunB promotes cell survival in CD4$^+$ effector T cells both *in vivo* and *in vitro*. Hence, JunB is required for maintaining cell survival since the early stage of CD4$^+$ T cell differentiation. However, JunB may play roles in other stages of CD4$^+$ T cell differentiation. For example, JunB might be a potential inhibitor in T cell exhaustion during Th2 differentiation, as JunB directly binds and represses the expression of exhaustion marker *Lag3* in Th2 cells (Fig. 19, 22). To explore this possibility, it is important to investigate whether JunB prevents T cell exhaustion *in vivo*.

In OVA peptide/adjuvants immunization experiments, most of OT-II cells became activated (Fig. 15) and a large proportion of *Junb*-deficient OT-II underwent cell death at 5 days post immunization (Fig. 16). Since JunB is necessary for accumulation of antigen-primed T helper cells, the current CD4-cre-dependent JunB knockout model is not suitable to evaluate the role of JunB in the events following to the priming of naïve CD4$^+$ T cells. Analysis of the effect of deletion of JunB in exhausted T cells using conditional knockout models with tamoxifen inducible *Cre* recombinase such as CD4-creERT2 might address this question.

It is also interesting to see the role of JunB in T helper cells activated with different strength of TCR signal. In this thesis, I used an OVA peptide that shows high affinity to

OT-II TCR. The role of JunB in T helper cells activated with weaker TCR signal should be addressed in the future.

Chapter 5: Future directions

Part I. The requirement of Bim for increased apoptosis in *Junb*-deficient $CD4^+$ T cells

My data suggest that one of the critical roles of JunB in $CD4^+$ T cells is to inhibit the expression of Bim. To further analyze the importance of JunB-dependent regulation of Bim expression, the effect of Bim knockout in *Junb*-deficient $CD4^+$ T cell should be evaluated with CRISPR-CAS9-mediated gene deletion. In this experiment, naïve $CD4^+$ T cells from $Junb^{fl/fl}Cd4^{cre}$ (*Junb*-deficient) mice will be electroporated with Cas9 proteins and guide RNA targeting *Bcl2l11* (gBim). After 72h activation under *in-vitro* Th1-, Th2-, and Th17-polarizing conditions, I will examine whether knockout of Bim can increase cell survival.

Part II. The molecular mechanism of action of JunB in control of Bim-mediated apoptosis in various $CD4^+$ effector T cells

Abundance of the apoptosis inducer Bim should be strictly regulated to prevent premature apoptosis in activated $CD4^+$ T cells. Previous studies showed that ligation of TCR and antigens decrease the expression of Bim mRNA (154, 155), suggesting that a TCR-induced repressor for Bim might exist in $CD4^+$ T cell differentiation. My data suggest that JunB is a critical regulator of Bim-mediated apoptosis, as deletion of JunB increased cell death as well as upregulation of Bim both *in vitro* and *in vivo* (Fig. 11C, 17C, 19). Furthermore, JunB colocalizes with BATF and IRF4 on *Bcl2l11* locus, suggesting that JunB directly regulates expression of *Bcl2l11* (Fig. 22).

JunB might regulate the expression of Bim through facilitating the binding of BATF and IRF4 to *Bcl2l11* locus. Previous studies demonstrated that BATF and IRF4 are potential repressors of Bim, as deletion of BATF and IRF4 upregulated expression of *Bcl2l11* in activated T cells (66, 113). Mouse *Bcl2l11* locus contains several conserved noncoding sequences (CNS) (Fig. 27), one of which starts at 9 kb upstream of the transcription starting site of *Bcl2l11* (CNS-9, Fig. 26). My ChIP-Seq analysis demonstrated that JunB colocalized with BATF and IRF4 only at CNS-9 in *Bcl2l11* locus, suggesting that CNS-9 might be an important cis-regulatory element for JunB to regulate Bim-induced apoptosis during $CD4^+$ T cell differentiation.

Furthermore, the complex formed by JunB, BATF and IRF4 might also compete with the known Bim activators such as Forkhead box O3A (Foxo3A) to inhibit *Bcl2l11* expression (156). I searched Foxo3A-binding motif across the entire mouse genome and identified several genomic regions containing potential binding sites for Foxo3A on *Bcl2l11* locus (Fig. 27). Among them, one Foxo3A binding site also locates within CNS-9 and are only 485 bp to the center regions of the JunB/BATF/IRF4-colocalizing

peaks (Fig. 27), suggesting a potential competition in DNA bindings between JunB-BATF/IRF4 complex and Foxo3A proteins.

To investigate whether the binding to CNS-9 region of BATF, IRF4 and Foxa3A is JunB-dependent, ChIP-PCR assay will be performed between *Junb*-deficient $CD4^+$ T cells and controls cells with antibodies to BATF, IRF4 and Foxa3A. In this experiment, naïve $CD4^+$ T cells from $Junb^{fl/fl}Cd4^{cre}$ (*Junb*-deficient) and $Junb^{fl/fl}$ (control) mice will be activated under Th1-, Th2-, and Th17-polarizing conditions. After 72 h, chromatins will be collected and real time PCR assay will be performed to reveal whether *Junb*-deficient $CD4^+$ T cells exhibit altered bindings of BATF, IRF4, and Foxa3A at the CNS-9 of *Bcl2l11* locus.

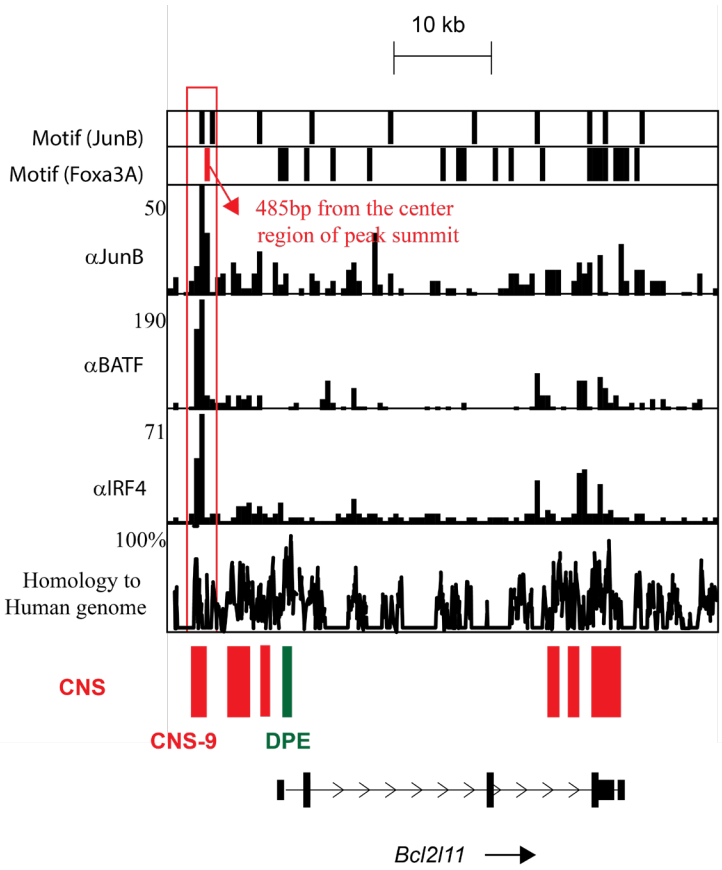

Fig. 27. JunB-mediated DNA binding of other transcription factors on *Bcl2l11* locus.

Schematic of JunB-binding motif, Foxa3A-binding motif, ChIP-seq peaks for JunB, BATF, and IRF4 in mouse *Bcl2l11* locus, and conserved regions between mouse and human *Bcl2l11* locus. JunB- and Foxo3A-binding motifs were identified through scanning the motif sequence across the entire mouse genome (ver. *mm10*). A consensus JunB ChIP-seq peak dataset was obtained from the union of JunB ChIP-seq data for Th1 cells and Th17 subsets (GSE86535). Conserved regions between mouse and human *Bcl2l11* locus were identified by ECR browser by comparing mouse and human genome (ver. *hg19* and ver. *mm10*) (157). Conserved regions that locate within 10 kbp upstream of transcription starting site of *Bcl2l11* or within the gene body are labelled. The overlapping region between Foxa3A-binding site, JunB/BATF/IRF4-colocalizing peak, and CNS-9 region are highlighted. The Foxa3a-binding site is 485 bp from the center region of JunB/BATF/IRF4-colocalizing peak. CNS, conserved noncoding region; DPE, downstream promoter element.

Part III. The role of JunB in aged CD4$^+$ T cells

Recent studies have suggested that the induction of Bim plays critical roles in eliminating functionally defective naïve CD4$^+$ T cells from aged individuals (158).

Naïve $CD4^+$ T cells from aged mice exhibit several functional defects during activation, including impaired proliferation, low cytokine production and poor abilities in helping B cell to produce antibodies (159–161). To ensure a healthy turnover of naïve $CD4^+$ T cells in peripheral tissues, Bim is continuously induced and the expression level of Bim should be kept higher than its antagonist, Bcl-2. In naïve $CD4^+$ T cells from young mice, the ratio of Bim to Bcl-2 is kept around 1.6 so that peripheral naive $CD4^+$ T cells are relatively susceptible to apoptosis. However, the expression level of Bim decreases during aging and the ratio of Bim to Bcl-2 also decreases to below 1.0 (158). As a result, dysfunctional naïve $CD4^+$ T cells accumulate in aged mice. Once activated, those $CD4^+$ T cells exhibit defective IL-2 secretion and cannot efficiently help B cells to undergo class switch to IgG (158, 162).

A small-scale study using six human subjects has demonstrated that the expression of main JunB partner, BATF, is increased in activated $CD4^+$ T cells from aged individuals (older than 60 years) (163). Hence, it is interesting to investigate whether the induction of JunB is higher in $CD4^+$ T cells in aged mice than those in young mice. To address this, aged (> 80 weeks) and young (<10 weeks) OT-II mice will be immunized with $OVA_{323-339}$. Throughout the immunization, the expression levels of JunB of activated OT-II T cells from both aged and young mice will be analyzed. Meanwhile, whether the expression of Bim in activated OT-II cells from aged mice is lower than those from young mice will also be confirmed.

If the results are in line with my hypothesis, then the next step is to investigate what factors cause the increased induction of JunB in $CD4^+$ T cells of aged mice. One hypothesis is the increased plasma IL-6 level during aging. Our lab has revealed that in addition to antigen stimulation, pro-inflammatory cytokines such as IL-6 can also augment the expression of JunB in activated $CD4^+$ T cells (100). Several clinical studies using human subjects also revealed that plasma IL-6 level is increased in older individuals compared to young individuals (164–167). To address this, plasma IL-6 level will be determined in aged and young OT-II mice. We can further treat aged mice with anti-IL-6 antibodies to see if IL-6 depletion can decrease the level of JunB in $CD4^+$ T cells of aged mice. Collectively, these studies will help us to understand the immune regulation mediated by IL-6-JunB-Bim axis during aging.

Part IV. The role of JunB in cell-type-specific regulation

My RNA-seq data identified many JunB target genes in a specific $CD4^+$ effector T subset. Depending on cell-type-specific chromatin landscape JunB may bind and regulate different sets of genes in $CD4^+$ effector T subsets. To investigate this possibility, the binding of JunB on its Th-subset-specific targets, including *Eomes*, *Il12rb2*, *Il13*, *Il4ra* and *Il17a,* will be examined by ChIP-PCR assay in cells cultured under Th1-,

Th2- and Th17-polarizing conditions. Furthermore, whether JunB facilitates BATF and IRF4 binding to these loci will be examined by ChIP-PCR assay in *Junb*-deficient $CD4^+$ T cells with antibodies to BATF and IRF4.

Part V. The role of JunB in chromatin remodeling

BATF has been reported to regulate global chromatin structures during Th17 differentiation (91). As the major BATF-interacting partner, JunB may also possess similar chromatin remodeling activities. To address this, the global chromatin accessibility between *Junb*-deficient and control cells, activated under Th1-, Th2-, and Th17-polarizing conditions, will be examined by using Assay for Transposase-Accessible Chromatin sequencing (ATAC-seq) (168). The differential ATAC-seq peaks will be overlapped with my RNA-seq data set to reveal whether JunB-mediated chromatin modeling affects gene expression in each Th subset.

Part VI. The JunB-mediated protein interactome

My study reveal that JunB potentially interacts with various family proteins to regulate gene expression (Fig. 25). Previous studies also demonstrated JunB likely interacts with BACH2 and c-Maf in regulating differentiation of $CD8^+$ T and Th2 cells, respectively (169, 170). Thus, JunB-mediated protein interactomes might exist in regulating effector functions and differentiation of various $CD4^+$ effector T cells. To decipher the JunB-mediated protein interactomes, JunB-interacting proteins will be harvested from Th1, Th2, and Th17 cells by immunoprecipitation with anti-JunB antibodies. The harvested proteins will be crosslinked, digested, and further analyzed by proteomics method. We can adopt data-independent acquisition mass spectrometry (DIA MS) technique, which allows us to identify the JunB-interacting partners in a full mass to charge (*m/z*) range without being restricted to predefined peptides of interest (171, 172). Moreover, through introducing a synthesized peptide with known concentrations, we can further quantify the relative abundance of complexes formed by JunB and BACH2, c-Maf and BATF in each $CD4^+$ T cell effector subsets.

Reference

1. Akira, S., S.Uematsu, andO.Takeuchi. 2006. Pathogen recognition and innate immunity. *Cell* 124: 783–801.
2. Medzhitov, R. 2001. TOLL-LIKE RECEPTORS AND INNATE IMMUNITY. *Nat. Rev. Immunol.* 1: 135–145.
3. Janeway, C. A., andR.Medzhitov. 2002. Innate immune recognition. *Annu. Rev. Immunol.* 20: 197–216.
4. Blom, B., andH.Spits. 2006. Development of human lymphoid cells. *Annu. Rev. Immunol.* 24: 287–320.
5. Holers, V. M. 2014. Complement and its receptors: New insights into human disease. *Annu. Rev. Immunol.* 32: 433–459.
6. Uribe-Querol, E., andC.Rosales. 2020. Phagocytosis: Our Current Understanding of a Universal Biological Process. *Front. Immunol.* 11: 1066.
7. Vidard, L., M.Kovacsovics-Bankowski, S. K.Kraeft, L. B.Chen, B.Benacerraf, andK. L.Rock. 1996. Analysis of MHC class II presentation of particulate antigens of B lymphocytes. *J. Immunol.* 156: 2809–18.
8. Savina, A., andS.Amigorena. 2007. Phagocytosis and antigen presentation in dendritic cells. *Immunol. Rev.* 219: 143–156.
9. Zhou, F. 2009. Molecular mechanisms of IFN-γ to up-regulate MHC class i antigen processing and presentation. *Int. Rev. Immunol.* 28: 239–260.
10. Pestka, S., C. D.Krause, D.Sarkar, M. R.Walter, Y.Shi, andP. B.Fisher. 2004. Interleukin-10 and related cytokines and receptors. *Annu. Rev. Immunol.* 22: 929–979.
11. Massagué, J., S. W.Blain, andR. S.Lo. 2000. TGFβ signaling in growth control, cancer, and heritable disorders. *Cell* 103: 295–309.
12. Harriman, W., H.Völk, N.Defranoux, andM.Wabl. 1993. Immunoglobulin class switch recombination. *Annu. Rev. Immunol.* 11: 361–384.
13. Martin, M. D., andV. P.Badovinac. 2018. Defining memory CD8 T cell. *Front. Immunol.* 9: 2692.
14. Sun, J. C., M. A.Williams, andM. J.Bevan. 2004. CD4+ T cells are required for the maintenance, not programming, of memory CD8+ T cells after acute infection. *Nat. Immunol.* 5: 927–933.
15. Williams, M. A., A. J.Tyznik, andM. J.Bevan. 2006. Interleukin-2 signals during priming are required for secondary expansion of CD8+ memory T cells. *Nature* 441: 890–893.
16. Lisco, A., P.Ye, C. S.Wong, L.Pei, A. P.Hsu, E. M.Mace, J. S.Orange, S. L.Lage, A. J.Ward, S. A.Migueles, M.Connors, M.V.Anderson, C. M.Buckner, S.Moir, A.Rupert, A.Dulau-Florea, P.Ogbogu, D.Timberlake, L. D.Notarangelo, S.Pittaluga, R. S.Abraham, andI.Sereti. 2021. Lost in Translation: Lack of CD4 Expression due to

a Novel Genetic Defect. *J. Infect. Dis.* 223: 645–654.
17. Douek, D. C., L. J.Picker, andR. A.Koup. 2003. T cell dynamics in HIV-1 infection. *Annu. Rev. Immunol.* 21: 265–304.
18. Lucas, C., P.Wong, J.Klein, T. B. R.Castro, J.Silva, M.Sundaram, M. K.Ellingson, T.Mao, J. E.Oh, B.Israelow, T.Takahashi, M.Tokuyama, P.Lu, A.Venkataraman, A.Park, S.Mohanty, H.Wang, A. L.Wyllie, C. B. F.Vogels, R.Earnest, S.Lapidus, I. M.Ott, A. J.Moore, M. C.Muenker, J. B.Fournier, M.Campbell, C. D.Odio, A.Casanovas-Massana, A.Obaid, A.Lu-Culligan, A.Nelson, A.Brito, A.Nunez, A.Martin, A.Watkins, B.Geng, C.Kalinich, C.Harden, C.Todeasa, C.Jensen, D.Kim, D.McDonald, D.Shepard, E.Courchaine, E. B.White, E.Song, E.Silva, E.Kudo, G.DeIuliis, H.Rahming, H. J.Park, I.Matos, J.Nouws, J.Valdez, J.Fauver, J.Lim, K. A.Rose, K.Anastasio, K.Brower, L.Glick, L.Sharma, L.Sewanan, L.Knaggs, M.Minasyan, M.Batsu, M.Petrone, M.Kuang, M.Nakahata, M.Campbell, M.Linehan, M. H.Askenase, M.Simonov, M.Smolgovsky, N.Sonnert, N.Naushad, P.Vijayakumar, R.Martinello, R.Datta, R.Handoko, S.Bermejo, S.Prophet, S.Bickerton, S.Velazquez, T.Alpert, T.Rice, W.Khoury-Hanold, X.Peng, Y.Yang, Y.Cao, Y.Strong, R.Herbst, A. C.Shaw, R.Medzhitov, W. L.Schulz, N. D.Grubaugh, C.DelaCruz, S.Farhadian, A. I.Ko, S. B.Omer, andA.Iwasaki. 2020. Longitudinal analyses reveal immunological misfiring in severe COVID-19. *Nature* 584: 463–469.
19. Hoffmann, M., H.Kleine-Weber, S.Schroeder, N.Krüger, T.Herrler, S.Erichsen, T. S.Schiergens, G.Herrler, N. H.Wu, A.Nitsche, M. A.Müller, C.Drosten, andS.Pöhlmann. 2020. SARS-CoV-2 Cell Entry Depends on ACE2 and TMPRSS2 and Is Blocked by a Clinically Proven Protease Inhibitor. *Cell* 181: 271-280.e8.
20. Xu, X., andX.-M.Gao. 2004. *Immunological Responses against SARS-Coronavirus Infection in Humans*,.
21. Davanzo, G. G., A. C.Codo, N. S.Brunetti, V.Boldrini, T. L.Knittel, L. B.Monterio, D.deMoraes, A. J.R Ferrari, G. F.deSouza, S. P.Muraro, G. S.Profeta, N. S.Wassano, L. N.Santos, V. C.Carregari, A. H.S Dias, J.Victor Virgilio-da-Silva, Í.Castro, L. C.Silva-Costa, A.Palma, E.Mansour, R. G.Ulaf, A. F.Bernardes, T. A.Nunes, L. C.Ribeiro, M.VAgrela, M.Luiza Moretti, L. I.Buscaratti, F.Crunfli, R. G.Ludwig, J. A.Gerhardt, R.Seste-Costa, J.Forato, M. R.Amorin, D. A.T Texeira, P. L.Parise, M. C.Martini, K.Bispo-dos-Santos, C. L.Simeoni, F.Granja, V. C.Silvestrini, E. B.deOliveira, V. M.Faça, M.Carvalho, B. G.Castelucci, A. B.Pereira, L. D.Coimbra, P. B.Rodrigues, A. S.Bernardo P Gomes, F. B.Pereira, L. M.B Santos, A. C.Sposito, R. F.Carvalho, A. S.Vieira, M. A.R Vinolo, A.Damasio, L. A.Velloso, H. I.Nakaya, H.Marques-Souza, R. E.Marques, D.Martins-de-Souza, M. S.Skaf, J.Luiz Proença-Modena, P. M.Moraes-Vieira, M. A.Mori, andA. S.Farias. 2020. SARS-CoV-2 Uses CD4 to Infect T Helper Lymphocytes. *medRxiv* 2020.09.25.20200329.

22. Dupage, M., andJ. A.Bluestone. 2016. Harnessing the plasticity of CD4+ T cells to treat immune-mediated disease. *Nat. Rev. Immunol.* 16: 149–163.
23. Saravia, J., N. M.Chapman, andH.Chi. 2019. Helper T cell differentiation. *Cell. Mol. Immunol.* 16: 634–643.
24. Zhu, J., H.Yamane, andW. E.Paul. 2010. Differentiation of effector CD4+ T cell populations. *Annu. Rev. Immunol.* 28: 445–489.
25. O'Shea, J. J., R.Lahesmaa, G.Vahedi, A.Laurence, andY.Kanno. 2011. Genomic views of STAT function in CD4 + T helper cell differentiation. *Nat. Rev. Immunol.* 11: 239–250.
26. Mosmann, T. R., H.Cherwinski, M. W.Bond, M. A.Giedlin, andR. L.Coffman. 1986. Two types of murine helper T cell clone. I. Definition according to profiles of lymphokine activities and secreted proteins. *J. Immunol.* 136: 2348–57.
27. Szabo, S. J., S. T.Kim, G. L.Costa, X.Zhang, C. G.Fathman, andL. H.Glimcher. 2000. A Novel Transcription Factor, T-bet, Directs Th1 Lineage Commitment. *Cell* 100: 655–669.
28. Zhu, J., D.Jankovic, A. J.Oler, G.Wei, S.Sharma, G.Hu, L.Guo, R.Yagi, H.Yamane, G.Punkosdy, L.Feigenbaum, K.Zhao, andW. E.Paul. 2012. The Transcription Factor T-bet Is Induced by Multiple Pathways and Prevents an Endogenous Th2 Cell Program during Th1 Cell Responses. *Immunity* 37: 660–673.
29. M, A., S.JR, Y.J, J.NG, C.N, Y.SY, M.TL, andM.KM. 2002. T-bet is a STAT1-induced regulator of IL-12R expression in naïve CD4+ T cells. *Nat. Immunol.* 3: 549–557.
30. Schroder, K., P. J.Hertzog, T.Ravasi, andD. A.Hume. 2004. Interferon-γ: an overview of signals, mechanisms and functions. *J. Leukoc. Biol.* 75: 163–189.
31. PC, R., andA.BB. 1999. TNF-induced signaling in apoptosis. *J. Clin. Immunol.* 19: 350–364.
32. Trinchieri, G. 2003. Interleukin-12 and the regulation of innate resistance and adaptive immunity. *Nat. Rev. Immunol.* 3: 133–146.
33. Fan, H., C. S.Walters, G. M.Dunston, andR.Tackey. 2002. IL-12 plays a significant role in the apoptosis of human T cells in the absence of antigenic stimulation. *Cytokine* 19: 126–137.
34. Barnes, P. J. 2018. Targeting cytokines to treat asthma and chronic obstructive pulmonary disease. *Nat. Rev. Immunol.* 18: 454–466.
35. Schmitz, J., A.Owyang, E.Oldham, Y.Song, E.Murphy, T. K.McClanahan, G.Zurawski, M.Moshrefi, J.Qin, X.Li, D. M.Gorman, J. F.Bazan, andR. A.Kastelein. 2005. IL-33, an interleukin-1-like cytokine that signals via the IL-1 receptor-related protein ST2 and induces T helper type 2-associated cytokines. *Immunity* 23: 479–490.
36. Kaplan, M. H., M. M.Hufford, andM. R.Olson. 2015. The development and in

vivo function of T helper 9 cells. *Nat. Rev. Immunol.* 15: 295–307.
37. Veldhoen, M., C.Uyttenhove, J.vanSnick, H.Helmby, A.Westendorf, J.Buer, B.Martin, C.Wilhelm, andB.Stockinger. 2008. Transforming growth factor-β "reprograms" the differentiation of T helper 2 cells and promotes an interleukin 9-producing subset. *Nat. Immunol.* 9: 1341–1346.
38. Chang, H. C., S.Sehra, R.Goswami, W.Yao, Q.Yu, G. L.Stritesky, R.Jabeen, C.McKinley, A. N.Ahyi, L.Han, E. T.Nguyen, M. J.Robertson, N. B.Perumal, R. S.Tepper, S. L.Nutt, andM. H.Kaplan. 2010. The transcription factor PU.1 is required for the development of IL-9-producing T cells and allergic inflammation. *Nat. Immunol.* 11: 527–534.
39. Faulkner, H., J. C.Renauld, J.VanSnick, andR. K.Grencis. 1998. Interleukin-9 enhances resistance to the intestinal nematode Trichuds muris. *Infect. Immun.* 66: 3832–3840.
40. Wu, X., J.Tian, andS.Wang. 2018. Insight into non-pathogenic Th17 cells in autoimmune diseases. *Front. Immunol.* 9: 1112.
41. Gaffen, S. L., R.Jain, A.V.Garg, andD. J.Cua. 2014. The IL-23-IL-17 immune axis: From mechanisms to therapeutic testing. *Nat. Rev. Immunol.* 14: 585–600.
42. Esplugues, E., S.Huber, N.Gagliani, A. E.Hauser, T.Town, Y. Y.Wan, W.O'connor, A.Rongvaux, N.VanRooijen, A. M.Haberman, Y.Iwakura, V. K.Kuchroo, J. K.Kolls, J. A.Bluestone, K. C.Herold, andR. A.Flavell. 2011. Control of T H 17 cells occurs in the small intestine. *Nature*.
43. Hirota, K., J. E.Turner, M.Villa, J. H.Duarte, J.Demengeot, O. M.Steinmetz, andB.Stockinger. 2013. Plasticity of TH 17 cells in Peyer's patches is responsible for the induction of T cell-dependent IgA responses. *Nat. Immunol.* 14: 372–379.
44. McGeachy, M. J., K. S.Bak-Jensen, Y.Chen, C. M.Tato, W.Blumenschein, T.McClanahan, andD. J.Cua. 2007. TGF-β and IL-6 drive the production of IL-17 and IL-10 by T cells and restrain TH-17 cell-mediated pathology. *Nat. Immunol.* 8: 1390–1397.
45. Zheng, Y., D. M.Danilenko, P.Valdez, I.Kasman, J.Eastham-Anderson, J.Wu, andW.Ouyang. 2007. Interleukin-22, a TH17 cytokine, mediates IL-23-induced dermal inflammation and acanthosis. *Nature* 445: 648–651.
46. Langrish, C. L., Y.Chen, W. M.Blumenschein, J.Mattson, B.Basham, J. D.Sedgwick, T.McClanahan, R. A.Kastelein, andD. J.Cua. 2005. IL-23 drives a pathogenic T cell population that induces autoimmune inflammation. *J. Exp. Med.* 201: 233–240.
47. Chen, Y., C. L.Langrish, B.Mckenzie, B.Joyce-Shaikh, J. S.Stumhofer, T.McClanahan, W.Blumenschein, T.Churakovsa, J.Low, L.Presta, C. A.Hunter, R. A.Kastelein, andD. J.Cua. 2006. Anti-IL-23 therapy inhibits multiple inflammatory

pathways and ameliorates autoimmune encephalomyelitis. *J. Clin. Invest.* 116: 1317–1326.
48. Chackerian, A. A., S. J.Chen, S. J.Brodie, J. D.Mattson, T. K.McClanahan, R. A.Kastelein, andE. P.Bowman. 2006. Neutralization or absence of the interleukin-23 pathway does not compromise immunity to mycobacterial infection. *Infect. Immun.* 74: 6092–6099.
49. Ivanov, I. I., B. S.McKenzie, L.Zhou, C. E.Tadokoro, A.Lepelley, J. J.Lafaille, D. J.Cua, andD. R.Littman. 2006. The Orphan Nuclear Receptor RORγt Directs the Differentiation Program of Proinflammatory IL-17+ T Helper Cells. *Cell* 126: 1121–1133.
50. Harrington, L. E., R. D.Hatton, P. R.Mangan, H.Turner, T. L.Murphy, K. M.Murphy, andC. T.Weaver. 2005. Interleukin 17-producing CD4+ effector T cells develop via a lineage distinct from the T helper type 1 and 2 lineages. *Nat. Immunol.* 6: 1123–1132.
51. Liu, X., R. I.Nurieva, andC.Dong. 2013. Transcriptional regulation of follicular T-helper (Tfh) cells. *Immunol. Rev.* 252: 139–145.
52. Nurieva, R. I., Y.Chung, G. J.Martinez, X. O.Yang, S.Tanaka, T. D.Matskevitch, Y. H.Wang, andC.Dong. 2009. Bcl6 mediates the development of T follicular helper cells. *Science (80-.).* 325: 1001–1005.
53. Yu, D., S.Rao, L. M.Tsai, S. K.Lee, Y.He, E. L.Sutcliffe, M.Srivastava, M.Linterman, L.Zheng, N.Simpson, J. I.Ellyard, I. A.Parish, C. S.Ma, Q. J.Li, C. R.Parish, C. R.Mackay, andC. G.Vinuesa. 2009. The Transcriptional Repressor Bcl-6 Directs T Follicular Helper Cell Lineage Commitment. *Immunity* 31: 457–468.
54. Bollig, N., A.Brüstle, K.Kellner, W.Ackermann, E.Abass, H.Raifer, B.Camara, C.Brendel, G.Giel, E.Bothur, M.Huber, C.Paul, A.Elli, R. A.Kroczek, R.Nurieva, C.Dong, R.Jacob, T. W.Mak, andM.Lohoff. 2012. Transcription factor IRF4 determines germinal center formation through follicular T-helper cell differentiation. *Proc. Natl. Acad. Sci. U. S. A.* 109: 8664–8669.
55. Breitfeld, B. D., L.Ohl, E.Kremmer, J.Ellwart, F.Sallusto, M.Lipp, andR.Förster. 2000. Follicular B Helper T Cells Express CXC Chemokine Receptor 5 , Localize to B Cell Follicles , and Support Immunoglobulin Production. 192.
56. Shi, J., S.Hou, Q.Fang, X.Liu, X.Liu, andH.Qi. 2018. PD-1 Controls Follicular T Helper Cell Positioning and Function Article PD-1 Controls Follicular T Helper Cell Positioning and Function. *Immunity* 49: 264-274.e4.
57. Koizumi, S., andH.Ishikawa. 2019. Transcriptional Regulation of Differentiation and Functions of Effector T Regulatory Cells. *Cells* 8: 939.
58. Chinen, T., A. K.Kannan, A. G.Levine, X.Fan, U.Klein, Y.Zheng, G.Gasteiger, Y.Feng, J. D.Fontenot, andA. Y.Rudensky. 2016. An essential role for the IL-2

receptor in T reg cell function. *Nat. Immunol. 2016 1711* 17: 1322–1333.
59. Walker, L. S. K. 2013. Treg and CTLA-4: Two intertwining pathways to immune tolerance. *J. Autoimmun.* 45: 49–57.
60. Chen, W., W.Jin, N.Hardegen, K.Lei, L.Li, N.Marinos, G.McGrady, andS. M.Wahl. 2003. Conversion of Peripheral CD4+CD25− Naive T Cells to CD4+CD25+ Regulatory T Cells by TGF-β Induction of Transcription Factor Foxp3. *J. Exp. Med.* 198: 1875–1886.
61. Bettelli, E., Y.Carrier, W.Gao, T.Korn, T. B.Strom, M.Oukka, H. L.Weiner, andV. K.Kuchroo. 2006. Reciprocal developmental pathways for the generation of pathogenic effector TH17 and regulatory T cells. *Nature* 441: 235–238.
62. Gagliani, N., M. C.Amezcua Vesely, A.Iseppon, L.Brockmann, H.Xu, N. W.Palm, M. R.DeZoete, P.Licona-Limón, R. S.Paiva, T.Ching, C.Weaver, X.Zi, X.Pan, R.Fan, L. X.Garmire, M. J.Cotton, Y.Drier, B.Bernstein, J.Geginat, B.Stockinger, E.Esplugues, S.Huber, andR. A.Flavell. 2015. TH17 cells transdifferentiate into regulatory T cells during resolution of inflammation. *Nature* 523: 221–225.
63. Dominguez-Villar, M., C. M.Baecher-Allan, andD. A.Hafler. 2011. Identification of T helper type 1-"like, Foxp3 + regulatory T cells in human autoimmune disease. *Nat. Med.* 17: 673–675.
64. Koch, M. A., G.Tucker-Heard, N. R.Perdue, J. R.Killebrew, K. B.Urdahl, andD. J.Campbell. 2009. The transcription factor T-bet controls regulatory T cell homeostasis and function during type 1 inflammation. *Nat. Immunol.* 10: 595–602.
65. Lu, K. T., Y.Kanno, J. L.Cannons, R.Handon, P.Bible, A. G.Elkahloun, S. M.Anderson, L.Wei, H.Sun, J. J.O'Shea, andP. L.Schwartzberg. 2011. Functional and Epigenetic Studies Reveal Multistep Differentiation and Plasticity of In Vitro-Generated and In Vivo-Derived Follicular T Helper Cells. *Immunity* 35: 622–632.
66. Yao, S., B. F.Buzo, D.Pham, L.Jiang, E. J.Taparowsky, andM. H.Kaplan. 2013. Interferon Regulatory Factor 4 Sustains CD8 + T Cell Expansion and Effector Differentiation. *Immunity* 39: 833–845.
67. Huber, M., A.Brüstle, K.Reinhard, A.Guralnik, G.Walter, A.Mahiny, E.VonLöw, andM.Lohoff. 2008. IRF4 is essential for IL-21-mediated induction, amplification, and stabilization of the Th17 phenotype. *Proc. Natl. Acad. Sci. U. S. A.* 105: 20846–20851.
68. Man, K., M.Miasari, W.Shi, A.Xin, D. C.Henstridge, S.Preston, M.Pellegrini, G. T.Belz, G. K.Smyth, M. A.Febbraio, S. L.Nutt, andA.Kallies. 2013. The transcription factor IRF4 is essential for TCR affinity-mediated metabolic programming and clonal expansion of T cells. *Nat. Immunol.* 14: 1155–1165.
69. Brüstle, A., S.Heink, M.Huber, C.Rosenplänter, C.Stadelmann, P.Yu, E.Arpaia, T. W.Mak, T.Kamradt, andM.Lohoff. 2007. The development of inflammatory TH-17

cells requires interferon-regulatory factor 4. *Nat. Immunol.* 8: 958–966.
70. Tominaga, N., K.Ohkusu-Tsukada, H.Udono, R.Abe, T.Matsuyama, andK.Yui. 2003. Development of Th1 and not Th2 immune responses in mice lacking IFN-regulatory factor-4. *Int. Immunol.* 15: 1–10.
71. Staudt, V., E.Bothur, M.Klein, K.Lingnau, S.Reuter, N.Grebe, B.Gerlitzki, M.Hoffmann, A.Ulges, C.Taube, N.Dehzad, M.Becker, M.Stassen, A.Steinborn, M.Lohoff, H.Schild, E.Schmitt, andT.Bopp. 2010. Interferon-Regulatory Factor 4 Is Essential for the Developmental Program of T Helper 9 Cells. *Immunity* 33: 192–202.
72. Vasanthakumar, A., K.Moro, A.Xin, Y.Liao, R.Gloury, S.Kawamoto, S.Fagarasan, L. A.Mielke, S.Afshar-Sterle, S. L.Masters, S.Nakae, H.Saito, J. M.Wentworth, P.Li, W.Liao, W. J.Leonard, G. K.Smyth, W.Shi, S. L.Nutt, S.Koyasu, andA.Kallies. 2015. The transcriptional regulators IRF4, BATF and IL-33 orchestrate development and maintenance of adipose tissue-resident regulatory T cells. *Nat. Immunol.* 16: 276–285.
73. Zheng, Y., A.Chaudhry, A.Kas, P.DeRoos, J. M.Kim, T. T.Chu, L.Corcoran, P.Treuting, U.Klein, andA. Y.Rudensky. 2009. Regulatory T-cell suppressor program co-opts transcription factor IRF4 to control TH2 responses. *Nature* 458: 351–356.
74. Mahnke, J., V.Schumacher, S.Ahrens, N.Käding, L. M.Feldhoff, M.Huber, J.Rupp, F.Raczkowski, andH. W.Mittrücker. 2016. Interferon Regulatory Factor 4 controls T H1 cell effector function and metabolism. *Sci. Rep.* 6.
75. Ahyi, A.-N. N., H.-C.Chang, A. L.Dent, S. L.Nutt, andM. H.Kaplan. 2009. IFN Regulatory Factor 4 Regulates the Expression of a Subset of Th2 Cytokines. *J. Immunol.* 183: 1598–1606.
76. Lohoff, M., andT. W.Mak. 2005. Roles of interferon-regulatory factors in T-helper-cell differentiation. *Nat. Rev. Immunol.* 5: 125–135.
77. Brass, A. L., E.Kehrli, C. F.Eisenbeis, U.Storb, andH.Singh. 1996. Pip, a lymphoid-restricted IRF, contains a regulatory domain that is important for autoinhibition and ternary complex formation with the Ets factor PU.1. *Genes Dev.* 10: 2335–2347.
78. Li, P., R.Spolski, W.Liao, L.Wang, T. L.Murphy, K. M.Murphy, andW. J.Leonard. 2012. BATF–JUN is critical for IRF4-mediated transcription in T cells. *Nature* 490: 543–546.
79. Glasmacher, E., S.Agrawal, A. B.Chang, T. L.Murphy, W.Zeng, B.VanderLugt, A. A.Khan, M.Ciofani, C. J.Spooner, S.Rutz, J.Hackney, R.Nurieva, C. R.Escalante, W.Ouyang, D. R.Littman, K. M.Murphy, andH.Singh. 2012. A genomic regulatory element that directs assembly and function of immune-specific AP-1 - IRF complexes. *Science (80-.).* 338: 975–980.
80. Rengarajan, J., K. A.Mowen, K. D.McBride, E. D.Smith, H.Singh, andL.

H.Glimcher. 2002. Interferon regulatory factor 4 (IRF4) interacts with NFATc2 to modulate interleukin 4 gene expression. *J. Exp. Med.* 195: 1003–1012.
81. Lohoff, M., H. W.Mittrücker, S.Prechtl, S.Bischof, F.Sommer, S.Kock, D. A.Ferrick, G. S.Duncan, A.Gessner, andT. W.Mak. 2002. Dysregulated T helper cell differentiation in the absence of interferon regulatory factor 4. *Proc. Natl. Acad. Sci. U. S. A.* 99: 11808–11812.
82. Cretney, E., A.Xin, W.Shi, M.Minnich, F.Masson, M.Miasari, G. T.Belz, G. K.Smyth, M.Busslinger, S. L.Nutt, andA.Kallies. 2011. The transcription factors Blimp-1 and IRF4 jointly control the differentiation and function of effector regulatory T cells. *Nat. Immunol.* 12: 304–312.
83. Angel, P., andM.Karin. 1991. The role of Jun, Fos and the AP-1 complex in cell-proliferation and transformation. *BBA - Rev. Cancer* 1072: 129–157.
84. Vinson, C., M.Myakishev, A.Acharya, A. A.Mir, J. R.Moll, andM.Bonovich. 2002. Classification of Human B-ZIP Proteins Based on Dimerization Properties. *Mol. Cell. Biol.* 22: 6321–6335.
85. Shaulian, E., andM.Karin. 2002. AP-1 as a regulator of cell life and death. *Nat. Cell Biol.* 4: E131–E136.
86. Murphy, T. L., R.Tussiwand, andK. M.Murphy. 2013. Specificity through cooperation: BATF-IRF interactions control immune-regulatory networks. *Nat. Rev. Immunol.* 13: 499–509.
87. Tussiwand, R., W. L.Lee, T. L.Murphy, M.Mashayekhi, W.Kc, J. C.Albring, A. T.Satpathy, J. A.Rotondo, B. T.Edelson, N. M.Kretzer, X.Wu, L. A.Weiss, E.Glasmacher, P.Li, W.Liao, M.Behnke, S. S. K.Lam, C. T.Aurthur, W. J.Leonard, H.Singh, C. L.Stallings, L.David Sibley, R. D.Schreiber, andK. M.Murphy. 2012. Compensatory dendritic cell development mediated by BATF-IRF interactions. *Nature* 490: 502–507.
88. Pham, D., C. E.Moseley, M.Gao, D.Savic, C. J.Winstead, M.Sun, B. L.Kee, R. M.Myers, C. T.Weaver, andR. D.Hatton. 2019. Batf Pioneers the Reorganization of Chromatin in Developing Effector T Cells via Ets1-Dependent Recruitment of Ctcf. *Cell Rep.* 29: 1203-1220.e7.
89. Schraml, B. U., K.Hildner, W.Ise, W. L.Lee, W. A. E.Smith, B.Solomon, G.Sahota, J.Sim, R.Mukasa, S.Cemerski, R. D.Hatton, G. D.Stormo, C. T.Weaver, J. H.Russell, T. L.Murphy, andK. M.Murphy. 2009. The AP-1 transcription factor Batf controls TH17 differentiation. *Nature* 460: 405–409.
90. Bao, K., T.Carr, J.Wu, W.Barclay, J.Jin, M.Ciofani, andR. L.Reinhardt. 2016. BATF Modulates the Th2 Locus Control Region and Regulates CD4 + T Cell Fate during Antihelminth Immunity. *J. Immunol.* 197: 4371–4381.
91. Ise, W., M.Kohyama, B. U.Schraml, T.Zhang, B.Schwer, U.Basu, F. W.Alt,

J.Tang, E. M.Oltz, T. L.Murphy, andK. M.Murphy. 2011. The transcription factor BATF controls the global regulators of class-switch recombination in both B cells and T cells. *Nat. Immunol.* 12: 536–43.
92. Ciofani, M., A.Madar, C.Galan, M.Sellars, K.MacE, F.Pauli, A.Agarwal, W.Huang, C. N.Parkurst, M.Muratet, K. M.Newberry, S.Meadows, A.Greenfield, Y.Yang, P.Jain, F. K.Kirigin, C.Birchmeier, E. F.Wagner, K. M.Murphy, R. M.Myers, R.Bonneau, andD. R.Littman. 2012. A validated regulatory network for Th17 cell specification. *Cell* 151: 289–303.
93. Sahoo, A., A.Alekseev, K.Tanaka, L.Obertas, B.Lerman, C.Haymaker, K.Clise-Dwyer, J. S.McMurray, andR.Nurieva. 2015. Batf is important for IL-4 expression in T follicular helper cells. *Nat. Commun.* 6: 1–10.
94. Jabeen, R., R.Goswami, O.Awe, A.Kulkarni, E.Nguyen, A.Attenasio, D.Walsh, M.Olson, M.Kim, R.Tepper, J.Sun, C.Kim, E.Taparowsky, B.Zhou, andM.Kaplan. 2013. Th9 cell development requires a BATF-regulated transcriptional network. *J. Clin. Invest.* 123: 4641–4653.
95. Betz, B. C., K. L.Jordan-Williams, C.Wang, S. G.Kang, J.Liao, M. R.Logan, C. H.Kim, andE. J.Taparowsky. 2010. Batf coordinates multiple aspects of B and T cell function required for normal antibody responses. *J. Exp. Med.* 207: 933–42.
96. C, X., F.Y, L.S, T.J, L.X, Q.R, D.H, Y.C, Z.C, W.J, K.MH, andY.K. 2021. BATF Regulates T Regulatory Cell Functional Specification and Fitness of Triglyceride Metabolism in Restraining Allergic Responses. *J. Immunol.* 206: 2088–2100.
97. Hayatsu, N., T.Miyao, M.Tachibana, R.Murakami, A.Kimura, T.Kato, E.Kawakami, T. A.Endo, R.Setoguchi, H.Watarai, T.Nishikawa, T.Yasuda, H.Yoshida, andS.Hori. 2017. Analyses of a Mutant Foxp3 Allele Reveal BATF as a Critical Transcription Factor in the Differentiation and Accumulation of Tissue Regulatory T Cells. *Immunity* 47: 268-283.e9.
98. Fu, Y., B.Koh, M.Kuwahara, B. J.Ulrich, R.Kharwadkar, M.Yamashita, andM. H.Kaplan. 2019. BATF-Interacting Proteins Dictate Specificity in Th Subset Activity. *J. Immunol.* 203: 1989–1998.
99. Yamazaki, S., Y.Tanaka, H.Araki, A.Kohda, F.Sanematsu, T.Arasaki, X.Duan, F.Miura, T.Katagiri, R.Shindo, H.Nakano, T.Ito, Y.Fukui, S.Endo, andH.Sumimoto. 2017. The AP-1 transcription factor JunB is required for Th17 cell differentiation. *Sci. Rep.* 7.
100. Hasan, Z., S. I.Koizumi, D.Sasaki, H.Yamada, N.Arakaki, Y.Fujihara, S.Okitsu, H.Shirahata, andH.Ishikawa. 2017. JunB is essential for IL-23-dependent pathogenicity of Th17 cells. *Nat. Commun.* 8: 15628.
101. Carr, T. M., J. D.Wheaton, G. M.Houtz, andM.Ciofani. 2017. JunB promotes Th17 cell identity and restrains alternative CD4+ T-cell programs during

inflammation. *Nat. Commun.* 8: 301.
102. Koizumi, S. ichi, D.Sasaki, T. H.Hsieh, N.Taira, N.Arakaki, S.Yamasaki, K.Wang, S.Sarkar, H.Shirahata, M.Miyagi, andH.Ishikawa. 2018. JunB regulates homeostasis and suppressive functions of effector regulatory T cells. *Nat. Commun.* 9: 5344.
103. Katagiri, T., S.Yamazaki, Y.Fukui, K.Aoki, H.Yagita, T.Nishina, T.Mikami, S.Katagiri, A.Shiraishi, S.Kimura, K.Tateda, H.Sumimoto, S.Endo, H.Kameda, andH.Nakano. 2019. JunB plays a crucial role in development of regulatory T cells by promoting IL-2 signaling. *Mucosal Immunol.* 12: 1104–1117.
104. Wheaton, J. D., andM.Ciofani. 2020. JunB Controls Intestinal Effector Programs in Regulatory T Cells. *Front. Immunol.* 11: 1–18.
105. Hartenstein, B., S.Teurich, J.Hess, J.Schenkel, M.Schorpp-Kistner, andP.Angel. 2002. Th2 cell-specific cytokine expression and allergen-induced airway inflammation depend on JunB. *EMBO J.* 21: 6321–6329.
106. Kuroda, S., M.Yamazaki, M.Abe, K.Sakimura, H.Takayanagi, andY.Iwai. 2011. Basic leucine zipper transcription factor, ATF-like (BATF) regulates epigenetically and energetically effector CD8 T-cell differentiation via Sirt1 expression. *Proc. Natl. Acad. Sci. U. S. A.* 108: 14885–14889.
107. Kuwahara, M., W.Ise, M.Ochi, J.Suzuki, K.Kometani, S.Maruyama, M.Izumoto, A.Matsumoto, N.Takemori, A.Takemori, K.Shinoda, T.Nakayama, O.Ohara, M.Yasukawa, T.Sawasaki, T.Kurosaki, andM.Yamashita. 2016. Bach2-Batf interactions control Th2-type immune response by regulating the IL-4 amplification loop. *Nat. Commun.* 7.
108. Martínez-Reyes, I., andN. S.Chandel. 2020. Mitochondrial TCA cycle metabolites control physiology and disease. *Nat. Commun.* 11: 1–11.
109. Fox, C. J., P. S.Hammerman, andC. B.Thompson. 2005. Fuel feeds function: Energy metabolism and the T-cell response. *Nat. Rev. Immunol.* 5: 844–852.
110. Wang, R., andD. R.Green. 2012. Metabolic checkpoints in activated T cells. *Nat. Immunol.* 13: 907–915.
111. Berod, L., C.Friedrich, A.Nandan, J.Freitag, S.Hagemann, K.Harmrolfs, A.Sandouk, C.Hesse, C. N.Castro, H.BäHre, S. K.Tschirner, N.Gorinski, M.Gohmert, C. T.Mayer, J.Huehn, E.Ponimaskin, W. R.Abraham, R.MüLler, M.Lochner, andT.Sparwasser. 2014. De novo fatty acid synthesis controls the fate between regulatory T and T helper 17 cells. *Nat. Med.* 20: 1327–1333.
112. Semenza, G. L. 2012. Hypoxia-inducible factors in physiology and medicine. *Cell* 148: 399–408.
113. Kurachi, M., R. A.Barnitz, N.Yosef, P. M.Odorizzi, M. A.Diiorio, M. E.Lemieux, K.Yates, J.Godec, M. G.Klatt, A.Regev, E. J.Wherry, andW. N.Haining.

2014. The transcription factor BATF operates as an essential differentiation checkpoint in early effector CD8 + T cells. *Nat. Immunol.* 15: 373–383.
114. Cho, Y. L., M.Flossdorf, L.Kretschmer, T.Höfer, D. H.Busch, andV. R.Buchholz. 2017. TCR Signal Quality Modulates Fate Decisions of Single CD4+ T Cells in a Probabilistic Manner. *Cell Rep.* 20: 806–818.
115. Green, D. R., N.Droin, andM.Pinkoski. 2003. Activation-induced cell death in T cells. *Immunol. Rev.* 193: 70–81.
116. Nagata, S., andM.Tanaka. 2017. Programmed cell death and the immune system. *Nat. Rev. Immunol.* 17: 333–340.
117. Strasser, A., L.O'Connor, andV. M.Dixit. 2000. Apoptosis signaling. *Annu. Rev. Biochem.* 69: 217–245.
118. Akiyama, T., P.Bouillet, T.Miyazaki, Y.Kadono, H.Chikuda, U.IlChung, A.Fukuda, A.Hikita, H.Seto, T.Okada, T.Inaba, A.Sanjay, R.Baron, H.Kawaguchi, H.Oda, K.Nakamura, A.Strasser, andS.Tanaka. 2003. Regulation of osteoclast apoptosis by ubiquitylation of proapoptotic BH3-only Bcl-2 family member Bim. *EMBO J.* 22: 6653–6664.
119. Fanzo, J. C., C. M.Hu, S. Y.Jang, andA. B.Pernis. 2003. Regulation of lymphocyte apoptosis by interferon regulatory factor 4 (IRF-4). *J. Exp. Med.* 197: 303–314.
120. Logan, M. R., K. L.Jordan-Williams, S.Poston, J.Liao, andE. J.Taparowsky. 2012. Overexpression of Batf induces an apoptotic defect and an associated lymphoproliferative disorder in mice. *Cell Death Dis.* 3: 1–9.
121. Dijkers, P. F., R. H.Medema, J. W. J.Lammers, L.Koenderman, andP. J.Coffer. 2000. Expression of the pro-apoptotic Bcl-2 family member Bim is regulated by the forkhead transcription factor FKHR-L1. *Curr. Biol.* 10: 1201–1204.
122. Sunters, A., S.Fernández De Mattos, M.Stahl, J. J.Brosens, G.Zoumpoulidou, C. A.Saunders, P. J.Coffer, R. H.Medema, R. C.Coombes, andE. W. F.Lam. 2003. FoxO3a Transcriptional Regulation of Bim Controls Apoptosis in Paclitaxel-treated Breast Cancer Cell Lines. *J. Biol. Chem.* 278: 49795–49805.
123. Luciano, F., A.Jacquel, P.Colosetti, M.Herrant, S.Cagnol, G.Pages, andP.Auberger. 2003. Phosphorylation of Bim-EL by Erk1/2 on serine 69 promotes its degradation via the proteasome pathway and regulates its proapoptotic function. *Oncogene* 22: 6785–6793.
124. Seki, A., andS.Rutz. 2018. Optimized RNP transfection for highly efficient CRI SPR/Cas9-mediated gene knockout in primary T cells. *J. Exp. Med.* 215: 985–997.
125. Saeidipour, B., andS.Bakhshi. 2013. Cutadapt Removes Adapter Sequences From High-Throughput Sequencing Reads. *Adv. Environ. Biol.* 7: 2803–2809.
126. Patro, R., G.Duggal, M. I.Love, R. A.Irizarry, andC.Kingsford. 2017. Salmon

provides fast and bias-aware quantification of transcript expression. *Nat. Methods* 14: 417–419.
127. Love, M. I., W.Huber, andS.Anders. 2014. Moderated estimation of fold change and dispersion for RNA-seq data with DESeq2. *Genome Biol.* 15: 1–21.
128. Edward Y Chen, Christopher M Tan, Yan Kou, Qiaonan Duan, Zichen Wang, Gabriela Vaz Meirelles, Neil R Clark, A. M. 2013. Enrichr: interactive and collaborative HTML5 gene list enrichment analysis tool. *BMC Bioinformatics* 14: 1–14.
129. Kuleshov, M.V., M. R.Jones, A. D.Rouillard, N. F.Fernandez, Q.Duan, Z.Wang, S.Koplev, S. L.Jenkins, K. M.Jagodnik, A.Lachmann, M. G.McDermott, C. D.Monteiro, G. W.Gundersen, andA.Ma'ayan. 2016. Enrichr: a comprehensive gene set enrichment analysis web server 2016 update. *Nucleic Acids Res.* 44: W90–W97.
130. Pasakarnis, T. S., C. A.Gorski, E.O'Loughlin, G. F.Parkin, andM. M.Scherer. 2006. TopHat2: accurate alignment of transcriptomes in the presence of insertions, deletions and gene fusions. *Genome Biol.* 46: 957–961.
131. Khan, A., andA.Mathelier. 2017. Intervene: A tool for intersection and visualization of multiple gene or genomic region sets. *BMC Bioinformatics* 18: 1–8.
132. Tang, Q., Y.Chen, C.Meyer, T.Geistlinger, M.Lupien, Q.Wang, T.Liu, Y.Zhang, M.Brown, andX. S.Liu. 2011. A comprehensive view of nuclear receptor cancer cistromes. *Cancer Res.* 71: 6940–6947.
133. Wang, S., H.Sun, J.Ma, C.Zang, C.Wang, J.Wang, Q.Tang, C. A.Meyer, Y.Zhang, andX. S.Liu. 2013. Target analysis by integration of transcriptome and ChIP-seq data with BETA. *Nat. Protoc.* 8: 2502–2515.
134. Breitling, R., P.Armengaud, A.Amtmann, andP.Herzyk. 2004. Rank products: A simple, yet powerful, new method to detect differentially regulated genes in replicated microarray experiments. *FEBS Lett.* 573: 83–92.
135. Lohoff, M., H.Mittrücker, A.Brüstle, F.Sommer, B.Casper, M.Huber, D. A.Ferrick, G. S.Duncan, andT. W.Mak. 2004. Enhanced TCR-induced Apoptosis in Interferon Regulatory Factor 4 – deficient CD4 + Th Cells. *J. Exp. Med.* 200: 247–253.
136. Semprini, S., T. J.Troup, N.Kotelevtseva, K.King, J. R. E.Davis, L. J.Mullins, K. E.Chapman, D. R.Dunbar, andJ. J.Mullins. 2007. Cryptic loxP sites in mammalian genomes: Genome-wide distribution and relevance for the efficiency of BAC/PAC recombineering techniques. *Nucleic Acids Res.* 35: 1402–1410.
137. Loonstra, A., M.Vooijs, H. B.Beverloo, B.AlAllak, E.VanDrunen, R.Kanaar, A.Berns, andJ.Jonkers. 2001. Growth inhibition and DNA damage induced by Cre recombinase in mammalian cells. *Proc. Natl. Acad. Sci. U. S. A.* 98: 9209–9214.
138. Moon, J. J., H. H.Chu, J.Hataye, A. J.Pagán, M.Pepper, J. B.McLachlan, T.Zell,

andM. K.Jenkins. 2009. Tracking epitope-specific T cells. *Nat. Protoc.* 4: 565–581.
139. Barnden, M. J., J.Allison, W. R.Heath, andF. R.Carbone. 1998. Defective TCR expression in transgenic mice constructed using cDNA- based α- and β-chain genes under the control of heterologous regulatory elements. *Immunol. Cell Biol.* 76: 34–40.
140. Robertson, J. M., P. E.Jensen, andB. D.Evavold. 2000. DO11.10 and OT-II T Cells Recognize a C-Terminal Ovalbumin 323–339 Epitope. *J. Immunol.* 164: 4706–4712.
141. Halim, T. Y. F., C. A.Steer, L.Mathä, M. J.Gold, I.Martinez-Gonzalez, K. M.McNagny, A. N. J.McKenzie, andF.Takei. 2014. Group 2 innate lymphoid cells are critical for the initiation of adaptive T helper 2 cell-mediated allergic lung inflammation. *Immunity* 40: 425–435.
142. Pape, K. A., A.Khoruts, andM. K.Jenkins. 2020. Inflammatory cytokines enhance the in vivo clonal expansion and differentiation of antigen-activated CD4+ T cells.
143. Kim, J., J. Y.Lee, K.Cho, S.-W.Hong, K. S.Kim, J.Sprent, S.-H.Im, C. D.Surh, andJ.-H.Cho. 2018. Spontaneous Proliferation of CD4+ T Cells in RAG-Deficient Hosts Promotes Antigen-Independent but IL-2-Dependent Strong Proliferative Response of Naïve CD8+ T Cells. *Front. Immunol.* 0: 1907.
144. Velardi, E., J. J.Tsai, andM. R. M.van denBrink. 2021. T cell regeneration after immunological injury. *Nat. Rev. Immunol.* 21: 277–291.
145. Dienz, O., andM.Rincon. 2009. The effects of IL-6 on CD4 T cell responses. *Clin. Immunol.* 130: 27–33.
146. Yang, Y., J.Xu, Y.Niu, J. S.Bromberg, andY.Ding. 2008. T-bet and Eomesodermin Play Critical Roles in Directing T Cell Differentiation to Th1 versus Th17. *J. Immunol.* 181: 8700.
147. JJ, de J., B.C, O.T, A.SD, andB.F. 2019. The MYO6 interactome: selective motor-cargo complexes for diverse cellular processes. *FEBS Lett.* 593: 1494–1507.
148. Chen, L., J. N. M.Glover, P. G.Hogan, A.Rao, andS. C.Harrison. 1998. Structure of the DNA-binding domains from NFAT, Fos and Jun bound specifically to DNA. *Nat. 1998 3926671* 392: 42–48.
149. Gabryšová, L., M.Alvarez-Martinez, R.Luisier, L. S.Cox, J.Sodenkamp, C.Hosking, D.Pérez-Mazliah, C.Whicher, Y.Kannan, K.Potempa, X.Wu, L.Bhaw, H.Wende, M. H.Sieweke, G.Elgar, M.Wilson, J.Briscoe, V.Metzis, J.Langhorne, N. M.Luscombe, andA.O'Garra. 2018. C-Maf controls immune responses by regulating disease-specific gene networks and repressing IL-2 in CD4+ T cells article. *Nat. Immunol.* 19: 497–507.
150. Fujita, N., Y.Kato, M.Naito, andT. T.S R. 1996. A NOVEL ANTI-Thy-1 (CD90) MONOCLONAL ANTIBODY INDUCES APOPTOSIS IN MOUSE MALIGNANT

T-LYMPHOMA CELLS IN SPITE OF INDUCING bcl-2 EXPRESSION. 66: 544–550.
151. Yoo, J. K., J. H.Cho, S. W.Lee, andY. C.Sung. 2002. IL-12 Provides Proliferation and Survival Signals to Murine CD4+ T Cells Through Phosphatidylinositol 3-Kinase/Akt Signaling Pathway. *J. Immunol.* 169: 3637–3643.
152. Reinhart, R., andT.Kaufmann. 2018. IL-4 enhances survival of in vitro-differentiated mouse basophils through transcription-independent signaling downstream of PI3K. *Cell Death Dis. 2018 97* 9: 1–12.
153. Malek, T. R., andI.Castro. 2010. Interleukin-2 Receptor Signaling: At the Interface between Tolerance and Immunity. *Immunity* 33: 153–165.
154. Hildeman, D. A., Y.Zhu, T. C.Mitchell, P.Bouillet, A.Strasser, andJ.Kappler. 2002. *Activated T Cell Death In Vivo Mediated by Proapoptotic Bcl-2 Family Member Bim Signaling through the Fas receptor directly activates apoptosis through the re-cruitment and activation of caspase enzymes (Cohen*,.
155. Bouillet, P., J. F.Purton, D. I.Godfrey, L. C.Zhang, L.Coultas, H.Puthalakath, M.Pellegrini, S.Cory, J. M.Adams, andA.Strasser. 2002. BH3-only Bcl-2 family member Bim is required for apoptosis of autoreactive thymocytes. *Nature* 415: 922–926.
156. Eijkelenboom, A., M.Mokry, L. M.Smits, E. E.Nieuwenhuis, andB. M. T.Burgering. 2013. FOXO3 selectively amplifies enhancer activity to establish target gene regulation. *Cell Rep.* 5: 1664–1678.
157. Ovcharenko, I., M. A.Nobrega, G. G.Loots, andL.Stubbs. 2004. ECR Browser: A tool for visualizing and accessing data from comparisons of multiple vertebrate genomes. *Nucleic Acids Res.* 32: W280.
158. Tsukamoto, H., G. E.Huston, J.Dibble, D. K.Duso, andS. L.Swain. 2010. Bim Dictates Naive CD4 T Cell Lifespan and the Development of Age-Associated Functional Defects. *J. Immunol.* 185: 4535–4544.
159. Lu, Y., A.Biancotto, F.Cheung, E.Remmers, N.Shah, J. P.McCoy, andJ. S.Tsang. 2016. Systematic Analysis of Cell-to-Cell Expression Variation of T Lymphocytes in a Human Cohort Identifies Aging and Genetic Associations. *Immunity* 45: 1162–1175.
160. Haynes, L., andS. L.Swain. 2006. Why Aging T Cells Fail: Implications for Vaccination. *Immunity* 24: 663–666.
161. Bruunsgaard, H., A. N.Pedersen, M.Schroll, P.Skinhøj, andB. K.Pedersen. 2000. Proliferative responses of blood mononuclear cells (BMNC) in a cohort of elderly humans: Role of lymphocyte phenotype and cytokine production. *Clin. Exp. Immunol.* 119: 433–440.
162. Tsukamoto, H., K.Clise-Dwyer, G. E.Huston, D. K.Duso, A. L.Buck, L.

L.Johnson, L.Haynes, andS. L.Swain. 2009. Age-associated increase in lifespan of naïve CD4 T cells contributes to T-cell homeostasis but facilitates development of functional defects. *Proc. Natl. Acad. Sci. U. S. A.* 106: 18333–18338.
163. Hu, B., G.Li, Z.Ye, C. E.Gustafson, L.Tian, C. M.Weyand, andJ. J.Goronzy. 2019. Transcription factor networks in aged naïve CD4 T cells bias lineage differentiation. *Aging Cell* 18.
164. Ferrucci, L., A.Corsi, F.Lauretani, S.Bandinelli, B.Bartali, D. D.Taub, J. M.Guralnik, andD. L.Longo. 2005. The origins of age-related proinflammatory state. *Blood* 105: 2294–2299.
165. Harris, T. B., L.Ferrucci, R. P.Tracy, M. C.Corti, S.Wacholder, W. H.Ettinger, H.Heimovitz, H. J.Cohen, andR.Wallace. 1999. Associations of elevated Interleukin-6 and C-Reactive protein levels with mortality in the elderly. *Am. J. Med.* 106: 506–512.
166. Hager, K., U.Machein, S.Krieger, D.Platt, G.Seefried, andJ.Bauer. 1994. Interleukin-6 and selected plasma proteins in healthy persons of different ages. *Neurobiol. Aging* 15: 771–772.
167. Wei, J., H.Xu, J. L.Davies, andG. P.Hemmings. 1992. Increase of plasma IL-6 concentration with age in healthy subjects. *Life Sci.* 51: 1953–1956.
168. Corces, M. R., A. E.Trevino, E. G.Hamilton, P. G.Greenside, N. A.Sinnott-Armstrong, S.Vesuna, A. T.Satpathy, A. J.Rubin, K. S.Montine, B.Wu, A.Kathiria, S. W.Cho, M. R.Mumbach, A. C.Carter, M.Kasowski, L. A.Orloff, V. I.Risca, A.Kundaje, P. A.Khavari, T. J.Montine, W. J.Greenleaf, andH. Y.Chang. 2017. An improved ATAC-seq protocol reduces background and enables interrogation of frozen tissues. *Nat. Methods 2017 1410* 14: 959–962.
169. Roychoudhuri, R., D.Clever, P.Li, Y.Wakabayashi, K. M.Quinn, C. A.Klebanoff, Y.Ji, M.Sukumar, R. L.Eil, Z.Yu, R.Spolski, D. C.Palmer, J. H.Pan, S. J.Patel, D. C.Macallan, G.Fabozzi, H. Y.Shih, Y.Kanno, A.Muto, J.Zhu, L.Gattinoni, J. J.O'Shea, K.Okkenhaug, K.Igarashi, W. J.Leonard, andN. P.Restifo. 2016. BACH2 regulates CD8 + T cell differentiation by controlling access of AP-1 factors to enhancers. *Nat. Immunol.* 17: 851–860.
170. Li, B., C.Tournier, R. J.Davis, andR. A.Flavell. 1999. Regulation of IL-4 expression by the transcription factor JunB during T helper cell differentiation. *EMBO J.* 18: 420–432.
171. Lin, Y.-H., R. V.Eguez, M. G.Torralba, H.Singh, P.Golusinski, W.Golusinski, M.Masternak, K. E.Nelson, M.Freire, andY.Yu. 2019. Self-Assembled STrap for Global Proteomics and Salivary Biomarker Discovery. *J. Proteome Res.* 18: 1907–1915.
172. Doerr, A. 2014. DIA mass spectrometry. *Nat. Methods 2015 121* 12: 35–35.